

論文 / 著書情報
Article / Book Information

| | |
|-------------------|---|
| 題目(和文) | |
| Title(English) | Preparation and Characterization of Mo/HNa-Y and Their Catalytic Activity. |
| 著者(和文) | 小松隆之 |
| Author(English) | TAKAYUKI KOMATSU |
| 出典(和文) | 学位:理学博士, 学位授与機関:東京工業大学, 報告番号:甲第1700号, 授与年月日:1986年3月26日, 学位の種別:課程博士, 審査員: |
| Citation(English) | Degree:Doctor of Science, Conferring organization: , Report number:甲第1700号, Conferred date:1986/3/26, Degree Type:Course doctor, Examiner: |
| 学位種別(和文) | 博士論文 |
| Type(English) | Doctoral Thesis |

b-19

PREPARATION AND CHARACTERIZATION OF Mo/HNa-Y
ZEOLITES AND THEIR CATALYTIC ACTIVITY

TAKAYUKI KOMATSU

Yashima Laboratory

Department of Chemistry

Tokyo Institute of Technology

CONTENTS

| | page |
|---|------|
| Chapter 1 Introduction | |
| 1-1 General aspects of molybdenum catalysts | 1 |
| 1-2 Molybdenum supported catalysts | 3 |
| 1-2-1 MoO ₃ supported catalysts | 4 |
| 1-2-2 New molybdenum supported catalysts | 11 |
| 1-2-3 Catalytic reactions on molybdenum supported catalysts | 18 |
| 1-3 Purpose of this study | 24 |
| References | 27 |
| Chapter 2 Preparation of Mo/HNa-Y | |
| 2-1 Introduction | 32 |
| 2-2 Experimental | 33 |
| 2-2-1 Materials | 33 |
| 2-2-2 Preparation of Mo/HNa-Y | 33 |
| 2-2-3 Infrared spectroscopy | 33 |
| 2-2-4 Temperature programmed decomposition | 35 |
| 2-2-5 X-ray photoelectron spectroscopy (XPS) | 35 |
| 2-3 Results and discussion | 35 |
| 2-3-1 Adsorption and decomposition of Mo(CO) ₆ | 35 |
| 2-3-2 Loading of molybdenum | 43 |
| 2-4 Conclusion | 50 |
| References | 52 |
| Chapter 3 Oxidation state of molybdenum | |
| 3-1 Introduction | 53 |

| | | |
|--|--|-----|
| 3-2 | Experimental | 54 |
| 3-2-1 | Average oxidation number of molybdenum | 54 |
| 3-2-2 | X-ray photoelectron spectroscopy (XPS) | 55 |
| 3-2-3 | Infrared spectroscopy | 56 |
| 3-2-4 | Electron spin resonance spectroscopy | 56 |
| 3-3 | Results and discussion | 57 |
| 3-3-1 | Average oxidation number of molybdenum | 57 |
| 3-3-2 | XPS study | 66 |
| 3-3-3 | Adsorption of CO | 76 |
| 3-3-4 | ESR study | 81 |
| 3-4 | Conclusion | 85 |
| | References | 87 |
| Chapter 4 Dispersion of molybdenum | | |
| 4-1 | Introduction | 89 |
| 4-2 | Experimental | 90 |
| 4-2-1 | Chemisorption of oxygen | 90 |
| 4-2-2 | Ultraviolet spectroscopy | 90 |
| 4-3 | Results and discussion | 91 |
| 4-3-1 | Chemisorption of oxygen | 91 |
| 4-3-2 | Ultraviolet spectra | 97 |
| 4-4 | Conclusion | 100 |
| | References | 101 |
| Chapter 5 Catalytic activity of Mo/HNa-Y | | |
| 5-1 | Introduction | 102 |
| 5-2 | Experimental | 103 |
| 5-2-1 | Polymerization of ethylene | 103 |
| 5-2-2 | Hydrogenation of ethylene | 103 |

| | | |
|-----------|----------------------------|-----|
| 5-2-3 | Metathesis of propylene | 104 |
| 5-3 | Results and discussion | 104 |
| 5-3-1 | Polymerization of ethylene | 104 |
| 5-3-2 | Hydrogenation of ethylene | 110 |
| 5-3-3 | Metathesis of propylene | 115 |
| 5-4 | Conclusion | 122 |
| | References | 123 |
| Chapter 6 | Conclusion | 125 |
| | Acknowledgment | 129 |

Chapter 1 Introduction

1-1 General aspects of molybdenum catalysts

Molybdenum is the element which can possess the formal oxidation states from -2 to +6 and its coordination numbers are in the range from 4 to 8. Therefore, molybdenum exhibits extensive variety in chemical properties. As a catalyst, molybdenum presents also the wide variety in its application. Molybdenum compounds have been used as industrial catalysts for a lot of reactions, and most of these catalysts are employed in heterogeneous reaction systems. Some representative applications of the molybdenum catalysts are shown in Table 1. These catalysts are classified into three catalyst systems;

- a) MoO_3 supported on other oxides
- b) Multicomponent composite oxides
- c) Heteropoly acids

Among these three catalyst systems, MoO_3 supported catalysts are most widely used for many kinds of reactions. In the MoO_3 supported catalysts, molybdenum occupies two or three different oxidation states by reduction treatments. Therefore, the variety in the chemical properties of molybdenum is reflected in the MoO_3 supported catalysts more extensively than in the other two catalyst systems.

In recent years, new molybdenum supported catalysts have been prepared to clarify what kind of molybdenum species possesses catalytic activity for an individual reaction. These new catalysts are prepared by using the different molybdenum compounds or complexes from the molybdates used in the MoO_3 sup-

Table 1

Molybdenum catalysts for various reactions

| Catalyst | Reaction |
|--------------------------------------|--------------------------------|
| $\text{MoO}_3/\text{Al}_2\text{O}_3$ | Hydrodesulfurization |
| Co-Mo/ Al_2O_3 | Hydrodenitrogenation |
| Ni-Mo/ Al_2O_3 | Hydrocracking of parafin |
| etc. | Hydrogenation of olefin |
| | Liquefaction of coal |
| | Isomerization of olefin |
| | Metathesis of olefin |
| | Polymerization of olefin |
| $\text{Bi}_2\text{O}_3\text{-MoO}_3$ | Ammoxidation of propylene |
| $\text{V}_2\text{O}_5\text{-MoO}_3$ | Selective oxidation of olefin |
| Fe-Bi-Mo oxides | Selective oxidation of alcohol |
| P-V-Mo oxides | Oxidation of aromatics |
| etc. | |
| Heteropoly acids | Hydration of olefin |
| | Dehydration of alcohol |
| | Isomerization of olefin |
| | Selective oxidation of olefin |

ported catalysts. I review these two types of molybdenum supported catalysts and refer to the catalytic activity of molybdenum in an individual reaction in the next section.

1-2 Molybdenum supported catalysts

As mentioned in the previous section, MoO_3 supported catalysts are widely applied to many kinds of reactions. Supporting MoO_3 on other oxides which have high surface areas results in higher dispersion of active molybdenum species. The other effects of the supports, that is, mechanical and thermal stabilities, geometrical influence, electronic effect, and so on, are also expected. The MoO_3 catalysts supported on other oxides are often used with some promoters such as Co, Ni, V, etc. to increase the activity and selectivity for hydrodesulfurization, hydrogenolysis, etc. in petroleum refining processes. However, the surface molybdenum species on the MoO_3 supported catalysts are usually heterogeneous in the oxidation states, particle size, interaction with supports, etc.. Consequently, there exists certain complexity in studying the catalytic properties of molybdenum when the MoO_3 supported catalysts are used.

For the purpose of overcoming this complexity, some investigators have recently paid their attention to a new class of molybdenum supported catalysts. These new catalysts have been prepared by using some molybdenum complexes or compounds as molybdenum sources instead of the molybdates which are usually used for the MoO_3 supported catalysts. It has been progressively

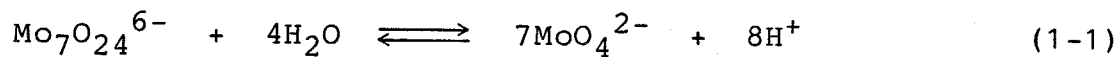
revealed that the new catalysts have many advantages to study the catalytic properties of molybdenum.

In this section, I review the studies on both the MoO_3 supported catalysts and the new molybdenum supported catalysts and point out the differences in the nature of supported molybdenum species and their catalytic activity for several reactions.

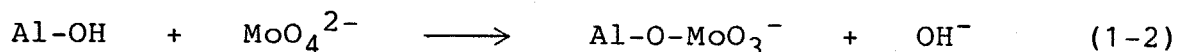
1-2-1 MoO_3 supported catalysts

First, I refer to the conventional MoO_3 supported catalysts. As a support, alumina has been generally used. In addition, silica, silica-alumina and magnesia supports have been industrially used, while titania [1] and zeolites [2] have been adapted as supports to the studies on the catalytic properties of molybdenum. Adding a promoter may complicate such studies on the catalytic properties, so that it is difficult to obtain a clear conclusion. I mention hereinafter the preparation, redox behavior and characterization of the MoO_3 supported catalysts, mainly $\text{MoO}_3/\text{Al}_2\text{O}_3$ without any promoters.

$\text{MoO}_3/\text{Al}_2\text{O}_3$ catalysts have been usually prepared by using an incipient wetness impregnation method with the aqueous solution of ammonium paramolybdate, ($(\text{NH}_4)_6\text{Mo}_7\text{O}_{24}$). A certain amount of the ammonium paramolybdate solution which corresponds to the total pore volume of the alumina is added to the alumina support. Subsequently, the mixture is dried and calcined to obtain $\text{MoO}_3/\text{Al}_2\text{O}_3$. The polyanion of this paramolybdate has an equilibrium in water;



Therefore, the increase in pH results in the degradation of the polyanion. Jeziorowski and Knözinger [3] have reported that when the polymolybdate solution of pH 6 is used for the impregnation, the ion exchange occurs on the alumina surface;

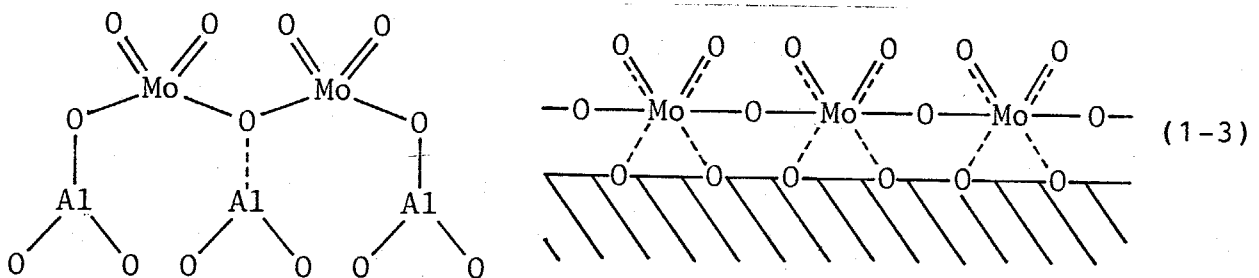


As a result, the local pH near the catalyst surface increased and the anion was adsorbed via MoO_4^{2-} . They have concluded that the adsorption process of the anion is not so extensively affected by using the molybdate solutions of various pH.

In order to diminish the change in the local pH in the impregnation solution, Wang and Hall [4] have prepared molybdenum supported catalysts by their equilibrium adsorption method using an excess amount of the dilute aqueous solution of ammonium paramolybdate. They found that the pH change did not occur so much during the impregnation, and that the anion was adsorbed via MoO_4^{2-} at pH = 8.6, $\text{Mo}_7\text{O}_{24}^{6-}$ at pH = 2.0 or $\text{Mo}_8\text{O}_{26}^{4-}$ at pH = 0.8. Thus they have suggested the possibility to control the degree of the aggregation of Mo species on calcination, that is, higher pH prefers less degree of aggregation. However, at the higher pH, less amount of adsorbed anion causes low loading of molybdenum.

In addition to the pH of the impregnation solution, the content of molybdenum has some effect on the nature of the supported Mo species. Zingg et al. [5] have reported that the Mo

species of $\text{MoO}_3/\text{Al}_2\text{O}_3$ prepared by the conventional impregnation method are divided into four types; tetrahedral interaction species, octahedral interaction species, $\text{Al}_2(\text{MoO}_4)_3$ and MoO_3 . The tetrahedral interaction species were the primary species at the low content of Mo. Below monolayer coverage, the two interaction species were formed, while above monolayer coverage, both $\text{Al}_2(\text{MoO}_4)_3$ and MoO_3 were identified. Vagin et al. [6] have proposed three types of Mo species on $\text{MoO}_3/\text{Al}_2\text{O}_3$ in view of their studies on the reduction kinetics. This proposal corresponds to the result of Zingg et al. [5], since these three species are the interaction species, $\text{Al}_2(\text{MoO}_4)_3$ and MoO_3 . The structures of these two interaction species have been reported as follows [7,8];

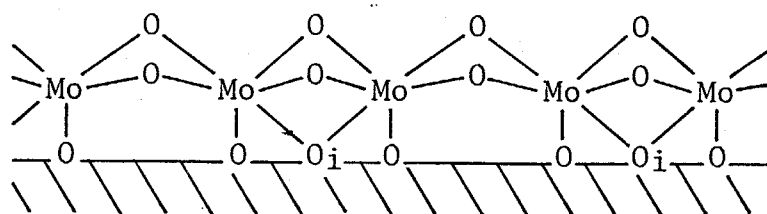


However, these structures may be subject to further discussion, because the structures of Mo species should depend on the structure of the alumina surface. Weigold [9] has proposed a surface attached oligomer model from two findings;

- 1) The adsorption of molybdate anions occurred through the interaction between the anions and the hydroxyl groups on alumina.
- 2) A significant proportion of these hydroxyl groups remaining on the surface of partially dehydroxylated alumina were located

in rows.

His oligomer model is represented by the structure below;

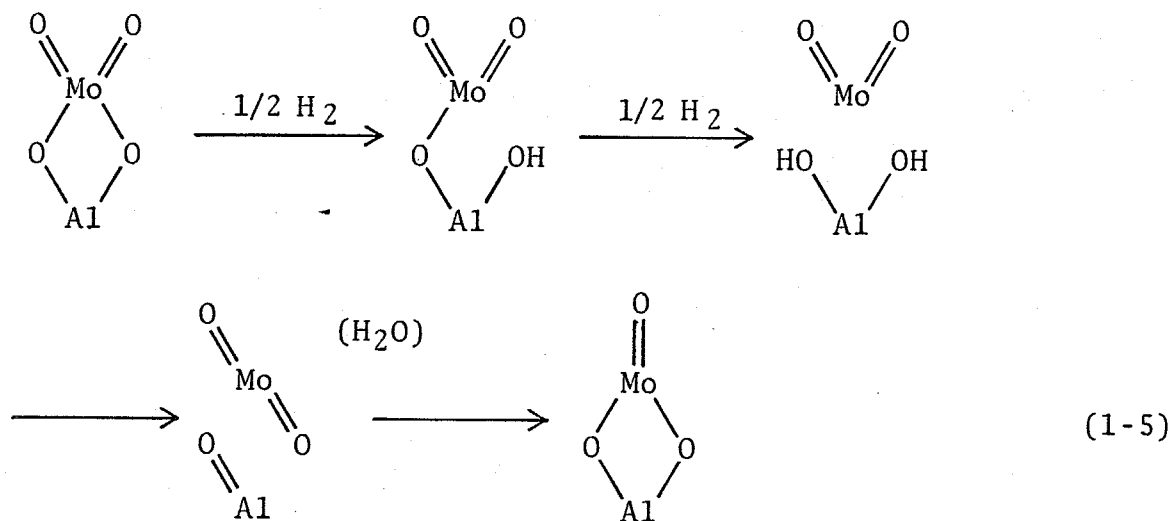


(1-4)

where O_i is the interstitial oxygen atom located in a vacancy of alumina layer. He has suggested that molybdenum is strongly attached through the Mo-O-Mo bond in addition to the Al-O-Mo bond, and that the $(Al-O)_2Mo$ structure does not exist because the distance between two adjacent Mo atoms in this structure is too long for the formation of the Mo-O-Mo bond.

Reduction process is often necessary for the MoO_3 supported catalysts to generate the sufficient activity for some kinds of reactions. The reduction has usually been carried out at $500^\circ C$ or so with hydrogen. Although a certain amount of Mo(VI) is reduced to Mo(IV) during this reduction, all of the Mo(VI) species can hardly be reduced homogeneously to Mo(IV) species. Besides, Mo species with the oxidation number of less than +4 cannot easily be obtained by the ordinal reduction treatment, that is, a hydrogen treatment at about $500^\circ C$.

Fransen et al. [10] and Millman et al. [11] have reported that their IR studies indicate the formation of new hydroxyl groups during the reduction of MoO_3/Al_2O_3 . The new hydroxyl band was attributed to the hydroxyl groups on alumina. This result led to the suggestion for the reduction mechanism [11];



Considering the proportion of Mo(IV), Mo(V) and Mo(VI) determined from XPS spectra, Zingg et al. [5], however, have reported that the tetrahedral interaction species formed at low contents of Mo are reduced not to Mo(IV) but to Mo(V). This is consistent with the other reports [12,13] that Mo species on the MoO₃/Al₂O₃ with low contents of molybdenum (< 3 wt%) are difficult to be reduced. On the other hand, Houalla et al. [14] have measured the surface Mo/Al ratio of MoO₃/Al₂O₃ with a monolayer coverage (8.1 wt%) and observed the decrease in this Mo/Al ratio of about 20 % during the reduction. They have suggested that the above mechanism (1-5) can not sufficiently account for their result and that MoO₂ crystallites are probably formed.

Thus the reduction of MoO₃ on supports is rather complex because the reduction behaviour varies with the content of molybdenum. In order to characterize the calcined, reduced or sulfided MoO₃ supported catalysts, a lot of physical method have been applied. Electron spin resonance (ESR) spectra can provide

the existence of Mo(V). However, the amount of Mo(V) measured from ESR spectra was significantly less than that estimated from the stoichiometric uptakes of H₂ and O₂ or from XPS spectra [15 - 18]. Petrakis et al. [16] have measured both XPS and ESR spectra of reduced MoO₃/Al₂O₃ and indicated the difference between the amounts of Mo(V) determined from the two methods, that is, 50 % of total molybdenum from XPS spectra and 0.6 % from ESR spectra. Such a difference has been interpreted by the formation of Mo(V) pairs which are inactive for ESR [19]. These Mo(V) pairs were assumed to be formed through Mo-O-Mo bonds [19] or Mo-Mo bonds [9]. Thus the application of XPS technique seems useful to determine the total amount of Mo(V) if one can adapt the deconvolution instruments for the measured spectra. The results of XPS studies have indicated that the Mo species with the oxidation number less than +4 are not formed during the reduction by H₂ at 500 °C [5,18] or during the sulfidation of MoO₃/Al₂O₃ [20].

UV spectra can detect the charge transfer from O²⁻ to Mo⁶⁺ of oxomolybdenum species. Therefore, the UV spectra of calcined MoO₃ supported catalysts measured using a diffuse reflectance method give the information about the oxygen coordination around Mo(VI). The oxomolybdenum species with an octahedral coordination have given the adsorption bands at 300 - 330 and 230 - 240 nm and those with a tetrahedral coordination at 260 - 290 and 230 - 240 nm [21]. Giordano et al. [7] have reported for MoO₃/Al₂O₃ that the low loading of molybdenum and the low temperature of calcination lead to the formation of tetrahedrally coordinated oxomolybdenum species and that the higher loading or the higher calcination temperature leads to the formation of octahedral

species which probably consist in bulk MoO_3 . Wang and Hall [22] have investigated the $\text{MoO}_3/\text{Al}_2\text{O}_3$ prepared by their equilibrium adsorption method and found that the tetrahedral species are preferably formed when the impregnation solution of higher pH (8.6) is used.

Raman spectra and infrared spectra provide some informations about molybdenum-oxygen bonds. The supports like Al_2O_3 and SiO_2 have intense background absorptions below 1000 cm^{-1} in their IR spectra. When Mo-O-Mo bonds exist, the Mo species are likely to form two or three dimensional aggregates. In the Raman spectra, the bands attributed to Mo-O-Mo bond vibrations appear at $850 - 700\text{ cm}^{-1}$ (antisymmetric), $600 - 400\text{ cm}^{-1}$ (symmetric) and $250 - 200\text{ cm}^{-1}$ (deformation). Jeziorowski and Knözinger [3] have reported from their observations on Raman spectra that the polymerization of the isolated tetrahedral species through the Mo-O-Mo bridges occurs during drying and calcination of the molybdates impregnated on alumina. They found that the degree of this polymerization depended on the Mo content and the temperature of calcination. These results are consistent with the UV studies by Giordano et al. [7]. On titania supports, as long as the loading was below a monolayer coverage, no Raman band attributed to MoO_3 was observed when the catalyst was prepared by the incipient impregnation method [1-B].

In recent years, extended X-ray absorption fine structure (EXAFS) has been applied to solid catalysts. It provides the local structure of any atom in amorphous materials. Clausen et al. [23] have measured the EXAFS of Mo atoms in calcined and

sulfided $\text{MoO}_3/\text{Al}_2\text{O}_3$. In the Fourier transforms of these EXAFS, there appeared only one peak ($R = \text{ca. } 1.73 \text{ \AA}$) with the calcined sample and two peaks ($R = \text{ca. } 1.90, 2.86 \text{ \AA}$) with the sulfided sample. They have suggested that the Mo species before sulfidation have a highly disordered structure and that the ordering takes place to form MoS_2 like structure during the sulfidation.

Thus a lot of studies have been performed with various MoO_3 supported catalysts. However, a lot of ambiguity about the nature of molybdenum remains unsolved. For the detailed study on the catalytic properties of molybdenum, the MoO_3 supported catalysts have three disadvantages as follows;

- 1) The surface Mo species are heterogeneous. Three or four kinds of species coexist and their proportion changes in relation to the impregnation condition and the content of molybdenum.
- 2) The aggregation of molybdenum occurs through the formation of Mo-O-Mo bonds.
- 3) The oxidation state of molybdenum cannot be altered widely. It is difficult to obtain the molybdenum species with the oxidation number less than +4.

In order to overcome these disadvantages, new type molybdenum supported catalysts have been expected to be developed.

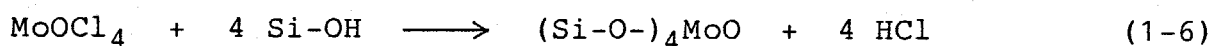
1-2-2 New molybdenum supported catalysts

To clarify the catalytic properties of molybdenum, some new molybdenum catalysts have been investigated. These catalysts have been prepared by using molybdenum complexes or compounds instead of the molybdates which are used for the preparation of

the MoO₃ supported catalysts. I review the new molybdenum catalysts, dividing this section into three parts, that is, the first part for the catalysts from MoCl₅, the second from molybdenum π-allyl complexes, and the third from Mo(CO)₆.

(A) Molybdenum catalysts prepared from MoCl₅

Dai and Lunsford [24] have prepared molybdenum supported Y-type zeolites by using a solid-solid cation exchange between MoCl₅ and HY or ultrastable HY zeolites. MoCl₅ was mechanically mixed with the zeolite followed by heating in flowing He at 400 °C. During the mixing in air much of the MoCl₅ was transformed into MoOCl₄ and the following reaction occurred by the heat treatment;



From the XPS spectra, they found that Mo(VI) was the main Mo species and that molybdenum was not concentrated on the outer surface of the zeolite crystallites. From X-ray diffraction studies, not so severe destruction of the zeolite framework structure was found to occur, and they have suggested that molybdenum is located at the cation exchange site of S_{II}.

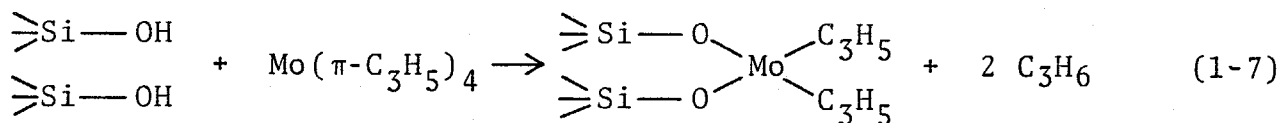
Johns and Howe [25] have prepared molybdenum supported mordenites by the vapour phase adsorption of MoCl₅ into H-mordenite. The MoCl₅ vapour was introduced into the dehydrated H-mordenite and the mixture was subsequently heated to decompose MoCl₅. After the decomposition at 100 °C, about 30 % of the total molybdenum was detected as Mo(V) in ESR spectra. They have

inferred that the other Mo species are Mo(V) dimers inactive for ESR. The maximum content of molybdenum corresponded to 6 wt% of Mo. The Mo species seemed to be located in the side pockets of the mordenite because the adsorption capacity of the mordenite did not change significantly.

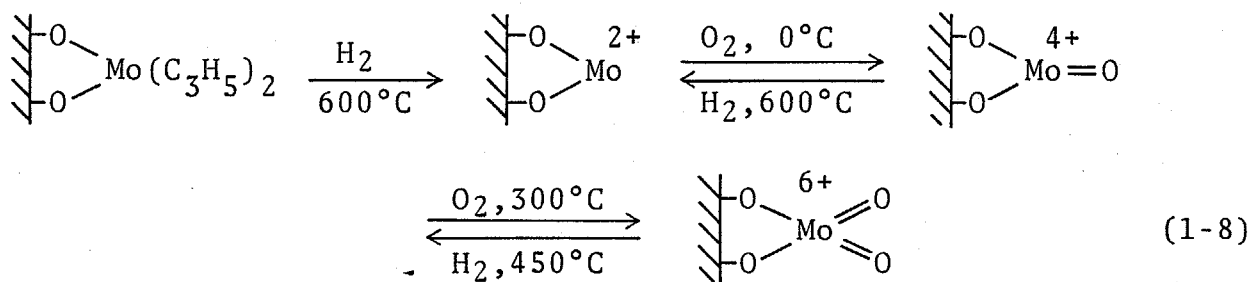
These two molybdenum supported zeolites have the advantage to limiting the aggregation of molybdenum, if the Mo species are distributed at the specific sites within the zeolite pores. However, it seems difficult to control the oxidation state of molybdenum widely, since the oxidation number of molybdenum in the starting materials is high (+5 and +6) like MoO₃ supported catalysts.

(B) Molybdenum catalysts prepared from π -allyl complexes

The SiO₂-supported molybdenum catalysts have been prepared by a ready reaction between molybdenum π -allyl complex and surface OH groups of the supports [26]. The pentane solution of Mo(π -C₃H₅)₄ was added to the precalcined SiO₂ under argon atmosphere at 20°C. Through the reaction as described below, molybdenum was supported on SiO₂ surface;



Additional H₂ treatments and O₂ treatments converted the Mo species as follows [26];

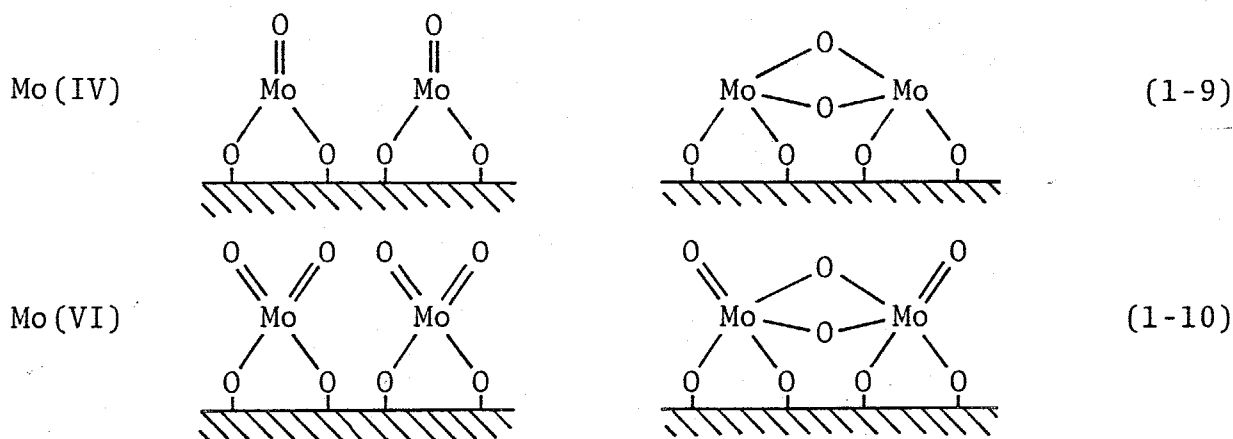


Individual steps were determined from the amount of H₂ or O₂ consumed during each step by the volumetrical measurements. In the case of alumina supports, molybdenum was supported in the same manner as silica supports except that the reduction of Mo(VI) directly converted it into Mo(II) [27]. Among above Mo species, Mo(VI) species were characterized as follows;

- a) Mo 3d_{5/2} binding energies observed in XPS spectra were higher than 232.6 eV indicating the existence of Mo(VI) [27].
- b) The IR band at 916 cm⁻¹ was attributed to the tetrahedral Mo(VI) species with two terminal O²⁻ [28].
- c) From the photoluminescence study, there existed only one kind of emitting Mo(VI) species, while two different emitting Mo(VI) species were found in MoO₃/SiO₂ prepared by the conventional impregnation method. This result indicates that the Mo(VI) species prepared from Mo(π -C₃H₅)₄ are homogeneous [27].

In this catalyst system, molybdenum is supported via the reaction between the π -allyl complex and the surface OH groups of the support. Consequently, it is suggested that rather high and homogeneous dispersion of molybdenum is obtained. In addition, the oxidation state of molybdenum could be easily altered down to Mo(II). However, the homogeneity of the Mo species may be reduced at the higher content of molybdenum.

Iwasawa et al. have prepared the supported Mo-pair catalysts using $\text{Mo}_2(\eta\text{-C}_3\text{H}_5)_4$ as a molybdenum source and alumina [29] or silica [30] as a support. Molybdenum was supported by the reaction between the complex and the support in the similar manner to the preparation process of the mononuclear catalysts from $\text{Mo}(\pi\text{-C}_3\text{H}_5)_4$. In this reaction, one complex molecule reacted with four adjacent OH groups on the support to form a Mo-pair with a Mo-Mo distance of ca. 3.3 Å, which was estimated from the EXAFS studies. Similar oxidation and reduction procedures which were carried out on the mononuclear catalysts produced reversibly Mo(II), Mo(IV), Mo(V) and Mo(VI). From the UV spectra and EXAFS study, they proposed two different structures for Mo(IV) and Mo(VI);



(C) Molybdenum catalysts prepared from $\text{Mo}(\text{CO})_6$

The preparation of molybdenum supported catalysts from $\text{Mo}(\text{CO})_6$ and Al_2O_3 , SiO_2 , ZnO , MgO or Y zeolites have been reported. The methods for the preparation of these catalysts involve two processes, that is, the attachment of $\text{Mo}(\text{CO})_6$ on the support and the decomposition of the attached $\text{Mo}(\text{CO})_6$. Two

procedures have been adapted for the first process;

a) The impregnation procedure with benzene or pentane solution of $\text{Mo}(\text{CO})_6$.

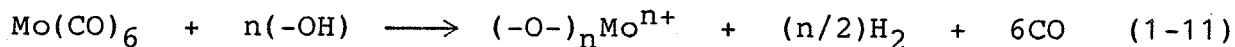
b) The adsorption of $\text{Mo}(\text{CO})_6$ on the support by contacting $\text{Mo}(\text{CO})_6$ vapour.

IR spectra of the adsorbed $\text{Mo}(\text{CO})_6$ had some additional bands to those observed for gas phase $\text{Mo}(\text{CO})_6$, which indicated the existence of the adsorbed species strongly interacting with the supports [31,32].

The procedure for the second process, that is, the decomposition of the attached $\text{Mo}(\text{CO})_6$, has been performed by heating in vacuo or in flowing He or H_2 . The heat treatment at 100 - 150°C produced the relatively stable subcarbonyl species. The adsorbed subcarbonyl, $\text{Mo}(\text{CO})_3$ (ads), was proposed to be the stable subcarbonyl on Al_2O_3 [32 - 35] or ZnO [36] from IR studies or the measurement of the eliminated CO. On HNa-Y zeolites, $\text{Mo}(\text{CO})_4$ (ads) was proposed as the subcarbonyl species [2,37,38]. Abdo and Howe [39] have reported from ESR studies that subcarbonyl species with the dimer structure, $\text{Mo}_2(\text{CO})_{10}^-$, are also contained in Mo/HNa-Y. However, on SiO_2 supports, no stable subcarbonyl was detected [40 - 43].

These subcarbonyl species were reversibly converted into $\text{Mo}(\text{CO})_6$ (ads) by contacting with CO gas [34]. However, there occurred the irreversible decomposition of the subcarbonyl species at the higher temperature. H_2 and methane were formed during this irreversible decomposition. Therefore, it has been considered that the oxidation of molybdenum by the surface hydro-

xyl groups of the support takes place as follows [33,37,42];



The IR absorption bands due to the surface OH groups decreased in intensity during this decomposition, which was also the evidence for the reaction (1-11) [32,37]. The oxidation state of Mo^{n+} formed on the support has been reported by several investigators. In the case of alumina supports, the oxidation state estimated from the amount of H_2 formed during the decomposition varied with the decomposition temperature [33]. When the alumina dehydroxylated at 950°C was used as a support, the average oxidation number of molybdenum which was determined by an O_2 titration method was +0.3 [44]. In this catalyst, $\text{Mo}(0)$ atoms were thought to aggregate on $\text{Mo}(\text{II})$ to form a cluster of about 40 Å in diameter. Whan et al. [45] have measured the XPS spectra to determine the oxidation state of molybdenum. They found that the binding energy of $\text{Mo } 3d_{5/2}$ shifted to the higher region by about 1 eV during the decomposition of Mo(CO)_6 . This is the evidence of the oxidation of $\text{Mo}(0)$, but they did not refer to the oxidation number of Mo after the decomposition. Abdo and Howe [39] have detected a significant amount of $\text{Mo}(\text{V})$ by ESR technique after the decomposition of Mo(CO)_6 on HNa-Y zeolite, but no $\text{Mo}(\text{V})$ was detected when Na-Y zeolite was used as a support. They have suggested that molybdenum supported on Na-Y zeolite is not oxidized readily.

Thus it has been possible to vary the oxidation state of the supported molybdenum widely using the π -allyl complex or Mo(CO)_6 as a molybdenum source. In addition, the high dispersion of molybdenum can be obtained because the Mo species are sup-

ported through the reaction between the complex and the support. Consequently, the new molybdenum supported catalysts prepared from the molybdenum complexes seem to be better catalysts for the study on the catalytic properties of molybdenum than the conventional MoO_3 supported catalysts.

1-2-3 Catalytic reactions on molybdenum supported catalysts

The catalytic properties of molybdenum have been studied with the various molybdenum supported catalysts mentioned in the previous section (1-2-2). The new catalysts prepared from the molybdenum complexes are revealed to have higher activity than that of the conventional MoO_3 supported catalysts for several reactions. The oxidation state of the active Mo species for these reactions has been investigated. In this section, I refer to what kind of Mo species are active for each reaction.

(A) Olefin metathesis

Since the metathesis of olefin was reported first by Banks and Bailey [46] with $\text{Mo}(\text{CO})_6/\text{Al}_2\text{O}_3$ catalysts, many investigations have been performed on various molybdenum supported catalysts.

In the case of $\text{MoO}_3/\text{Al}_2\text{O}_3$, the reduction of calcined catalysts has generated the activity for the propylene metathesis. Nakamura et al. [47] have reported that the reduction of $\text{Mo}(\text{VI})$ to Mo^{n+} ($n < 5$) causes the higher activity compared with the parent $\text{Mo}(\text{VI})$. However, the oxidation state of the active Mo species was not determined clearly, probably because the surface Mo species were rather heterogeneous. Hardee and Hightower [48]

have measured the amount of NO which is necessary to poison completely the reduced Co-Mo/Al₂O₃. They found that at most 14 % of the total molybdenum was the active site. The similar result has been reported by Giordano et al. [49]. They have studied the relation between the Mo(V) ESR signal and the activity for propylene metathesis by using the reduced MoO₃/Al₂O₃ and suggested that the active site is a Mo(V) pair whose structure is [OMo-O-MoO]⁴⁺.

Many investigations have been carried out also on the catalysts prepared from Mo(CO)₆. On the whole, these catalysts are more active than the MoO₃ supported catalysts. For example, Howe and Kemball [50] have reported that the catalyst prepared by the decomposition of Mo(CO)₆/SiO₂ at 200°C is about 200 fold as active as Co-Mo/Al₂O₃ catalysts for the propylene metathesis. Howe et al. [41] have found that the completely decarbonylated species on alumina are more active for the propylene metathesis than the subcarbonyl species. In the case of the silica support, the complete decomposition of Mo(CO)₆ also generated the high activity. Addition of oxygen onto the decomposed species caused the significant increase in activity with alumina as a support and the drastic decrease in activity with silica as a support. From these results, they have proposed that the active site for propylene metathesis is not Mo(0) but the Mo species of some higher oxidation state. In the case of a ZnO support, the complete decomposition of Mo(CO)₆ generated the activity for a cross metathesis of cis-2-butene-d₀ and cis-2-butene-d₈, which indicated that the active Mo species were some oxidized ones [36].

Brenner et al. [43] have found that the maximum metathesis

activity is obtained at 140°C when the temperature programmed decomposition (TPDE) of $\text{Mo}(\text{CO})_6/\text{SiO}_2$ is performed in flowing $\text{H}_2/\text{C}_3\text{H}_6$ mixture. In the TPDE experiment with flowing He, the rate of H_2 formation which resulted from the oxidation of molybdenum reached the maximum at 200°C. Consequently, the maximum activity was generated at the early stage of the oxidation of molybdenum, and the further oxidation led to the decrease in activity. They proposed the Mo(II) species to be the active site. On the other hand, Howe and Kemball [50] have proposed that the Mo(III) species is the active site because the most active catalyst prepared from $\text{Mo}(\text{CO})_6/\text{SiO}_2$ exhibits the most intense IR absorption bands attributed to $\text{Mo}^{3+}(\text{NO})$.

Thus the studies on the catalysts which consist of the Mo species in low oxidation states prepared from $\text{Mo}(\text{CO})_6$ have revealed the possibility that Mo(II) or Mo(III) is the active species for olefin metathesis in addition to Mo(IV).

In the case of the catalysts derived from π -allyl complexes, it has been reported that Mo(IV) species, especially Mo(IV) with two σ -allyl groups, are the most active for propylene metathesis [51,52]. In contrast with the results for the catalysts prepared from $\text{Mo}(\text{CO})_6$, Mo(II) and Mo(III) were much less active than Mo(IV). The dimer species prepared from the dinuclear complex were less active than the monomer species, and the activity also altered with the kind of supports (two types of silica or alumina).

(B) Olefin hydrogenation

Such metal catalysts as Ni, Pd, Pt, etc. are generally

used for the hydrogenation of olefin, while among oxides, Cr_2O_3 is known to be active. Molybdenum containing catalysts are not so much active as these catalysts. However, the studies of the olefin hydrogenation on molybdenum supported catalysts have been performed by many workers to know the catalytic properties of molybdenum.

From the studies on $\text{MoO}_3/\text{Al}_2\text{O}_3$ catalysts, the activity for propylene hydrogenation usually increases with increasing the extent of reduction. Millman and Hall [53] have found that the hydrogenation activity of the reduced $\text{MoO}_3/\text{Al}_2\text{O}_3$ is in proportion to the amount of chemisorbed oxygen at -78°C . Because the chemisorption of oxygen was believed to occur at the coordinatively unsaturated site (CUS) on Mo(IV), they have proposed that this CUS on Mo(IV) is the active site for propylene hydrogenation. Hall and Millman [54] and Lombardo et al. [55] have measured the amount of NO which completely poisons the hydrogenation of propylene. They have suggested that a few percent of the total molybdenum is the active site.

For the hydrogenation of ethylene, the activity increased also with increasing the extent of reduction on $\text{MoO}_3/\text{Al}_2\text{O}_3$, so that the CUS on Mo(IV) was believed to be the active site [56]. While for the hydrogenation of cis-2-butene, the reduction of Mo(VI) in $\text{MoO}_3/\beta\text{-TiO}_2$ to Mo(IV) generated the activity, and further reduction increased this activity [1-A]. This indicates that the Mo species with the oxidation number of less than +4 is the active site.

In the case of the catalyst prepared from $\text{Mo}(\text{CO})_6$, the activity for the ethylene hydrogenation reached the maximum when

$\text{Mo}(\text{CO})_6$ adsorbed on alumina was decomposed at 200 - 300°C in flowing $\text{H}_2/\text{C}_3\text{H}_6$ mixture [57]. In this temperature range, parts of the CO ligands were eliminated. Above 300°C, the oxidation of molybdenum occurred, which was evidenced by the formation of hydrogen. It has been considered that the subcarbonyl species which is not oxidized at all is the active site.

In the case of the catalysts prepared from the π -allyl complexes, Mo(II) species, especially with dimer structure, exhibited the higher activity than the Mo species whose oxidation numbers were +4 or +6 [58]. The initial activity of this most active catalyst was 10 fold as higher as $\text{MoO}_3/\text{SiO}_2$ catalysts prepared by the conventional impregnation method. It has been concluded that the active site is Mo(II).

Thus in any kind of molybdenum supported catalysts, the lower oxidation state of molybdenum leads to the higher activity for the hydrogenation of olefin.

(C) Ethylene polymerization

For the polymerization of ethylene, the studies by using reduced $\text{MoO}_3/\text{Al}_2\text{O}_3$ catalysts have been reported. Morris et al. [59] have measured the amount of Mo(V) from the ESR spectra and found that the activity increases with increasing the amount of Mo(V). They have proposed that the Mo(V) species are the active sites. Hashimoto et al. [60] have also measured the ESR spectra and identified three different Mo(V) species on the reduced $\text{MoO}_3/\text{Al}_2\text{O}_3$. The activity for the ethylene polymerization was measured with the catalysts of various Mo contents and of various extents of reduction. The activity was in good correspondence

with the amount of the specific Mo(V) which was soluble in water. This Mo(V) species were believed to be the active site for the ethylene polymerization.

(D) Miscellaneous reactions

It has been reported that the catalysts derived from $\text{Mo}(\text{CO})_6$ are active for the methanation. Brenner and Hucul [42] have measured the methanation activity of the catalyst prepared by the decomposition of $\text{Mo}(\text{CO})_6/\text{Al}_2\text{O}_3$ at about 200°C . This activity was about 1000 fold as active as that measured after the oxidation to Mo(VI) and was about 20 fold as active as that measured after the additional reduction on the Mo(VI). When alumina dehydroxylated at 950°C was used as a support, the initial activity was higher than the activity measured by using partially dehydroxylated alumina as a support [44]. The active species for the methanation were suggested to be the molybdenum in low oxidation states.

In the case of the hydrogenolysis of propane, the catalyst prepared from $\text{Mo}(\text{CO})_6$ and highly dehydroxylated alumina exhibited the high activity [61]. The Mo species in low oxidation states were believed to be the active species as in the case of the methanation. MoO_3 supported catalysts, especially with Co as a promoter, are used for the hydrodesulfurization. To generate the activity, these catalysts are usually sulfided with H_2S , CS_2 , thiophene, etc.. Therefore, the active species are thought to be MoS_2 crystallites or a kind of molybdenum oxysulfides which are different from the active species for the reactions mentioned previously in this section.

As described above, the different Mo species are proposed

to be the active site for the same reaction when the different kind of catalysts are used. Therefore, any definite conclusions have not been drawn as to what is the active site for each reaction. Generally speaking, however, the new type catalysts prepared from molybdenum complexes seem more active than the conventional impregnation catalysts such as $\text{MoO}_3/\text{Al}_2\text{O}_3$.

1-3 Purpose of this study

As mentioned in the previous sections, in order to clarify the catalytic properties of molybdenum, many studies on the nature of some new type molybdenum supported catalysts have been performed in addition to those on the conventional MoO_3 supported catalysts. These new catalysts generally exhibit higher activities for many reactions than the conventional catalysts. Besides, the conclusion as to the active Mo species differs with the kind of the catalysts used in the studies. I consider that this difference results from four reasons as follows;

- 1) The range of the oxidation state of molybdenum which can be controlled by changing the preparation conditions varies with the kind of catalysts.
- 2) The dispersion of molybdenum varies with the preparation conditions as well as with the kind of catalysts.
- 3) The chemical and morphological nature of the surface varies with the kind of supports.
- 4) Several different Mo species often coexist in a catalyst.

In order to obtain the clear conclusions as to the catalytic

properties of molybdenum, it is important to choose a molybdenum source and a support taking account of the effects which are induced by these reasons.

In this study, taking account of the oxidation state (reason 1), I used $\text{Mo}(\text{CO})_6$ as a molybdenum source which has a certain advantage in varying the oxidation state of molybdenum widely because it consists of $\text{Mo}(0)$. In addition, the dispersion of molybdenum (reason 2) is expected to be high because the molybdenum is supported through a reaction between $\text{Mo}(\text{CO})_6$ and the surface of the support. It is also expected that homogeneous Mo species (reason 4) can be obtained by controlling this reaction.

I used Y-type zeolite as a support. Zeolites have some definite framework structure, so that the nature of the surface is not so complicated as that of amorphous oxides (reason 3). The high dispersion of molybdenum is likely to be obtained because the framework structure of zeolites consists of small and uniform pores. Usually, transition metal cations can be anchored in the framework of zeolites by ion exchange methods with aqueous solutions of the metal salts. However, molybdenum is unstable in a cationic form in water, so that ordinary ion exchange methods with aqueous solutions cannot provide molybdenum supported zeolites. The only exception using an aqueous solution of $\text{Mo}_2(\text{en})_4\text{Cl}_4$ (en: ethylenediamine) has been reported [38,62]. However, the preparation in the presence of water may result in the oxidation of molybdenum, so that the Mo species in low oxidation state can hardly be formed by this method. Another example of the ion exchange is the method using a solid-solid cation

exchange with MoCl_5 and H-Y zeolite [24]. Because Mo(V) was used as a molybdenum source, only the Mo species of high oxidation states were obtained.

The preparation method of molybdenum supported Y zeolite from $\text{Mo}(\text{CO})_6$ and HNa-Y has been reported by Gallezot et al. [37]. The characterization of Mo/HNa-Y zeolites prepared by this method has been performed [31,38,39]. However, the catalytic properties of the supported Mo species have not been investigated, so that the relation between the nature of the Mo species and their catalytic activity are not clear.

In this study, I prepared molybdenum supported Y zeolites (Mo/HNa-Y) by using $\text{Mo}(\text{CO})_6$ and HNa-Y zeolites, and carried out some experiments and discussion with two purposes as follows;

- 1) To prepare the Mo species of various oxidation states and make them clearly defined species through some characterizations.
- 2) To clarify the relation between the nature of the Mo species and their catalytic activity for some reactions.

References

- 1 (A) K. Tanaka, K. Miyahara and K. Tanaka, *J. Mol. Catal.*, 15, 133 (1982); K. Tanaka, K. Miyahara and K. Tanaka, *Proc. 7th Intern. Congr. Catal*, (Tokyo, 1980), P. 1318
(B) K. Y. S. Ng and E. Gulari, *J. Catal.*, 92, 340 (1985)
- 2 (A) I. Balakrishnan, S. G. Hegde, B. S. Rao, S. B. Kulkarni and P. Ratnasamy, *Proc. 4th Intern. Conf. Chemistry and Uses of Molybdenum*, (Golden, 1982), P. 331
(B) W. W. Swanson, B. J. Streusand and G. A. Tsigdinos, *Proc. 4th Intern. Conf. Chemistry and Uses of Molybdenum*, (Golden, 1982), P. 323
(C) P. Kovacheva, N. Davidova and D. Shopov, *Zeolites*, 3, 92 (1983)
(D) R. Cid, F. J. G. Llambias, J. L. G. Fierro, A. L. Agudo and J. Villasenor, *J. Catal.*, 89, 478 (1984)
- 3 H. Jeziorowski and H. Knozinger, *J. Phys. Chem.*, 83, 1166 (1979)
- 4 L. Wang and W. K. Hall, *J. Catal.*, 66, 251 (1980)
- 5 D. S. Zingg, L. E. Makovsky, R. E. Tischer, F. R. Brown and D. M. Hercules, *J. Phys. Chem.*, 84, 2898 (1980)
- 6 A. I. Vagin, V. I. Erofeev and I. V. Kalechits, *React. Kinet. Catal. Lett.*, 21, 299 (1982)
- 7 N. Giordano, J. C. J. Bart, A. Vaghi, A. Castellan and G. Martinotti, *J. Catal.*, 36, 81 (1975)
- 8 J. Medema, C. Van Stam., V. H. J. de Beer, A. J. A. Konings and D. C. Koningsberger, *J. Catal.*, 53, 386 (1978)

- 9 H. Weigold, *J. Catal.*, 83, 85 (1983)
- 10 T. Fransen, O. van der Meer and P. Mars, *J. Catal.*, 42, 79 (1976)
- 11 W. S. Millman, M. Crespin, A. C. Cirillo, Jr., S. Abdo and W. K. Hall, *J. Catal.*, 60, 404 (1979)
- 12 F. E. Massoth, *J. Catal.*, 30, 204 (1973)
- 13 J. B. Perl, *J. Phys. Chem.*, 86, 1615 (1982)
- 14 M. Houalla, C. L. Kibby, L. Petrakis and D. M. Hercules, *J. Catal.*, 83, 50 (1983)
- 15 K. S. Seshadri and L. Petrakis, *J. Catal.*, 30, 195 (1973)
- 16 L. Petrakis, P. L. Meyer and T. P. Debies, *J. Phys. Chem.*, 84, 1020 (1980)
- 17 W. K. Hall and M. L. Jacono, *Proc. 6th Intern. Congr. Catal.*, (London, 1976), P. 246
- 18 T. A. Patterson, J. C. Carver, D. E. Leyden and D. M. Hercules, *J. Phys. Chem.*, 80, 1700 (1976)
- 19 S. Abdo, R. B. Clarkson and W. K. Hall, *J. Phys. Chem.*, 80, 2431 (1976); S. Abdo, A. Kazusaka and R. F. Howe, *ibid.*, 85, 1380 (1981)
- 20 C. P. Li and D. M. Hercules, *J. Phys. Chem.*, 88, 456 (1984)
- 21 M. Che, F. Figueras, M. Forissier, J. McAteer, M. Perrin, J. L. Portefaix and H. Praliaud, *Proc. 6th Intern. Congr. Catal.*, (London, 1976), Vol. 1, P. 261
- 22 L. Wang and W. K. Hall, *J. Catal.*, 77, 232 (1982)
- 23 B. S. Clausen, H. Topsoe, R. Candia, J. Villadsen, B. Lengeler, J. Als-Nielsen and F. Christensen, *J. Phys. Chem.*, 85, 3868 (1981)
- 24 P.-S. E. Dai and J. H. Lunsford, *J. Catal.*, 64, 173 (1980)

- 25 J. R. Johns and R. F. Howe, *Zeolites*, 5, 251 (1985)
- 26 Y. I. Yermakov and B. N. Kuznetsov, *Prepr. 2nd Japan-Soviet Catalysis Seminar, (Tokyo, 1973)*, P. 65
- 27 Y. Iwasawa and S. Ogasawara, *J. Chem. Soc., Faraday Trans. I*, 75, 1465 (1979)
- 28 Y. Iwasawa, Y. Nakano and S. Ogasawara, *J. Chem. Soc., Faraday Trans. I*, 74, 2968(1978)
- 29 Y. Iwasawa, Y. Sato and H. Kuroda, *J. Catal.*, 82, 289 (1983)
- 30 Y. Iwasawa and M. Yamagishi, *J. catal.*, 82, 373 (1983)
- 31 S. Abdo and R. F. Howe, *J. Phys. Chem.*, 87, 1713 (1983)
- 32 A. Kazusaka and R. F. Howe, *J. Mol. Catal.*, 9, 183 (1980)
- 33 A. Brenner and R. L. Burwell, Jr., *J. Catal.*, 52, 353 (1978)
- 34 A. Brenner and R. L. Burwell, Jr., *J. Am. Chem. Soc.*, 97, 2565 (1975)
- 35 T. L. Brown, *J. Mol. Catal.*, 12, 41 (1981)
- 36 K. Tanaka, Y. Zhai and K. Aomura, *Proc. 4th Intern. Conf. Chemistry and Uses of Molybdenum, (Golden, 1982)*, P. 278
- 37 P. Gallezot, G. Coudurier, M. Primet and B. Imelik, *ACS Symp. Ser., No. 40*, 144 (1977)
- 38 M. B. Ward and J. H. Lunsford, *Proc. 6th Intern. zeolite Conf., (Reno, 1983)*, P. 405
- 39 S. Abdo and R. F. Howe, *J. Phys. Chem.*, 87, 1722 (1983)
- 40 R. F. Howe, *Inorg. Chem.*, 15, 486 (1976)
- 41 R. F. Howe, D. E. Davidson and D. A. Whan, *J. Chem. Soc., Faraday Trans. I*, 68, 2266 (1972)
- 42 A. Brenner and D. A. Hucul, *Proc. 3rd Intern. Conf. Chemistry and Uses of Molybdenum, (Ann Arbor, 1979)*, P. 194

- 43 A. Brenner, D. A. Hucul and S. J. Hardwick, *Inorg. Chem.*, 18, 1478 (1979)
- 44 R. G. Bowman and R. L. Burwell, Jr., *J. Catal.*, 63, 463 (1980)
- 45 D. A. Whan, M. Barber and P. Swift, *J. Chem. Soc., Chem. Comm.*, 198 (1972)
- 46 R. L. Banks and G. C. Bailey, *Ind. Eng. Chem., Prod. Res. Develop.*, 3, 170 (1964)
- 47 R. Nakamura, Y. Morita and E. Echigoya, *Nippon Kagaku Kaishi* (1973) P. 244
- 48 J. R. Hardee and J. W. Hightower, *J. Catal.*, 83, 182 (1983)
- 49 N. Giordano, M. Padovan, A. Vaghi, J. C. J. Bart and A. Castellan, *J. Catal.*, 38, 1 (1975)
- 50 R. F. Howe and C. Kemball, *J. Chem. Soc., Faraday Trans. I*, 70, 1153 (1974)
- 51 Y. I. Yermakov, B. N. Kuznetzov, Y. P. Grabovski, A. N. Startzev, A. M. Lazutkin, V. A. Zakharov and A. I. Lazutkina, *J. Mol. Catal.*, 1, 93 (1975/76); B. N. Kuznetsov, A. N. Startsev and Y. I. Yermakov, *ibid.*, 8, 135 (1980)
- 52 Y. Iwasawa, H. Ichinose, S. Ogasawara and M. Soma, *J. Chem. Soc., Faraday Trans. I*, 77, 1763 (1981); Y. Iwasawa, H. Kubo and H. Hamamura, *J. Mol. catal.*, 28, 191 (1985)
- 53 W. S. Millman and W. K. Hall, *J. Catal.*, 59, 311 (1979)
- 54 W. K. Hall and W. S. Millman, *Proc. 7th Intern. Congr. Catal.*, (Tokyo, 1980) P. 1304
- 55 E. A. Lombardo, M. L. Jacono and W. K. Hall, *J. Catal.*, 64, 150 (1980)
- 56 E. A. Lombardo, M. Houalla and W. K. Hall, *J. Catal.*, 51, 256

(1978)

- 57 A. Brenner, *J. Mol. Catal.*, 5, 157 (1979)
- 58 Y. Iwasawa, M. Yamagishi and S. Ogasawara, *J. Chem. Soc., Chem. Comm.*, 871 (1980)
- 59 R. V. Morris, D. R. Waywell and J. w. Shepard, *J. Less - Common Metals*, 36, 395 (1974)
- 60 K. Hashimoto, S. Watanabe and K. Tarama, *Bull. Chem. Soc. Japan*, 49, 12 (1976)
- 61 R. Nakamura, R. G. Bowman and R. L. Burwell, Jr., *J. Am. Chem. Soc.*, 103, 673 (1981); R. Nakamura, D. Pioch, R. G. Bowman and R. L. Burwell, Jr., *J. Catal.*, 93, 388 (1985)
- 62 M. B. Ward, K. Mizuno and J. H. Lunsford, *J. Mol. Catal.*, 27, 1 (1984)

Chapter 2 Preparation of Mo/HNa-Y

2-1 Introduction

The preparation of molybdenum supported Y zeolites using $\text{Mo}(\text{CO})_6$ as a molybdenum source has been reported by Gallezot et al. [1]. They adsorbed $\text{Mo}(\text{CO})_6$ on HNa-Y zeolite by contacting HNa-Y with the $\text{Mo}(\text{CO})_6$ vapour, and subsequently decomposed the adsorbed $\text{Mo}(\text{CO})_6$ by heating in vacuo to form the Mo/HNa-Y zeolite. The similar method has been adapted with alumina supports [2]. The other method using $\text{Mo}(\text{CO})_6$ is the impregnation method with an organic solvent such as pentane as mentioned previously on alumina supports (1-2-2). When the characterization of the supported molybdenum is carried out with an in situ technique, the impregnation method sometimes cannot be applied, since the use of solvents is prohibited in many kinds of spectroscopic instruments. The preparation using the adsorption of $\text{Mo}(\text{CO})_6$ in vacuo is preferable from this point of view and is advantageous to preventing the catalyst from hydrocarbon contaminations.

Taking into account these considerations, I prepared the molybdenum supported HNa-Y zeolite (Mo/HNa-Y) using the adsorption of $\text{Mo}(\text{CO})_6$. The preparation procedure was designed based on that reported by Gallezot et al. [1]. In this chapter, I discuss the details of the preparation of Mo/HNa-Y and the loading behaviour of molybdenum on HNa-Y zeolites.

2-2 Experimental

2-2-1 Materials

Na-Y zeolites (Toyo Soda Ind. Co., Lot Y-30; unit cell composition: $\text{Na}_{49.5}\text{Al}_{49.5}\text{Si}_{142.5}\text{O}_{384}\cdot 233\text{H}_2\text{O}$) were treated with NH_4Cl aqueous solution to form $\text{NH}_4\text{Na-Y}$. After calcination at 470°C in air, $\text{H}(x)\text{Na-Y}$ was obtained, where x is the percent degree of proton exchange. Na-Y was washed with pure water, followed by drying at 120°C in air. Table 2 shows the conditions of NH_4^+ exchange and the specific surface areas of $\text{H}(x)\text{Na-Y}$ with x of 0 - 82 %. The content of sodium in $\text{H}(x)\text{Na-Y}$ was determined by flame emission spectroscopy.

$\text{Mo}(\text{CO})_6$ (Soekawa Chemical Co. Ltd.) was used without further purification.

2-2-2 Preparation of Mo/HNa-Y

The preparation procedure of Mo/HNa-Y zeolites which was designed based on the procedure reported by Gallezot et al. [1] is as follows. A specific amount of HNa-Y placed in a quartz tube was heated in vacuo at various temperatures to yield dehydrated HNa-Y. The desired amount of $\text{Mo}(\text{CO})_6$ was added to the dehydrated HNa-Y under nitrogen or argon atmosphere. After the nitrogen or argon was pumped out for 20 s, the tube was put in a thermostatted oven at 60°C and allowed to stand for 15 h to adsorb $\text{Mo}(\text{CO})_6$ on HNa-Y. Mo/HNa-Y was obtained by heating $\text{Mo}(\text{CO})_6/\text{HNa-Y}$ in vacuo at various temperatures.

The content of molybdenum in the Mo/HNa-Y was determined by atomic absorption spectroscopy.

2-2-3 Infrared spectroscopy

Infrared spectra were measured with Mo/HNa-Y prepared by

Table 2
 Ion exchange conditions and surface areas of Y zeolites

| Zeolite | Concentration of NH_4Cl aqueous solution/N | Temperature of ion exchange/ $^{\circ}\text{C}$ | Surface area / $\text{m}^2 \cdot \text{g}^{-1}$ |
|-----------|--|---|---|
| Na-Y | — | — | 942 |
| H(14)Na-Y | 0.05 | 25 | 933 |
| H(36)Na-Y | 0.05 | 25 | 947 |
| H(65)Na-Y | 0.05 | 25 | 884 |
| H(74)Na-Y | 0.05 | 60 | 779 |
| H(82)Na-Y | 0.5 | 60 | 690 |

using a self-supporting wafer of HNa-Y as a support. The HNa-Y wafer was placed in the quartz IR cell with KBr windows. The Mo/HNa-Y sample was prepared in situ from the HNa-Y wafer and $\text{Mo}(\text{CO})_6$. The IR spectra were measured at room temperature in each stage of the preparation on the Hitachi EPI G3 spectrometer.

2-2-4 Temperature programmed decomposition

Temperature programmed decomposition of $\text{Mo}(\text{CO})_6$ adsorbed on HNa-Y zeolite was carried out with a vacuum system. $\text{Mo}(\text{CO})_6$ /HNa-Y was heated in vacuo from 25 to 500°C at a heating rate of 2°C/min. CO (m/e = 28), H_2 (m/e = 2) and methane (m/e = 15) evolved during this heat treatment were monitored on the quadrupole mass spectrometer (ULVAC, MSQ-150A).

2-2-5 X-ray photoelectron spectroscopy (XPS)

The Mo/HNa-Y samples for X-ray photoelectron spectroscopic studies were prepared by using HNa-Y tablets. The loading of molybdenum and subsequent treatments were carried out in a Pyrex tube and the sample was then sealed in vacuo. The sample tablet was placed in the sample holder of the XPS apparatus under argon atmosphere. XPS spectra of Mo 3d and Si 2p regions were measured on the Shimadzu ESCA 750 spectrometer with $\text{Mg K}_{\alpha 1,2}$ X-rays (1253 eV) used as the exciting source.

2-3 Results and discussion

2-3-1 Adsorption and decomposition of $\text{Mo}(\text{CO})_6$

$\text{Mo}(\text{CO})_6$ is a volatile solid and has the vapour pressure of about 0.08 torr at room temperature [3]. Keeping the mixture of $\text{Mo}(\text{CO})_6$ and the dehydrated HNa-Y in vacuo caused the adsorption

of the volatilized $\text{Mo}(\text{CO})_6$ molecules on HNa-Y. The IR study was performed to observe the adsorbed $\text{Mo}(\text{CO})_6$ molecules. The result is shown in Fig. 1 (b). Intense absorption bands attributed to the CO stretching vibration appeared at 1900 - 2000 cm^{-1} . The IR spectra of gaseous $\text{Mo}(\text{CO})_6$ exhibited an intense band at 1996 cm^{-1} and two shoulders at 2080 and 1971 cm^{-1} . The spectrum of the $\text{Mo}(\text{CO})_6$ adsorbed on HNa-Y was slightly different from that of the gaseous molecules. Therefore, the $\text{Mo}(\text{CO})_6$ molecules are thought to be adsorbed strongly. In fact, the desorption of $\text{Mo}(\text{CO})_6$ was scarcely occurred at room temperature, which implies also the strong interaction between $\text{Mo}(\text{CO})_6$ and HNa-Y. Abdo and Howe [4] have measured the IR spectra of $\text{Mo}(\text{CO})_6/\text{HNa-Y}$ after the evacuation at various temperatures. They found the chemisorbed $\text{Mo}(\text{CO})_6$ in addition to the physisorbed $\text{Mo}(\text{CO})_6$. Their findings of the chemisorbed species are consistent with my proposal that $\text{Mo}(\text{CO})_6$ is adsorbed strongly.

Decomposition of $\text{Mo}(\text{CO})_6/\text{HNa-Y}$ at 100 °C led to the change in the spectrum (Fig. 1, c). This subcarbonyl species may be $\text{Mo}(\text{CO})_3$ (ads) taking into account the results of the temperature programmed decomposition of $\text{Mo}(\text{CO})_6/\text{H}(36)\text{Na-Y}$ mentioned later in this section. The further decomposition at 300 °C resulted in the disappearance of all carbonyl bands and the spectrum became similar to that of Fig. 1 (a). This indicates that $\text{Mo}(\text{CO})_6$ is completely decomposed up to 300 °C. Gallezot et al. [1] have measured the amount of CO evolved during the decomposition of $\text{Mo}(\text{CO})_6/\text{HNa-Y}$ and reported that six CO molecules per Mo atom are desorbed up to 300 °C. This result is consistent with the result

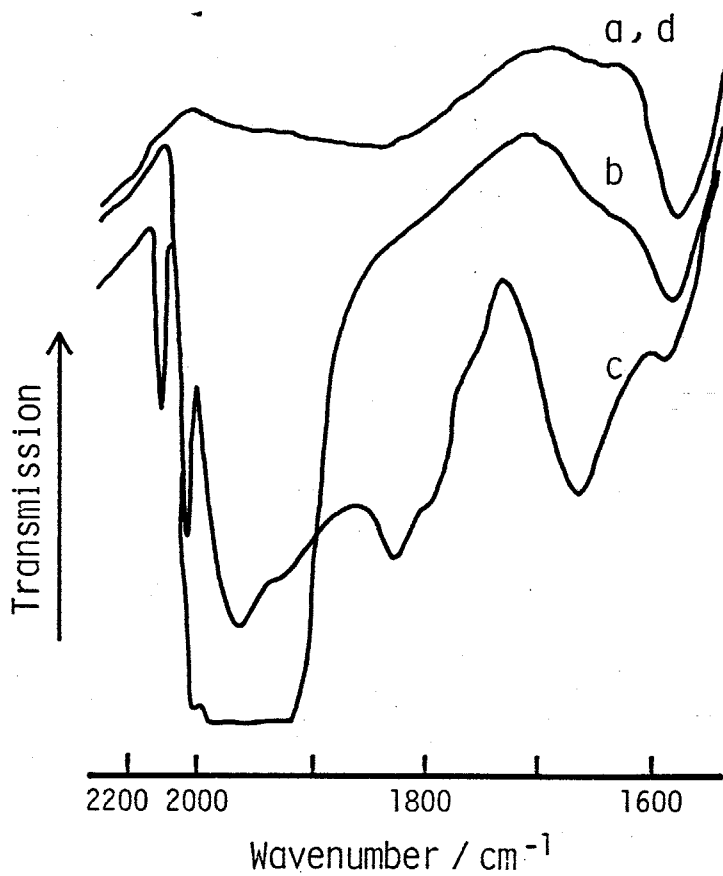
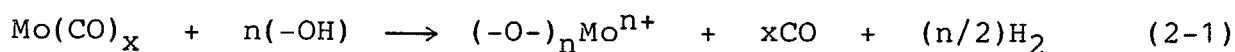


Fig. 1 IR spectra of Mo(CO)₆/H(82)Na-Y

- a: H(82)Na-Y dehydrated at 300°C for 2 h
- b: Mo(CO)₆ was added to sample a
- c: Sample b evacuated at 100°C for 10 min
- d: Sample c evacuated at 300°C for 1 h

of my IR study.

In order to clarify the decomposition process further, temperature programmed decomposition (TPDE) of $\text{Mo}(\text{CO})_6/\text{HNa-Y}$ was carried out. The TPDE curves of $\text{Mo}(\text{CO})_6/\text{H}(36)\text{Na-Y}$ are shown in Fig. 2. The curve for CO desorption had two peaks (P_1 , P_2), while the curve for the evolved H_2 or methane had a sharp peak (Q_1 or R_1) and a broad peak (Q_2 or R_2) at higher temperatures. The decarbonylation began at about 50°C and was almost completed at about 300°C . This result is in agreement with that from the IR study. At the temperature around the peak P_1 , a significant amount of H_2 was not formed and only CO was evolved. The two clearly separated CO peaks indicate that parts of the CO ligands are desorbed to form a rather stable subcarbonyl species, $\text{Mo}(\text{CO})_x$. Peak areas of the two CO peaks (P_1 and P_2) were nearly equal to each other, so that the subcarbonyl species is considered to be $\text{Mo}(\text{CO})_3$ (see Fig. 1, c). The formation of H_2 began at about 120°C and the formation curve reached the maximum at about 165°C (peak Q_1) accompanied with the other CO peak (P_2). In the case of the thermal decomposition of $\text{Mo}(\text{CO})_6$ adsorbed on alumina or silica [5] and HNa-Y [1], it has been reported that the hydrogen is formed as the result of the oxidation of molybdenum by the surface hydroxyl groups of the supports. This oxidation is expressed as follows;



It is suggested that such an oxidation of molybdenum occurs above 120°C . In addition, a certain amount of methane was formed (peak

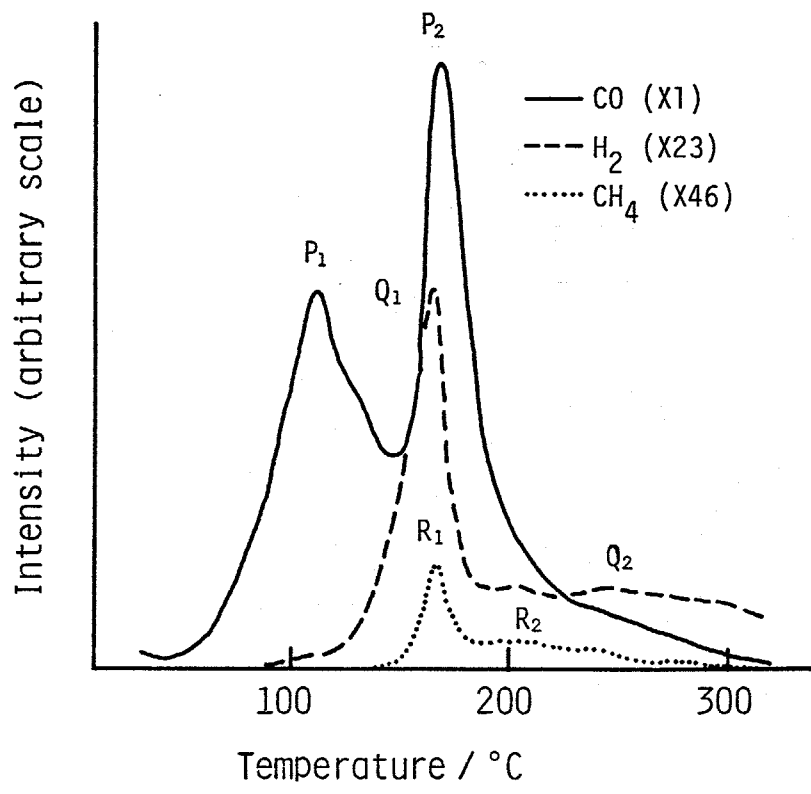
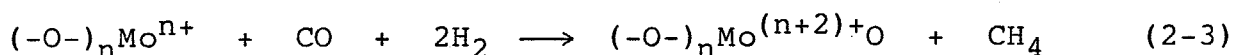


Fig. 2 Temperature programmed decomposition of Mo(CO)₆ adsorbed on H(36)Na-Y

Dehydration temperature of H(36)Na-Y: 400°C
 Mo content: 2 Mo-atoms/supercage
 Heating rate: 2 °C/min

R₁) at the similar temperature to that of the H₂ formation. This methane is produced through the reactions between H₂ and the CO ligand or the desorbed CO. These reactions can be expressed as follows [6];



Though H₂O is possibly formed in these reactions, the H₂O molecule is probably consumed to oxidize molybdenum. In any case, both reactions also cause the oxidation of molybdenum. At a higher temperature than that of peak P₂, the CO curve decreased, but the curve for H₂ formation had a broad peak at about 250°C. This indicates that further oxidation of molybdenum occurs after CO ligands are completely eliminated. This oxidation lasted above 300°C. A small amount of methane formed in the similar temperature range is probably generated from some strongly adsorbed CO.

Since the decomposition of adsorbed Mo(CO)₆ occurs with the concomitant oxidation of molybdenum by the hydroxyl groups of HNa-Y, the proton concentration of HNa-Y may affect the decomposition behaviour. Using four H(x)Na-Ys (x = 14, 36, 65 and 74) and Na-Y as supports, I obtained the TPDE curves of the adsorbed Mo(CO)₆. Figure 3 shows the profiles of CO desorption. With increasing the degree of proton exchange, P₂ peak shifted to lower temperatures and the separation between P₁ and P₂ peaks got ambiguous. This indicates that the subcarbonyl species are the

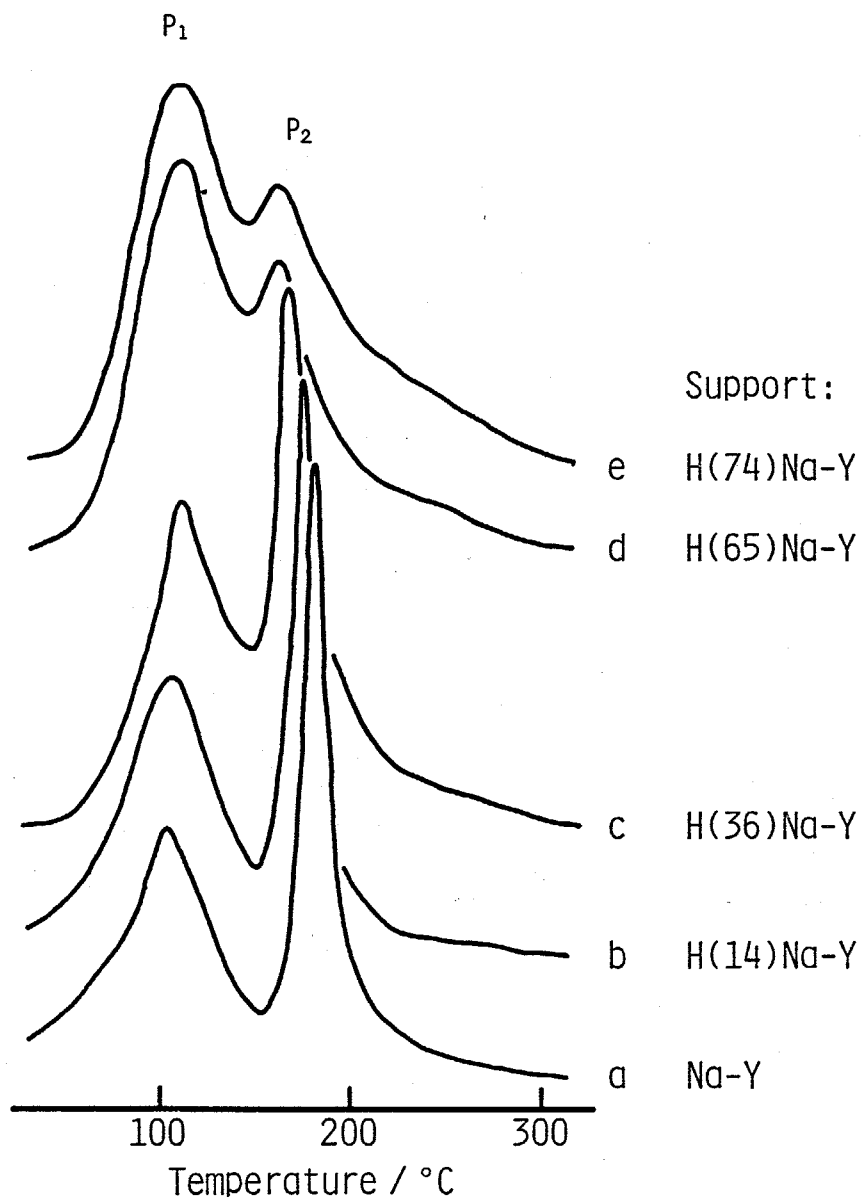


Fig. 3 CO desorption profiles during temperature programmed decomposition of $\text{Mo}(\text{CO})_6/\text{Y}$ zeolites
 Dehydration temperature of Y zeolite: 400°C
 Mo content: 2 Mo-atoms/supercage

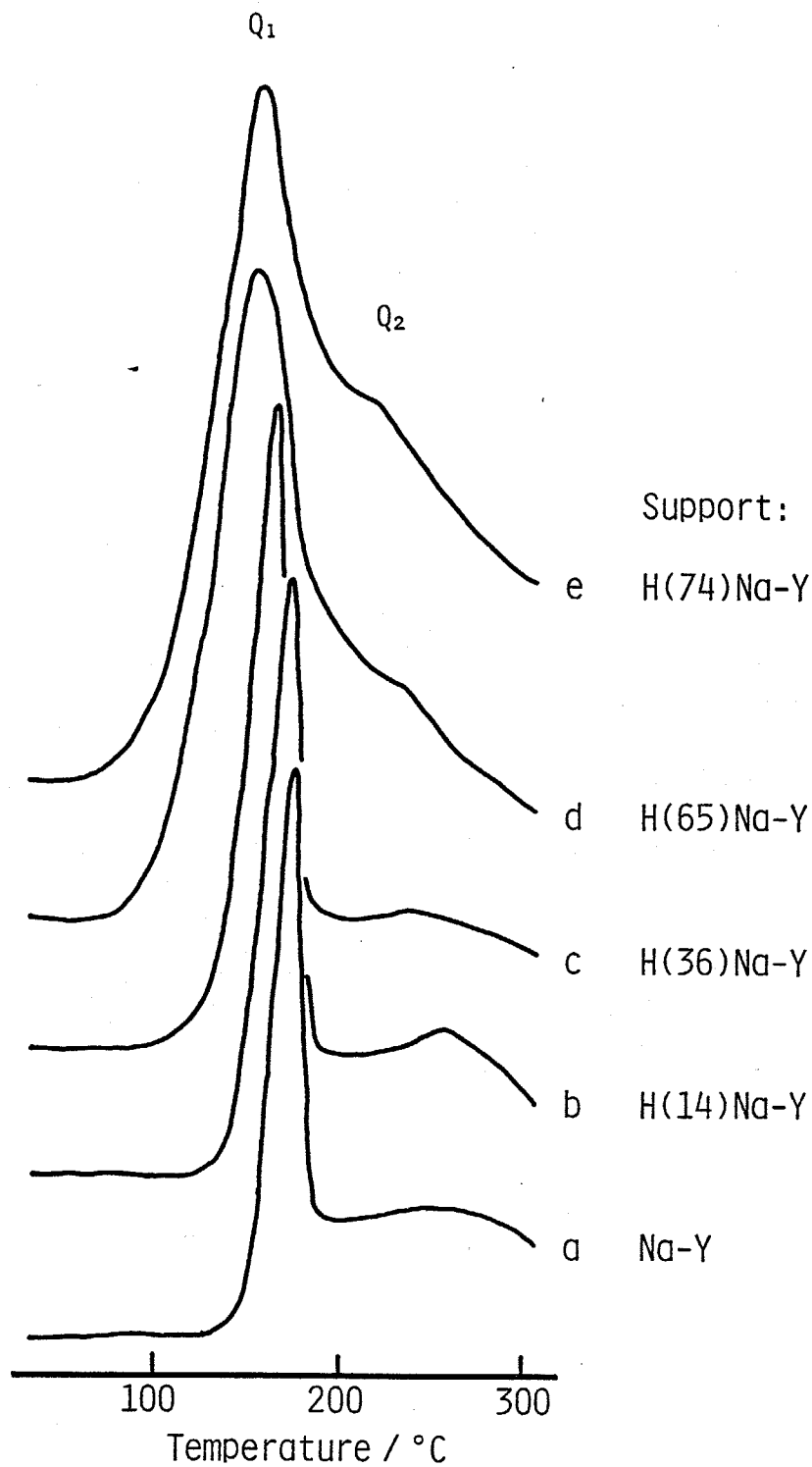


Fig. 4 H_2 formation profiles during temperature programmed decomposition of $Mo(CO)_6/Y$ zeolites
 Dehydration temperature of Y zeolite: $400^\circ C$
 Mo content: 2 Mo-atoms/supercage

less stable on HNa-Y with the higher proton concentration.

The formation of H_2 during the TPDE of the samples in Fig. 3 is described in Fig. 4. With increasing the degree of proton exchange in Y zeolites, Q_1 peak shifted to lower temperature as observed for the P_2 peak in Fig. 3. This indicates that molybdenum is oxidized at the lower temperatures on HNa-Y with the higher proton concentration. It is found that the surface OH groups with the higher concentration promote the reaction (2-1). Therefore, the subcarbonyl species is easily decomposed on the HNa-Y with the higher proton concentration as observed in Fig. 3. In addition, the Q_2 peak also shifted to the lower temperature region with increasing the degree of proton exchange, which indicates that the oxidation after the complete decomposition of subcarbonyl species is also promoted by the higher concentration of the OH groups.

2-3-2 Loading of molybdenum

It has been reported that $Mo(CO)_6$ is adsorbed in the supercage of dehydrated HNa-Y zeolite [1]. The supercage is the largest space in the porous structure of Y-type zeolites, having the diameter of about 13 Å and the aperture of about 8 Å. $Mo(CO)_6$ molecules have a molecular diameter of about 6.4 Å estimated from the bond lengths of Mo-C and C-O. Consequently, it seems easy for a $Mo(CO)_6$ molecule to enter a supercage. However, the number of the $Mo(CO)_6$ molecules which can simultaneously enter one supercage seems to be very small. Based on these

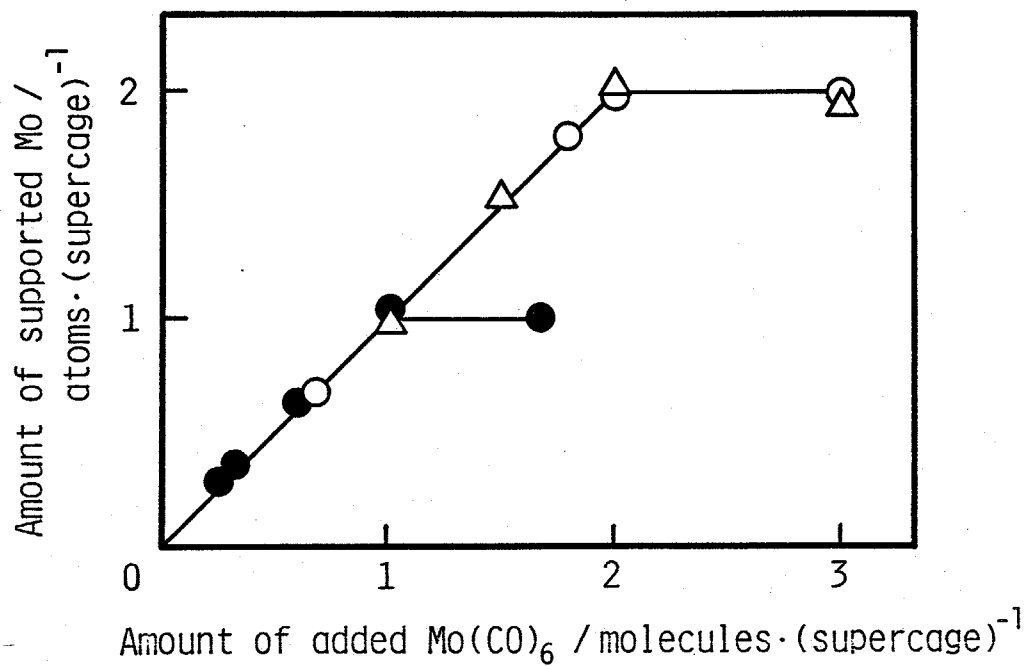


Fig. 5 Relation between the amount of added $\text{Mo}(\text{CO})_6$ and the amount of Mo supported on Y zeolites after decomposition of adsorbed $\text{Mo}(\text{CO})_6$

Support: Δ - Na-Y; \circ - H(36)Na-Y; \bullet - H(82)Na-Y
 Decomposition temperature of $\text{Mo}(\text{CO})_6$: 300°C

inferences, I measured the content of molybdenum in Mo/HNa-Y prepared from various amounts of $\text{Mo}(\text{CO})_6$ to clarify the loading behaviour.

Figure 5 shows the relation between the amount of added $\text{Mo}(\text{CO})_6$ and that of supported molybdenum after the decomposition of adsorbed $\text{Mo}(\text{CO})_6$. It is clear that the whole amount of the added Mo is supported on the HNa-Y, up to 1 Mo atom per supercage of Y zeolites (1 Mo-atoms/supercage), irrespective of the degree of proton exchange in Y zeolites. When H(82)Na-Y was used as a support, the content of molybdenum was restricted to this level, while in the case of H(36)Na-Y and Na-Y, the content linearly increased up to 2 Mo-atoms/supercage (which corresponds to about 9.5 wt% Mo). When H(14)Na-Y, H(65)Na-Y and H(74)Na-Y were used as supports, the maximum contents of Mo were 2.0, 2.0 and 1.9 Mo-atoms/supercage, respectively. These results indicate that no more $\text{Mo}(\text{CO})_6$ molecules can adsorb in the supercage which previously adsorbed two $\text{Mo}(\text{CO})_6$ molecules and that the amount of supported molybdenum is independent of the concentration of protons on the zeolite, except for the H(82)Na-Y.

The specific surface area of the H(82)Na-Y was certainly small compared with the other HNa-Y (see Table 2), which can be explained by the partial destruction of the framework structure of the H(82)Na-Y zeolite. Therefore, the decrease in the maximum content of molybdenum may result partly from a decrease in the concentration of supercages. Thus the maximum amount of supported molybdenum is determined by the saturated amount of adsorbed $\text{Mo}(\text{CO})_6$ which is the only function of the relation between the size of $\text{Mo}(\text{CO})_6$ molecules and the diameter of the supercages.

It is found that once the $\text{Mo}(\text{CO})_6$ molecules are adsorbed in the supercage, all of the Mo atoms are supported on zeolites by heating in vacuo without the sublimation of the adsorbed $\text{Mo}(\text{CO})_6$.

After decomposing $\text{Mo}(\text{CO})_6$ to remove bulky CO ligands, the space in the supercages nearly equal to that of the parent HNa-Y may be regenerated. Consequently, it seems possible that additional $\text{Mo}(\text{CO})_6$ molecules are adsorbed in this regenerated space. I added $\text{Mo}(\text{CO})_6$ to the Mo/HNa-Y with the content of 2 Mo-atoms/supercage. The results are shown in Fig. 6. The solid line represents the calculated value when all of the added Mo is supported on HNa-Y. The numbers in parentheses represent the number of adsorption-decomposition cycles repeated on the same sample. It is found that additional molybdenum is indeed supported on the Mo/HNa-Y, and that the increase in the molybdenum content permitted by each cycle is nearly equal to the content determined by the saturated amount of the adsorption (2 Mo-atoms/supercage). The loading behaviour were again the same for Na-Y and H(36)Na-Y. It is confirmed that the content of molybdenum is limited by the size of vacant space in the supercage which can adsorb $\text{Mo}(\text{CO})_6$, and that it is independent of the proton concentration of the zeolite supports.

XPS spectra can provide the surface composition in the range of dozens of angstrom depth. In the case of molybdenum supported on zeolites, the comparison of the surface composition with the bulk composition reveals whether molybdenum is supported on the external surface of the zeolite crystallites or inside the crystallites. Dai and Lunsford [8] have reported for Mo/Y zeo-

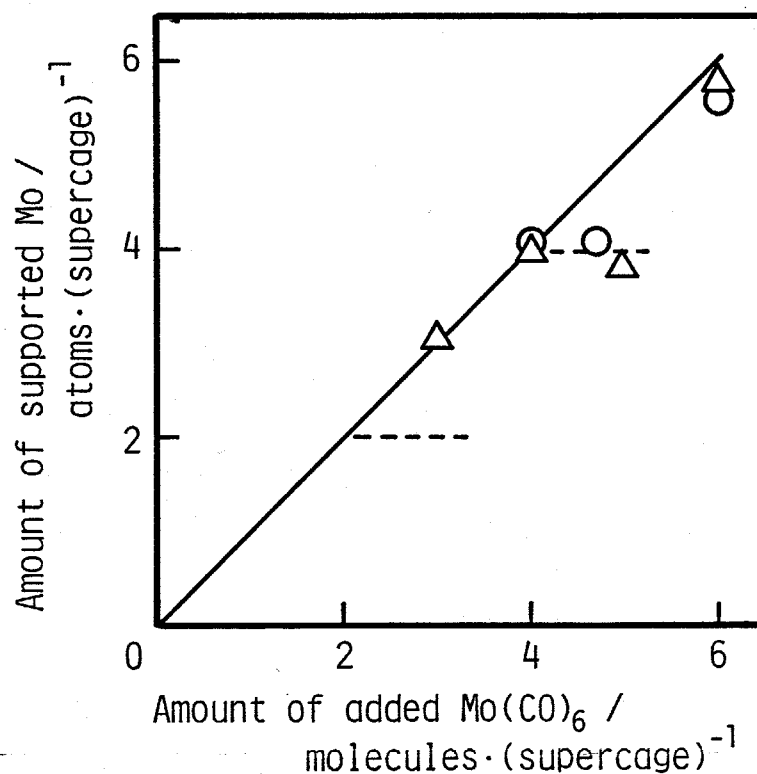


Fig. 6 Change in amount of supported Mo with repeated adsorption and decomposition of $\text{Mo}(\text{CO})_6$ on Mo/Y zeolites

Dehydration temperature of Y zeolite: 300°C

Decomposition temperature of $\text{Mo}(\text{CO})_6$: 300°C

Support: Δ - Na-Y; \circ - H(36)Na-Y

Numbers in parentheses: See text

lites prepared from MoCl_5 by a solid-solid cation exchange method that the Mo/Si ratio calculated from XPS data is not greater than the ratio determined from bulk composition. They have concluded that their method results in the exchange of protons by Mo inside the zeolite crystallites. Tri et al. [9] have prepared bimetallic Pt-Mo/Y zeolites and checked the homogeneity of the Mo distribution from XPS spectra in the similar manner to that of Dai and Lunsford [8]. They have concluded that no surface enrichment in molybdenum occurs for Pt-rich samples, and that large amounts of $\text{Mo}(\text{CO})_6$ are adsorbed and decomposed in the outer layer of zeolite crystallites for Mo-rich samples.

I calculated the Mo/Si ratio from the XPS spectra of Mo/HNa-Y by equations (2-4) and (2-5) [10];

$$\frac{n_2}{n_1} = \frac{N_2}{N_1} \times \frac{\sigma_1}{\sigma_2} \times \frac{f_1}{f_2} \times \frac{\lambda_1}{\lambda_2} \times \frac{S_1}{S_2} \quad (2-4)$$

$$f_i = 1 + \frac{\beta_i}{2} \left(\frac{3}{2} \sin^2 \theta - 1 \right) \quad (2-5)$$

where n is the concentration of the element, N is the photoelectron intensity, σ is the total photoionization cross section, f is the angular asymmetry factor, λ is the escaping depth, S is the transmission factor of the spectrometer, β is the asymmetry parameter and θ is the angle of photoelectron emission. I used the values of σ , β and λ which were reported by Scofield [11], Reilman et al. [12] and Penn [13], respectively, and those of S and θ presented in the manual of the spectrometer.

Table 3 shows the external surface Mo/Si ratios calculated from the peaks of Mo 3d and Si 2p in the XPS spectra together

Table 3

Bulk and external surface Mo/Si ratios

| Support | Dehydration temperature of zeolite /°C | Decomposition temperature of Mo(CO) ₆ /°C | Treatment | Mo/Si ^a (Mo 3d)/(Si 2p) ^b |
|-----------|--|--|------------------------|---|
| Na-Y | 500 | 300 | — | 0.10 |
| H(14)Na-Y | 300 | 300 | O ₂ , 300°C | 0.089 |
| H(65)Na-Y | 400 | 440 | — | 0.088 |
| H(74)Na-Y | 400 | 300 | H ₂ , 500°C | 0.092 |
| | | | | 0.046 |
| | | | | 0.051 |
| | | | | 0.048 |
| | | | | 0.026 |

^aValues derived from bulk composition.^bValues calculated from XPS spectra.

with the bulk Mo/Si ratios derived from the bulk composition. The molybdenum contents of these samples corresponded to 1.6 - 1.8 Mo atoms per supercage of HNa-Y. It is clear that the surface Mo/Si ratio is smaller than the bulk ratio in each Mo/HNa-Y, regardless of the degree of proton exchange in the zeolites and the preparation conditions. Consequently, I conclude that enrichment of molybdenum at the external surface of the zeolite crystallites does not occur, and that the Mo species are uniformly distributed within the crystallites. When each supercage of HNa-Y is saturated with the adsorbed $\text{Mo}(\text{CO})_6$ molecules (2 molecules per supercage), the $\text{Mo}(\text{CO})_6$ should be homogeneously dispersed within the zeolite crystallites. Therefore, I can also conclude that Mo atoms do not migrate toward the external surface of the zeolite crystallites during the decomposition of $\text{Mo}(\text{CO})_6$, oxidation by O_2 and reduction by H_2 .

2-4 Conclusion

Molybdenum can be supported on HNa-Y zeolites by the adsorption of $\text{Mo}(\text{CO})_6$ on the dehydrated HNa-Y and the subsequent decomposition of the adsorbed $\text{Mo}(\text{CO})_6$. Two $\text{Mo}(\text{CO})_6$ molecules can be adsorbed per supercage of HNa-Y. Heating the adsorbed $\text{Mo}(\text{CO})_6$ in vacuo first leads to the partial decomposition of $\text{Mo}(\text{CO})_6$ to form a subcarbonyl species, $\text{Mo}(\text{CO})_3$ (ads). Further heating at a higher temperature causes the elimination of the remaining CO ligands with the simultaneous formation of hydrogen and methane. It is found that the oxidation of molybdenum occurs during this

decomposition. The stability of the subcarbonyl species varies with the degree of proton exchange in Y zeolites. It is suggested that the higher proton concentration in HNa-Y results in the lower temperature of the oxidation of subcarbonyl species. From the XPS study, it is revealed that the supported molybdenum after the thermal decomposition is not located exclusively on the surface of the zeolite crystallites but is distributed within the crystallites. The content of molybdenum in Mo/HNa-Y is limited by the saturated amount of $\text{Mo}(\text{CO})_6$ which corresponds to two molecules per supercage. Once the $\text{Mo}(\text{CO})_6$ molecules are adsorbed in the supercage, their sublimation does not occur during the heating in vacuo, so that all of the Mo atoms are supported on zeolites. The saturated amount of adsorption is determined only by the size of the available space in a supercage for the adsorption of $\text{Mo}(\text{CO})_6$ and is independent of the proton concentration of HNa-Y.

References

- 1 P. Gallezot, G. Coudurier, M. Primet and B. Imelik, ACS Symp. Ser., No. 40, 144 (1977)
- 2 A. Brenner, D. A. Hucul and S. J. Hardwick, Inorg. Chem., 18, 1478 (1979)
- 3 R. R. Monchamp and F. A. Cotton, J. Chem. Soc., 1438 (1960)
- 4 S. Abdo and R. F. Howe, J. Phy. Chem., 87, 1713 (1983)
- 5 A. Brenner and R. L. Burwell, Jr., J. Catal., 52, 353 (1978)
- 6 R. G. Bowman and R. L. Burwell, Jr., J. Catal., 63 463 (1980)
- 7 A. Brenner and D. A. Hucul, Proc. 3rd Intern. Conf. Chemistry and Uses of Molybdenum, (Ann Arbor, 1979), p. 194
- 8 P. E. Dai and J. H. Lunsford, J. Catal., 64, 173 (1980)
- 9 T. M. Tri, J. -P. Candy, P. Gallezot, J. Massardier, M. Primet, J. C. Vadrine and B. Imelik, J. Catal., 79, 396 (1983)
- 10 S. T. Manson, J. Electron Spectrosc. Relat. Phenom., 1, 413 (1972/73)
- 11 J. H. Scofield, J. Electron Spectrosc. Relat. Phenom., 8, 129 (1976)
- 12 R. T. Reilman, A. Msezane and S. T. Manson, J. Electron Spectrosc. Relat. Phenom., 8, 389 (1976)
- 13 D. R. Penn, J. Electron Spectrosc. Relat. Phenom., 9, 29 (1976)

Chapter 3 Oxidation state of molybdenum

3-1 Introduction

Molybdenum has the high affinity to oxygen, so that the molybdenum in its highest oxidation state, namely Mo(VI) is the most stable in air. Consequently, in order to obtain the Mo species with lower oxidation states than Mo(VI), it is necessary to carry out the reductions at high temperatures. In the case of conventional $\text{MoO}_3/\text{Al}_2\text{O}_3$ catalysts, Mo(IV) has been easily obtained by the reduction with H_2 , but the Mo species whose oxidation number is lower than +4 has hardly been obtained unless the reduction under severe conditions is conducted [1,2]. In the cases of the hydrogenation of olefins, the hydrodesulfurization in petroleum refining, etc., the catalytic activity of the MoO_3 supported catalysts increased with increasing the extent of the reduction. Therefore, the activity of the Mo species with the oxidation number less than +4 should be one of the subjects to be resolved.

Such a low oxidation state of molybdenum has been obtained by Nakamura et al, [1]. They found the formation of Mo(0) by the reduction of $\text{MoO}_3/\text{Al}_2\text{O}_3$ with H_2 at 950°C . Perl [2] has also reported that the similar Mo(0) formation occurs by the reduction of the $\text{MoO}_3/\text{Al}_2\text{O}_3$ with H_2 at 800°C . On the other hand, the low oxidation states of molybdenum have been obtained under mild conditions using the new molybdenum supported catalysts prepared from molybdenum complexes. For example, Mo(0) clusters are formed by decomposing $\text{Mo}(\text{CO})_6$ adsorbed on fully dehydroxylated alumina at 500°C [1,3].

In order to clarify the catalytic properties of the Mo species in the low oxidation states, it is better to use the molybdenum supported catalyst in which the oxidation state of molybdenum can be controlled widely without treatments under severe conditions. I prepared Mo/HNa-Y with various oxidation states of molybdenum by altering the concentration of hydroxyl groups on HNa-Y and the decomposition temperature of $\text{Mo}(\text{CO})_6$, and discuss the oxidation states from the results of O_2 titration, X-ray photoelectron spectroscopic study, adsorption of CO, and so on.

3-2 Experimental

3-2-1 Average oxidation number of molybdenum

The average oxidation number (AON) of molybdenum in Mo/HNa-Y prepared by the decomposition of $\text{Mo}(\text{CO})_6$ adsorbed on HNa-Y was determined by two different methods as follows.

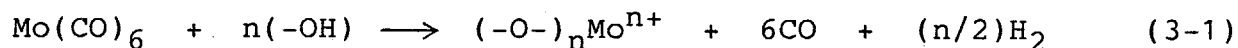
(A) O_2 titration method

Mo/HNa-Y was exposed to 200 torr of oxygen at room temperature. The sample was then heated at 300 - 500°C for 30 min. The amount of O_2 consumed during this oxidation was measured volumetrically. After O_2 was pumped out at room temperature, the amount of O_2 which was physisorbed on the Mo/HNa-Y was measured at room temperature under nearly the same pressure of O_2 as that after the first O_2 treatment. The amount of O_2 used to oxidize molybdenum was calculated by subtracting the amount of the physisorbed O_2 from the total amount of consumed O_2 during the first

treatment. I determined the AON of Mo from the amount of O₂ which oxidized molybdenum by assuming that all of the Mo species were oxidized to Mo(VI) during the first treatment.

(B) Measurement of the amount of H₂ formed during the decomposition-

As mentioned previously (2-3-1), molybdenum is oxidized by the surface hydroxyl groups of HNa-Y during the decomposition of the adsorbed Mo(CO)₆. In this decomposition, the overall stoichiometry can be expressed as follows;



Parts of these H₂ and CO were consumed to form methane, as shown in the equations (2-2) and (2-3) in the previous section. I measured the amounts of CO, H₂ and methane evolved during the decomposition by using quadrupole mass spectrometer (see 2-2-4), and calculated the AON of Mo from the relative amounts of these gases.

3-2-2 X-ray photoelectron spectroscopy (XPS)

The Mo/HNa-Y samples for XPS studies were prepared by an in situ procedure. A small drop of HNa-Y suspended in pure water was put on the tip of the sample holder of the XPS apparatus and then dried to form a very thin layer of HNa-Y. This tip was placed in a Pyrex tube which was connected to a vacuum system. The HNa-Y on the tip was dehydrated in vacuo. A certain amount of Mo(CO)₆ was added under argon atmosphere on the HNa-Y in the Pyrex tube. Mo(CO)₆ was adsorbed in vacuo and the sample was then sealed in vacuo at -196°C after the adsorption was com-

pleted. The $\text{Mo}(\text{CO})_6/\text{HNa-Y}$ thus prepared on the tip was placed in the sample holder in a glove box filled with argon. Immediately after the sample was inserted into the analyzer chamber, it was heated under vacuum (10^{-6} torr) to form $\text{Mo}/\text{HNa-Y}$.

The XPS spectra were measured on the Shimadzu ESCA 750 spectrometer with $\text{Mg K}_{\alpha 1,2}$ X-rays (1253 eV) used as the exciting source. The values of binding energies were determined from the $4f_{7/2}$ line of Au (83.7 eV) deposited on the sample after measurements of the spectra of other elements. The C 1s line was used as a secondary standard for each spectrum. The reproducibility of binding energies was ± 0.2 eV.

3-2-3 Infrared spectroscopy

The measurement of IR spectra was carried out with the $\text{Mo}/\text{HNa-Y}$ prepared from the self-supporting wafer of HNa-Y and $\text{Mo}(\text{CO})_6$. As described previously (2-2-3), $\text{Mo}/\text{HNa-Y}$ samples were prepared within the IR cell. After 50 torr of CO was adsorbed on $\text{Mo}/\text{HNa-Y}$ at room temperature, IR spectra were measured on the Hitachi EPI G3 spectrometer.

3-2-4 Electron spin resonance spectroscopy

The $\text{Mo}/\text{HNa-Y}$ samples for the measurements of ESR spectra were prepared in situ within a quartz tube of a 4 mm diameter. The ESR spectra were measured at -196°C on the JEOL JFS-PE-IX spectrometer (± 1000 G). The spin concentration of the sample was determined by using $\text{CuSO}_4 \cdot 5\text{H}_2\text{O}$ as a reference. The g-value was determined from the g-values of manganese.

3-3 Results and discussion

3-3-1 Average oxidation number of molybdenum

During the decomposition of $\text{Mo}(\text{CO})_6$ adsorbed on HNa-Y, molybdenum is oxidized by the hydroxyl groups of HNa-Y as mentioned in chapter 2. If the degree of this oxidation is controlled, the Mo species having a wide range of oxidation state will be prepared. There are two ways to control this oxidation, that is, to vary the concentration of the OH groups and to vary the temperature of the decomposition. It is known that the concentration of the surface OH groups on HNa-Y zeolites can be altered by heating in vacuo [4]. I prepared Mo/HNa-Y using H(82)Na-Y supports dehydrated in vacuo at various temperatures and determined the average oxidation number (AON) of the supported molybdenum by the O_2 titration method. The results are shown in Fig. 7. The AON of Mo decreased from +3.76 to +0.60 with increasing the dehydration temperature of H(82)Na-Y. The dehydration at higher temperatures directly leads to the decrease in the concentration of the OH groups on H(82)Na-Y. As a result, the oxidation of Mo is suppressed when the HNa-Y dehydrated at the higher temperatures is used.

I tried to control the AON of Mo also by varying the decomposition temperature of $\text{Mo}(\text{CO})_6$ adsorbed on H(82)Na-Y. Figure 8 shows the change in AON with the decomposition temperature. Every H(82)Na-Y support was dehydrated at 400°C and has the same concentration of the OH groups. The AON increased from +1.16 to +2.33 with increasing the decomposition temperature. It is found that the oxidation of Mo is accelerated at the higher temperatures.

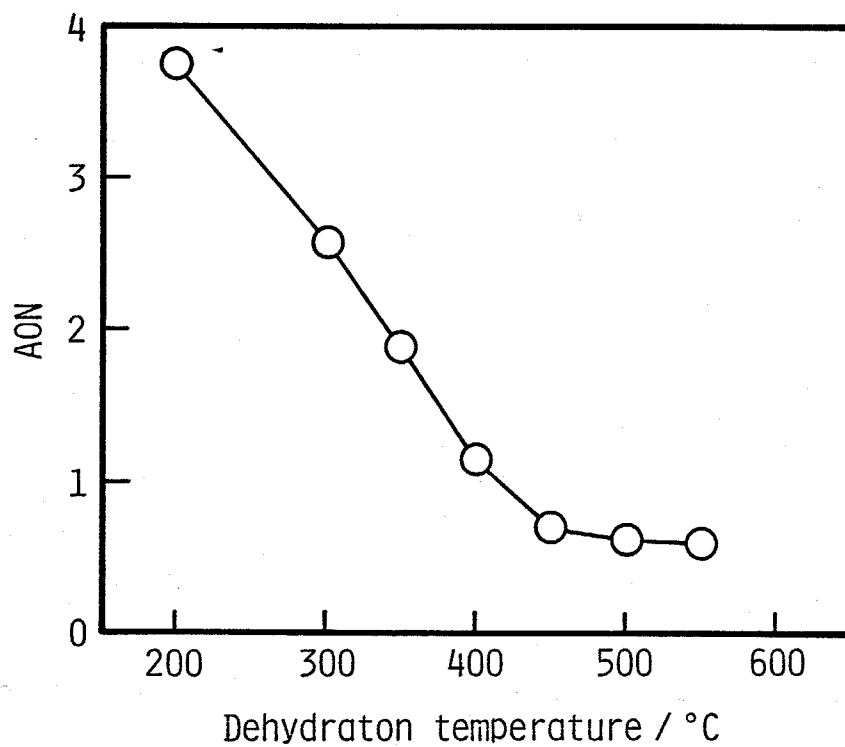


Fig. 7 Effect of dehydration temperature of H(82)Na-Y on average oxidation number of Mo in Mo/H(82)Na-Y

Decomposition temperature of $\text{Mo}(\text{CO})_6$: 300°C
 Mo content: 0.68 Mo-atoms/supercage

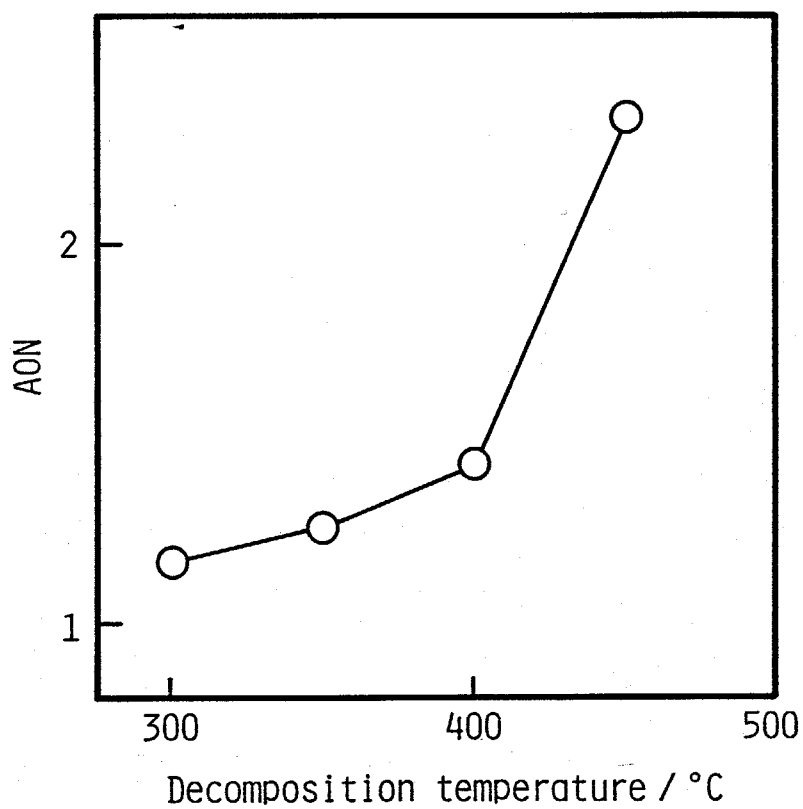


Fig. 8 Effect of decomposition temperature of adsorbed $\text{Mo}(\text{CO})_6$ on average oxidation number of Mo in $\text{Mo}/\text{H}(82)\text{Na}-\text{Y}$

Dehydration temperature of $\text{H}(82)\text{Na}-\text{Y}$: 400°C

Mo content: 0.68 Mo-atoms/supercage

Thus the AON of Mo was altered with both the dehydration temperature of H(82)Na-Y and the decomposition temperature of $\text{Mo}(\text{CO})_6$. Combining these two effects, I prepared the Mo species of various AON of Mo on the H(82)Na-Y support. Figure 9 shows the variation of AON with the decomposition and dehydration temperatures. At each decomposition temperature, an inverse correlation between the AON and the dehydration temperature was observed. On the other hand, at each dehydration temperature, the AON increased with increasing the decomposition temperature. However, when the H(82)Na-Y dehydrated at higher temperatures ($\geq 450^\circ\text{C}$) was used as a support, only a small increase in AON was observed with increasing the decomposition temperature. H(82)Na-Y zeolite has about five OH groups per supercage before the dehydration. Therefore, when two $\text{Mo}(\text{CO})_6$ molecules are coexist in one supercage, there exist about 2.5 OH groups per Mo atom on an average. The dehydration at the higher temperatures ($\geq 450^\circ\text{C}$) diminishes the concentration of OH groups to a considerable extent. Therefore, the AON of Mo does not increase so much at the higher decomposition temperatures on the HNa-Y dehydrated at such a high temperature.

Changing the preparation conditions as mentioned above, I could adjust the AON of Mo supported on H(82)Na-Y from +0.60 to +3.77. The oxidation states of this range are lower than those obtained by the reduction of $\text{MoO}_3/\text{Al}_2\text{O}_3$ under the usual condition (at 500°C with H_2). In addition, oxidation with O_2 could increase the AON of Mo in the Mo/HNa-Y to various extents. For example, the oxidation at room temperature caused the increase in AON of about 2, while the oxidation at 300°C transformed all Mo

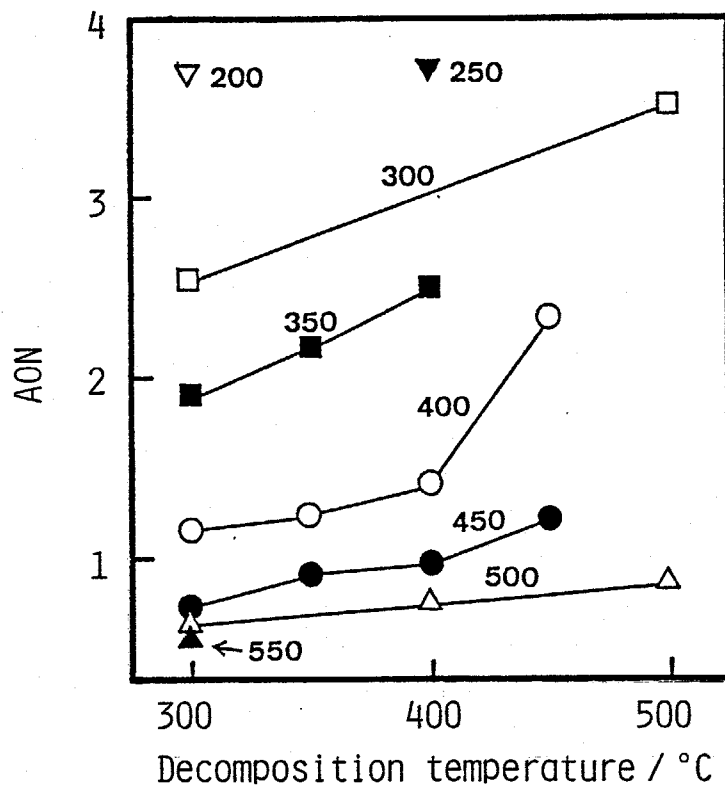


Fig. 9 Effect of dehydration temperature of H(82)Na-Y and decomposition temperature of adsorbed $\text{Mo}(\text{CO})_6$ on average oxidation number of Mo

Numbers in figure represent dehydration temperature of H(82)Na-Y

Mo content: 0.68 Mo-atoms/supercage

species into Mo(VI). By changing the preparation conditions and/or by conducting these oxidation treatments on the Mo/HNa-Y, the AON of Mo could be altered in the range from +0.60 to +6. Therefore, the Mo/HNa-Y prepared from $\text{Mo}(\text{CO})_6$ is of great advantage to investigating the relation between the oxidation state of Mo and its catalytic properties. However, most of Mo/HNa-Y did not exhibit the integral AON of Mo, so that two or more Mo species with different oxidation states are considered to coexist in one Mo/HNa-Y.

The concentration of the surface OH groups of HNa-Y can be controlled also by varying the degree of proton exchange in Y zeolites. Using the HNa-Y with a low degree of proton exchange or Na-Y as a support, Mo should not be oxidized so much. From the H_2 formation during TPDE (Fig. 4, in section 2-3-1), indeed, the oxidation of Mo required the higher temperatures with decreasing the degree of proton exchange.

Figure 10 shows the change in AON of Mo with the degree of proton exchange in Y zeolites. The AON clearly decreased with decreasing the exchange degree, which indicates that lowering the degree of proton exchange has the same effect on AON as that of increasing the dehydration temperature of HNa-Y supports. Na-Y zeolite has a Na^+ ion at each cation exchange site, so that the only terminal OH groups present at the end of crystallites and the defects of lattice structure can oxidize the molybdenum during the decomposition of $\text{Mo}(\text{CO})_6$. The low values of AON imply the presence of a considerable amount of Mo(0) species.

The Mo/HNa-Y with various AON of Mo were obtained by

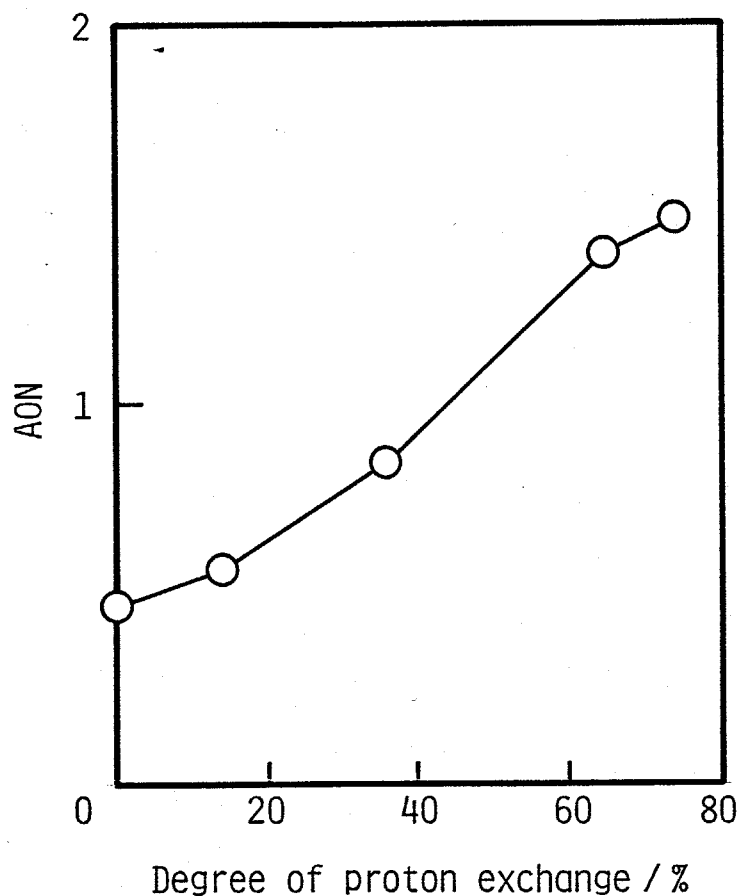


Fig. 10 Effect of degree of proton exchange in Y zeolites on average oxidation number of Mo in Mo/Y zeolites

Dehydration temperature of Y zeolite: 300°C

Decomposition temperature of $\text{Mo}(\text{CO})_6$: 300°C

Mo content: 2 Mo-atoms/supercage

changing both the degree of proton exchange in Y zeolites and the dehydration temperature of the HNa-Y. These AON are shown in Fig. 11. In the cases of H(74)Na-Y, H(65)Na-Y and H(36)Na-Y supports, the AON decreased with increasing the dehydration temperature, as observed in the case of H(82)Na-Y support (Fig. 7). When H(14)Na-Y or Na-Y was used as a support, however, the AON of Mo did not change so much. The proton concentrations of these zeolites are very low, so that the dehydration temperature has little influence on the AON. It is clear that, as a whole, the AON shown in Fig. 11 is smaller than that of Mo in Mo/H(82)Na-Y (Fig. 9). The content of Mo in Mo/HNa-Y used in Fig. 11 is 2 Mo-atoms/supercage, while that of the Mo/H(82)Na-Y used in Fig. 9 is 0.68 Mo-atoms/supercage. The number of OH groups of HNa-Y per added Mo atom is less than 2.3 for the former Mo/HNa-Y, while that for the latter is about 7.5. Though molybdenum is not oxidized by all of the OH groups, the lower concentrations of the OH groups in former HNa-Y lead to the smaller AON of Mo.

From the results on the temperature programmed decomposition (TPDE) of $\text{Mo}(\text{CO})_6/\text{HNa-Y}$ as described in the previous section (2-3-1), it is possible to determine the AON of supported molybdenum. The total amount of CO desorbed during the TPDE up to 300°C should correspond to $\text{CO}/\text{Mo} = 6$, because the decomposition of $\text{Mo}(\text{CO})_6$ is completed at this temperature. Therefore, integrating the TPDE curves, I can determine how many molecules of H_2 and methane per Mo atom are formed. From the equations (2-1), (2-2) and (2-3) presented before (see 2-3-1), the formation of one molecule of H_2 and methane per Mo atom corresponds to the in-

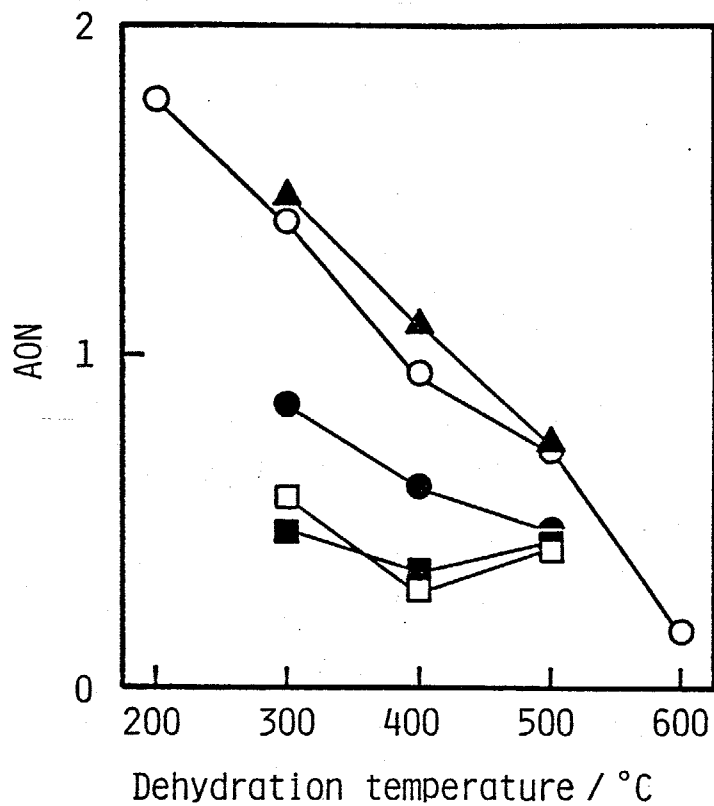


Fig. 11 Effect of dehydration temperature of Y zeolites on average oxidation number of Mo

Decomposition temperature of $\text{Mo}(\text{CO})_6$: 300°C

Mo content: 2 Mo-atoms/supercage

Degree of proton exchange (%):

■ - 0; □ - 14; ● - 36; ○ - 65; ▲ - 74

crease in AON of 2 and 6, respectively. The AONs thus calculated from the amount of H₂ and methane are shown in Table 4 together with those determined by the O₂ titration method. The two series of the AON determined for the same Mo/HNa-Y were nearly consistent with each other. It is revealed that the Mo/Na-Y contains a large proportion of Mo(0) also from the TPDE results.

3-3-2 XPS study

In the previous section (3-3-1), the average oxidation number of molybdenum in Mo/HNa-Y is investigated. The results indicates that AON is not always integral. Therefore, it seems that Mo species with different oxidation numbers coexist in a Mo/HNa-Y sample. In order to find out the individual oxidation number of the Mo species, I measured XPS spectra of Mo/HNa-Y.

The Mo species with low oxidation states are easily oxidized by oxygen at room temperature [3,5]. As the Mo species in Mo/HNa-Y have the AON below +6 (see Figs. 9 and 11), I should protect the Mo species from the oxidation to determine the precise oxidation state. I placed the Mo/HNa-Y sample in the sample holder of XPS apparatus under argon atmosphere using a glove box filled with argon. From the XPS spectra of the sample thus prepared, it was found that the oxidation state of Mo was rather high compared with the AON of Mo for the sample. Therefore, the Mo species may be oxidized by a trace amount of oxygen and/or water in the glove box. The possibility of a similar oxidation by the trace amount of oxygen when a glove box is used for the

Table 4

Average oxidation numbers of Mo determined by two different methods

| Catalyst | Dehydration temperature of zeolite /°C | Decomposition temperature of Mo(CO) ₆ /°C | Average oxidation number O ₂ titration | Measurement of amount of H ₂ |
|--------------|--|--|---|---|
| Mo/Na-Y | 400 | 300 | 0.36 | 0.21 |
| | 500 | 440 | 0.31 | 0.25 ^a |
| Mo/H(65)Na-Y | 400 | 300 | 0.94 | 0.63 |
| | 500 | 440 | 0.68 | 0.61 ^b |
| | 500 | 440 | 2.60 ^c | — |
| Mo/H(74)Na-Y | 400 | 300 | 1.10 | 1.34 |

^aSample corresponded to Fig. 13, a.^bSample corresponded to Fig. 13, b.^cOxidized by O₂ at 25°C; sample corresponded to Fig. 13, c.

measurement of XPS spectra has been reported by Leclercq et al. [6] for Pt⁰ in Pt-Mo/Y zeolites.

For the purpose of avoiding the oxidation of molybdenum, Mo/HNa-Y was prepared in the analyzer chamber of the XPS instruments. Heating the sample was achieved by an electric heater placed in the sample holder. In order to raise sufficiently the temperature on the upper side of the sample by the heater under the sample, I used a thin layer of HNa-Y, since the high vacuum ($< 10^{-6}$) causes the low thermal conduction.

Figure 12 shows the Mo 3d XPS spectra of Mo(CO)₆ adsorbed on H(36)Na-Y. I refer to the peak of Mo 3d_{5/2} since its intensity is higher than that of Mo 3d_{3/2}. In the first scan (a: scanning time was 68 s), a large peak was observed at a binding energy of 228.5 eV. However, the intensity of this peak decreased in the second scan (b: 68 s) and decreased moreover in third scan (c: 204 s), while the intensity of the peaks in the higher binding energy region increased. These results indicate that X-ray irradiation causes the decomposition of Mo(CO)₆ and the consequent oxidation of the Mo species.

Figure 13 shows the Mo 3d XPS spectra of some kinds of Mo/HNa-Y measured after the thermal decomposition carried out in the manner mentioned in this chapter (3-2-2). In the case of Mo/Na-Y (a), the spectrum exhibited a peak at 228.4 eV. This spectrum did not change significantly on repeated scans, so that I can exclude the change in the oxidation state of Mo caused by X-ray irradiation on the thermally decomposed products. In the case of Mo/H(65)Na-Y (b), a broad and split peak at about 229 eV was observed. It is clear that the oxidation state is certainly

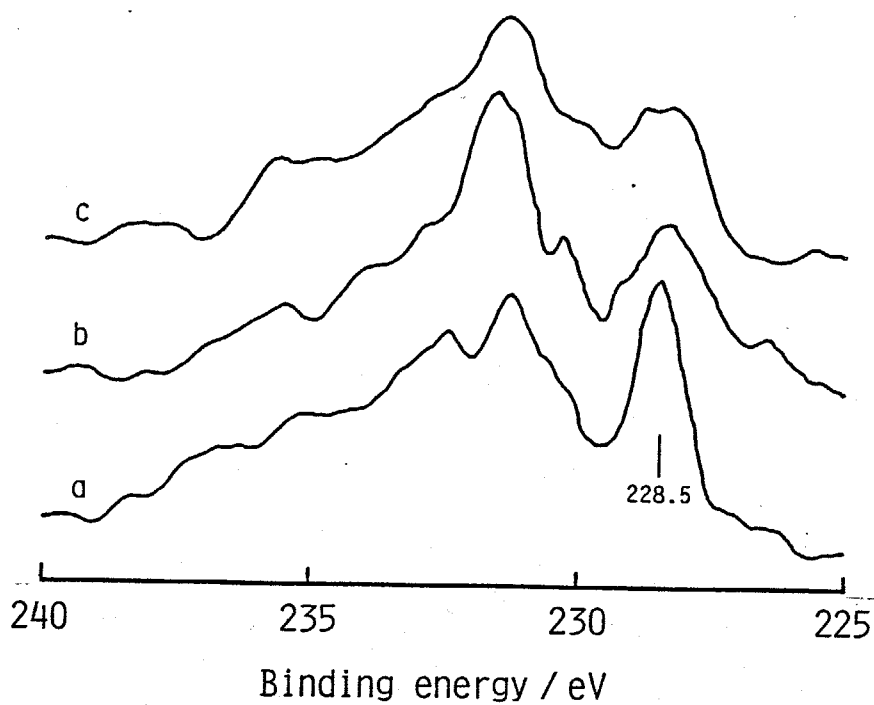


Fig. 12 Mo 3d XPS spectra of $\text{Mo}(\text{CO})_6$ adsorbed on $\text{H}(36)\text{Na-Y}$

Dehydration temperature of $\text{H}(36)\text{Na-Y}$: 400°C

a: First scan; scanning time was 68 s.

b: Second scan; scanning time was 68 s.

c: Third scan; scanning time was 204 s.

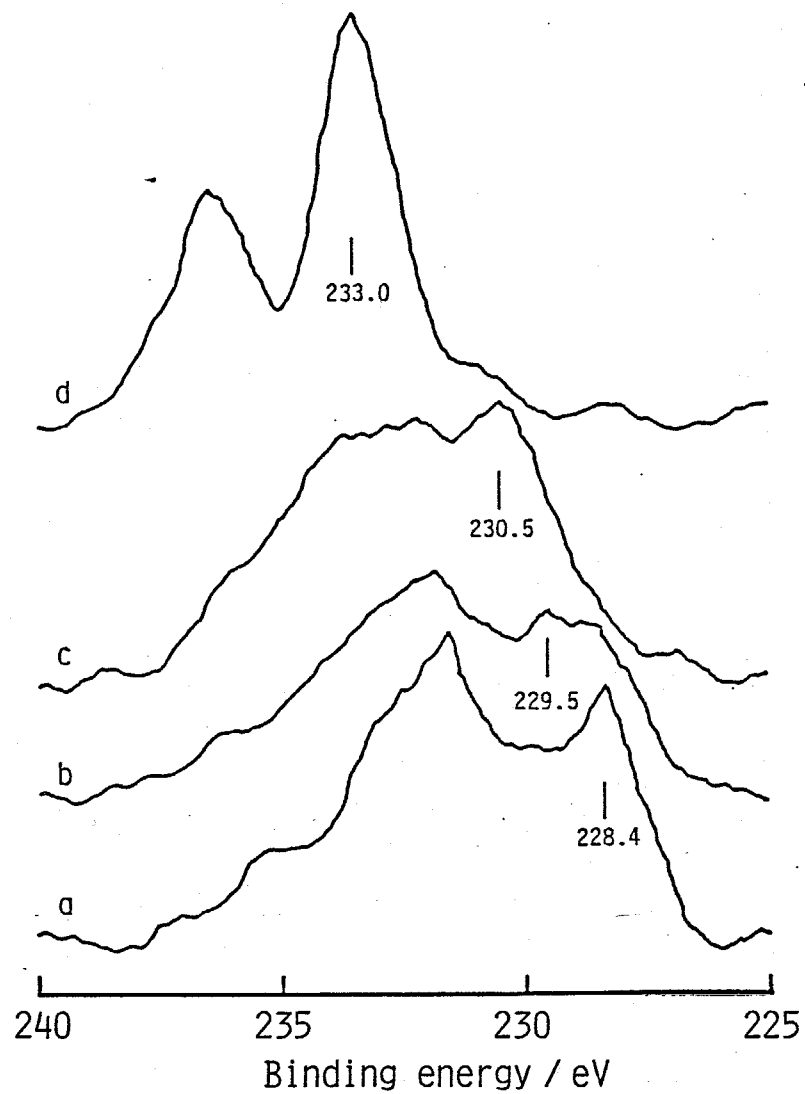


Fig. 13 Mo 3d XPS spectra of Mo/Y-zeolite

- a: Mo/Na-Y; dehydration temperature of Na-Y was 500°C
decomposition temperature of Mo(CO)₆ was 440°C
- b: Mo/H(65)Na-Y; preparation conditions were same as a
- c: Sample b exposed to air at 25°C
- d: Sample c exposed to air at 250°C

heterogeneous compared with Mo/Na-Y (a). This broad peak may consist of a peak at 229.5 eV in addition to a peak at 228.6 eV, which is nearly equal to the binding energy of the peak in spectrum (a). Spectrum (c) was obtained after the Mo/H(65)Na-Y (spectrum b) was oxidized by air at room temperature. A peak at 230.5 eV was observed, but the oxidation state was rather heterogeneous. When this sample was further oxidized by air at 250°C, spectrum (d) was obtained. This spectrum, having a peak at 233.0 eV, demonstrates the existence of the Mo species with a homogeneous oxidation state.

In order to clarify the oxidation number to which each peak in Fig. 13 corresponds, I measured the XPS spectra of Mo metal and several Mo compounds. The results are presented in Table 5 together with the data appeared in literatures [7 - 9]. In the case of data taken from Refs. 7, 8 and 9, corrections are made to the published $3d_{5/2}$ binding energies, taking into account the different referencing procedures (see footnotes a, b and c of Table 5). The binding energies used as reference standards in Refs. 7, 8 and 9 are 83.0 eV (Au $4f_{7/2}$), 284.0 eV (C 1s) and 83.8 eV (Au $4f_{7/2}$), respectively, while those used in this work are 83.7 eV (Au $4f_{7/2}$) and 284.5 eV (C 1s). From Table 5, the peak at 228.4 eV observed for Mo/Na-Y apparently corresponds to the molybdenum with an oxidation number between 0 and +2. Here I attribute this peak to Mo(0) for the following reasons.

(1) It has been reported [10] that the Mo $3d_{5/2}$ binding energy of $\text{Mo}(\text{CO})_6$ is higher by 0.5 eV than that of Mo metal. This indicates that the binding energy is high if Mo(0) has no metal

Table 5

Binding energies of molybdenum metal and some molybdenum compounds

| Sample | Oxidation number of Mo | Binding energy of Mo 3d5/2 /eV | Reference |
|--|------------------------|---|-------------------------|
| Mo metal | 0 | 227.9 227.7 ^a | This work [7] |
| Mo ₆ Cl ₁₂ | +2 | 229.2 ^b | [8] |
| MoCl ₃ | +3 | 229.6 229.7 ^a | This work [7] |
| MoO ₂ | +4 | 229.5 231.7 ^a | This work [7] |
| MoCl ₄ | +4 | 230.3 ^a | [7] |
| MoCl ₅ | +5 | 231.7 230.7 ^a | This work [7] |
| MoO ₃ | +6 | 232.7 232.4 ^a 232.4 ^c | This work [7] [9] |
| (NH ₄) ₆ Mo ₇ O ₂₄ ·4H ₂ O | +6 | 232.4 232.4 ^a | This work [7] |

^aValue corrected by +0.7 eV(see text).

^bValue corrected by +0.5 eV(see text).

^cValue corrected by -0.1 eV(see text).

bond. As shown in Fig. 12, $\text{Mo}(\text{CO})_6/\text{HNa-Y}$ gave a peak at 228.5 eV for the first scan. This seems to represent the peak corresponding to Mo(0) in $\text{Mo}(\text{CO})_6$.

(2) It has been reported [11] for Pt/Y zeolites that when Pt(0) is atomically dispersed, the binding energy of Pt(0) is higher by 1.3 eV than that in metal film and by 0.6 eV than that in particles of 10 - 20 Å in diameter (Table 6). This result has been explained by the change in the extra-atomic relaxation. A similar difference in binding energies (ca. 1.0 eV) depending on the particle size is observed for Ru(0) in Y zeolites [12] (Table 6).

In the case of $\text{Mo}/\text{HNa-Y}$, the dispersion of molybdenum is certainly high (see 4-3). I can, therefore, expect a similar increase in the binding energies of molybdenum in the $\text{Mo}/\text{HNa-Y}$.

It is clear that the peak at 233.0 eV (Fig. 13, d) corresponds to Mo(VI), because the binding energies of Mo(VI) in some compounds (Table 5) were below 233.0 eV. This assignment is confirmed by the fact that the color of the sample (Fig. 13, d) was white. From Fig. 13 and Table 5, the differences in the Mo(VI) binding energies between $\text{Mo}/\text{HNa-Y}$ and Mo compounds were 0.3 - 0.6 eV. Assuming that the same difference exists in the case of Mo(IV), I can attribute the peak at 230.5 eV (Fig. 13, c) to Mo(IV). From these assignments, the peak at about 229.5 eV (Fig. 13, b) clearly corresponds to the Mo species whose oxidation numbers are +1 - +3. From Table 5, the binding energies of Mo(III) and Mo(II) in molybdenum chlorides were lower than that of Mo(IV) in MoCl_4 by 0.6 - 0.7 eV and 1.1 eV, respectively. The binding energy of the peak at 229.5 eV was lower by 1.0 eV than

Table 6

Binding energy shifts in XPS spectra of various metals in zeolites

| Catalyst | Supported metal or cation | Binding energy Inside of zeolite | Binding energy Metal or compound | Reference |
|----------|---------------------------|--|----------------------------------|-----------|
| Mo/HNa-Y | Mo ⁶⁺ (3d 5/2) | 233.0 | 232.4 | This work |
| Pt/Na-Y | Pt ⁰ (4f 7/2) | 72.8 ^a 72.2 ^b | 71.5 | [11] |
| Ru/Na-Y | Ru ⁰ (3d 5/2) | 281.0 ^c 280.1 ^d | 280.0 ^e | [12] |
| | Ru ⁴⁺ (3d 5/2) | 281.9 | 281.0 ^f | [12] |
| NiNa-X | Ni ²⁺ (2p 3/2) | 857.6 | 852.1 - 856.5 | [13] |
| NiHZSM-5 | Ni ²⁺ (2p 3/2) | 856.5 | 855.8 | [14] |

^a Atomically dispersed Pt⁰ ^b Particles (diameter = 10 - 20 A)

^c Particles (diameter 10 A) ^d Particles (diameter 15 A)

^e Particles (diameter 250 A) on the external surface of Na-Y

^f RuO₂ on the external surface of Na-Y

that of the Mo(IV) peak in Mo/HNa-Y. Therefore, I can attribute the peak at 229.5 eV to Mo(II).

In these assignments, each binding energy is rather high compared with that in the corresponding Mo compound. Similar positive shifts of binding energies have been reported for metal cations in zeolites, as shown in Table 6. Pedersen and Lunsford [12] have reported that the Ru $3d_{5/2}$ binding energy for RuO₂ particles within the zeolite cage is higher by 0.9 eV than that located on the external surface of the zeolite. They have attributed this change in the binding energy to the metal-support interaction and the matrix effects of the zeolite, such as differences in the crystal field potential energy. In the case of NiNaX [13] and NiHZSM-5 [14], the positive shifts in Ni $2p_{3/2}$ binding energies are 1.1 eV and 0.7 eV, respectively, compared with Ni(II) compounds. Taking into account these investigations, I consider my assignments of the Mo $3d_{5/2}$ binding energies to be reasonable.

From the above assignments, it is concluded that Mo/Na-Y (Fig. 13, a) contains a considerable amount of Mo(0), and that Mo/H(65)Na-Y (Fig. 13, b) contains the Mo species whose oxidation numbers are 0 and +2. It is clear that the hydroxyl groups of H(65)Na-Y zeolite oxidize the Mo species to increase their oxidation numbers from 0 to +2. After oxidation at room temperature with air (Fig. 13, c), Mo(IV) is mainly formed, and further oxidation at 250°C converts all the Mo species to Mo(VI). The AONs of the samples a, b and c in Fig. 13 were 0.25, 0.61 and 2.7, respectively. These values are somewhat lower than those

estimated from the XPS spectra. However, the same tendencies are observed, that is, Mo(0) exists in Mo/Na-Y and some Mo species in Mo/HNa-Y have higher oxidation states than those in Mo/Na-Y.

An XPS study of Mo/Na-Y and Pt-Mo/Y prepared from Mo(CO)₆ has been carried out by Tri et al. [15]. They have reported that only Mo(IV), Mo(V) and Mo(VI) are detected, even in the Pt-containing samples. Because their samples were exposed to air and subsequently reduced by H₂ before the XPS measurements, I suppose that the oxidation state of Mo in the sample without exposure to air is lower than Mo(IV).

I conclude from my in situ XPS studies that the dominant Mo species in Mo/HNa-Y prepared from Mo(CO)₆ and HNa-Y zeolites have oxidation numbers of 0 and +2. When Na-Y is used as a support, the lack of surface hydroxyl groups in Na-Y results in the formation of nearly homogeneous Mo(0) species.

3-3-3 Adsorption of CO

The adsorption of CO provides some information about the oxidation state, the coordinative unsaturation, the structural environment, etc. of the metal as a adsorption site. IR spectroscopy is one of the vibrational spectroscopy which is used to characterize the metal or oxide surface with probe molecules such as CO, NO, NH₃, etc.. Many reports have referred to the IR spectra of CO adsorbed on some transition metals or their oxides. When CO is adsorbed on the metal atom through the M-CO σ -bond, the back donation of d-electron in the metal to the antibonding π^* -orbital occurs simultaneously. This back donation weakens the

C-O bond, which leads to the lower frequency of its IR absorption band. Therefore, the IR band of adsorbed CO provides the certain information about the oxidation state of metals.

Figure 14 shows the IR spectra of CO adsorbed on Mo/H(65)Na-Y. Addition of 50 torr of CO onto Mo/H(65)Na-Y (spectrum a) caused the intense absorption bands as indicated in spectrum (b). New peaks at 2163, 2132, 2084 and 2037 cm^{-1} and a broad band around 1970 cm^{-1} appeared. The evacuation at room temperature for 5 s (spectrum c) and for 10 min (spectrum d) led to the drastic decrease in intensity of the peak at 2163 cm^{-1} . It is found that this band is attributed to the physisorbed CO and that the other bands are attributed to the chemisorbed CO. By further evacuation at 100°C, all of the CO bands, especially higher frequency bands (2132 and 2084 cm^{-1}), decreased in intensity.

IR spectra of chemisorbed CO on various kinds of Mo/HNa-Y are shown in Fig. 15. When CO was adsorbed on Mo/H(36)Na-Y, two peaks were observed at 2130 and 1977 cm^{-1} (Fig. 15, b). These two bands were also observed on Mo/H(65)Na-Y (spectrum a). On the other hand, CO adsorbed on Mo/H(74)Na-Y which has a higher AON of Mo exhibited a IR band at 2161 cm^{-1} with a shoulder at about 2180 cm^{-1} . Additional $\text{Mo}(\text{CO})_6$ was adsorbed and decomposed on this Mo/H(74)Na-Y in the similar manner to that mentioned previously (2-3-2), and the IR spectrum of CO adsorbed on the resultant Mo/H(74)Na-Y was measured (spectrum d). Three bands at 2183, 2132 and 2025 cm^{-1} were observed. The last two bands were similar to those in the spectrum (a) (2132 and 2037 cm^{-1} , respectively).

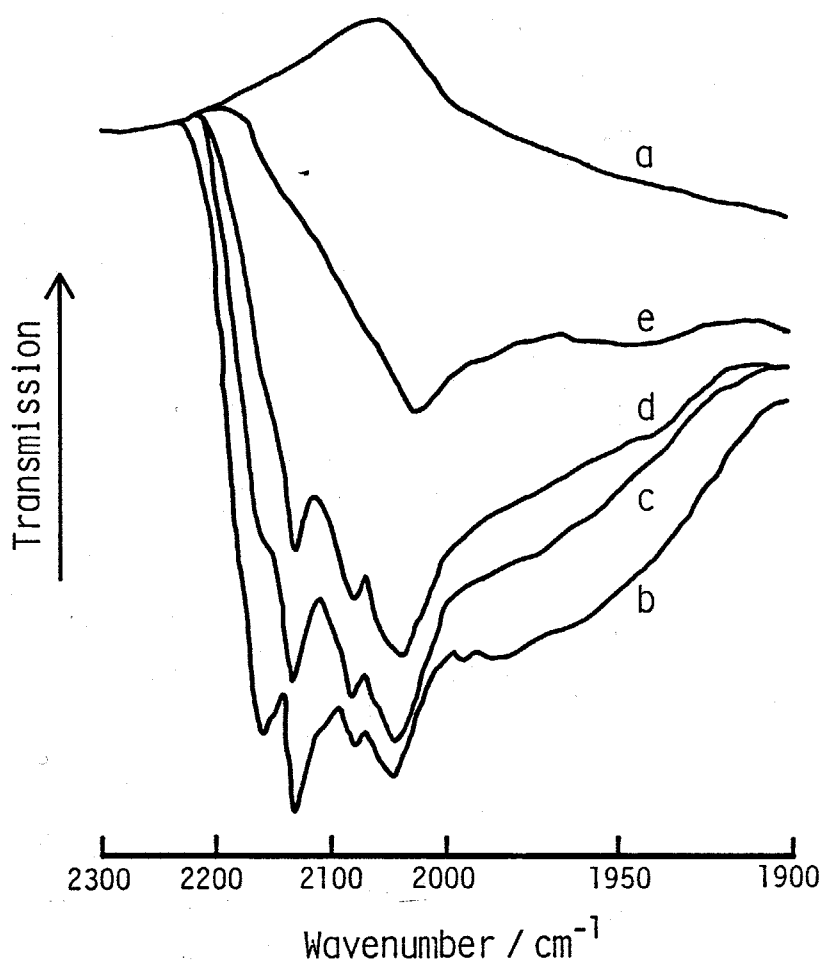


Fig. 14 IR spectra of CO adsorbed on Mo/H(65)Na-Y
 a: Mo/H(65)Na-Y; dehydration temperature was 400°C
 decomposition temperature was 300°C
 b: Sample a exposed to 50 torr of CO
 c: Sample b evacuated at 25°C for 5 s
 d: Sample c evacuated at 25°C for 10 min
 e: Sample d evacuated at 100°C for 10 min

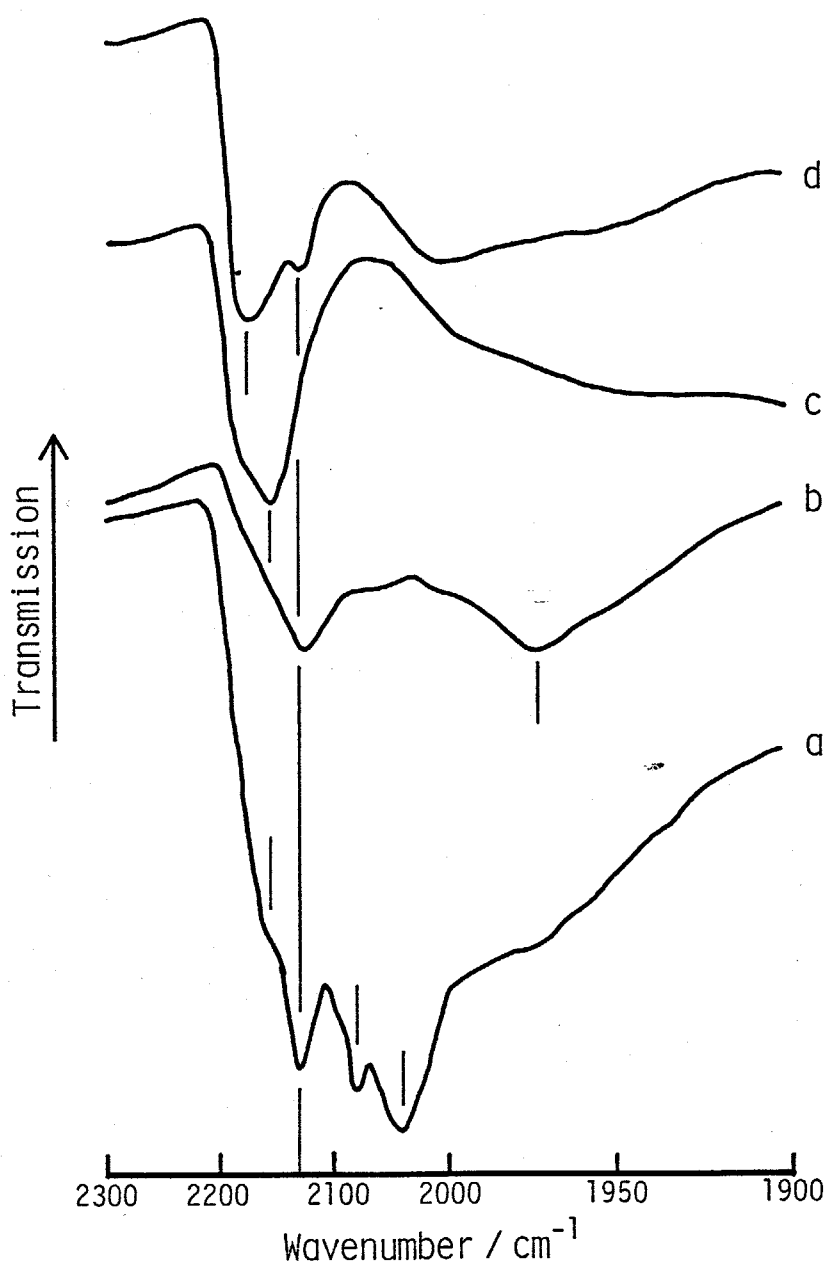


Fig. 15 IR spectra of CO adsorbed on various Mo/HNa-Y
 Spectra were recorded after 50 torr of CO was adsorbed
 and then pumped out at 25°C for 5 s.
 a: Mo/H(65)Na-Y; AON of Mo was 1.0
 b: Mo/H(36)Na-Y; AON of Mo was 0.6
 c: Mo/H(74)Na-Y; AON of Mo was 2.5
 d: Additional Mo(CO)₆ was adsorbed on sample c and
 then decomposed at 300°C

Kung and Kung [16] have reviewed the IR studies of the CO adsorbed on the surface of various oxides and indicated the wavenumbers of the IR bands. From their review, CO adsorbed on M^+ exhibits the IR band at $2170 - 2130 \text{ cm}^{-1}$, while CO adsorbed on M^{2+} and M^{3+} exhibits the band above 2172 cm^{-1} . Lokhov and Davydov [17] have reported from their IR studies that the wavenumbers of the IR bands for $M^0\text{CO}$ are below 2100 cm^{-1} , those for $M^+\text{CO}$ are in the region of $2120 - 2160 \text{ cm}^{-1}$, and those for $M^{2+}\text{CO}$ are above 2170 cm^{-1} . Considering these reports, I assign the bands at 1977 cm^{-1} (Fig. 15, b), $2025 - 2037 \text{ cm}^{-1}$ (a,d) and 2084 cm^{-1} (a) all to CO on Mo(0), while I assign the bands at $2129 - 2132 \text{ cm}^{-1}$ (a,b,d) and $2161 - 2163 \text{ cm}^{-1}$ (a,c) to CO on Mo(I). The band at 2183 cm^{-1} observed in the spectra (a), (c) and (d) in Fig. 15 is assigned to the CO adsorbed on the Mo species whose oxidation number is +2 or more.

From above assignments, it is suggested that the Mo/H(65)Na-Y (Fig. 15, a) and Mo/H(36)Na-Y (b) consist of mainly Mo(0) and Mo(I). The AON of Mo in these samples determined by the O_2 titration method were +1.0 and +0.6, respectively. Therefore, the existence of Mo(0) and Mo(I) suggested by the IR spectra are reasonable for these Mo/HNa-Y, but their proportion is not clear because the extinction coefficients of the individual CO are not known. The bridging CO on metals gives its IR band below 2000 cm^{-1} . Consequently, the band at 1977 cm^{-1} are assigned to the bridging CO on metallic Mo. This assignment is consistent with the result in chapter 4 that the Mo species on H(36)Na-Y support are aggregated to form Mo(0) clusters.

Repeated loading of Mo on Mo/H(74)Na-Y caused the new CO

band at 2025 cm^{-1} (Fig. 15, d). During the second loading, molybdenum may be less oxidized because the OH groups were already consumed by the reaction with Mo in the first loading. Therefore, the assignment of this band to Mo(0)CO is reasonable. However, the difference between the two Mo(0)CO bands in the spectrum (a) cannot be explained.

Perl [2] has measured the IR spectra of adsorbed CO on some reduced MoO₃/Al₂O₃ catalysts. He observed the IR band at 2190 cm^{-1} on the catalyst reduced at 700°C with hydrogen and two bands at 2040 and 2025 cm^{-1} on that reduced at 800°C. He attributed the former band to Mo(IV)CO and the latter bands to Mo(0)CO. This is consistent with my assignments, except that the exact oxidation number of Mo corresponding to the higher frequency CO band is not clear.

In addition to the previous XPS study, the IR study on the adsorbed CO ensures the existence of Mo(0) species. However, instead of Mo(II) which is suggested to consist in Mo/H(65)Na-Y, Mo(I) is suggested to exist from the IR spectra of CO adsorbed on the Mo/H(65)Na-Y though the existence of Mo(II) is not excluded from the IR spectra because CO molecules are adsorbed more weakly on Moⁿ⁺ ($n \geq 2$) than on Mo(0) or Mo(I).

3-3-4 ESR study

Because Mo(V) is an ESR active species, ESR spectra have been widely used for the characterization of molybdenum supported catalysts. It has been often reported that the catalytic activity for such reactions as the olefin hydrogenation, etc. is gene-

rated when the calcined MoO_3 supported catalysts are reduced. Some reports have been referred to the relation between the amount of Mo(V) and the catalytic activity [18 - 20]. In the case of Mo/HNa-Y, the AON of Mo is always below +4 without the oxidation by O_2 (see 3-3-1). However, the oxidation state is suggested to be heterogeneous as mentioned in the previous sections (3-3-1 - 3-3-3). Therefore, it is possible that Mo/HNa-Y contains a significant amount of Mo(V) species. Figure 16 shows the X-band ESR spectra of various kinds of Mo/HNa-Y measured at -196°C on the JEOL JFS-PE-IX spectrometer. Spectrum (a) measured for Mo/H(82)Na-Y (AON = +3.8) had a peak ($g_{\perp} = 1.948, g_{\parallel} = 1.883$). Table 7 shows the g-values of the ESR spectra attributed to Mo(V) reported with other molybdenum supported catalysts [21 - 24]. Comparing my data with other g-values, I assign the spectrum (a) to the ESR peak of Mo(V) species. Spectrum (b) was obtained after the oxidation of Mo/H(82)Na-Y (spectrum a) by air at room temperature. The peak attributed to Mo(V) ($g_{\perp} = 1.949, g_{\parallel} = 1.882$) was nearly the same as spectrum (a), but an additional peak ($g = 2.008$) appeared. This additional peak had a similar g-value to g_2 of O_2^- species formed on other molybdenum supported catalysts [22 - 25], so that it is assigned to the O_2^- on Mo/H(82)Na-Y. The amounts of Mo(V) in Mo/HNa-Y were calculated by the double integration of the ESR spectra as shown in Fig, 16. The fraction of Mo(V) did not change so much during the oxidation at room temperature. Consequently, it is found that little Mo(V) is formed by the oxidation at room temperature. Spectrum (c) was measured with Mo/H(82)Na-Y which consists of less oxidized Mo species (AON = +1.10). Only a weak signal ($g =$

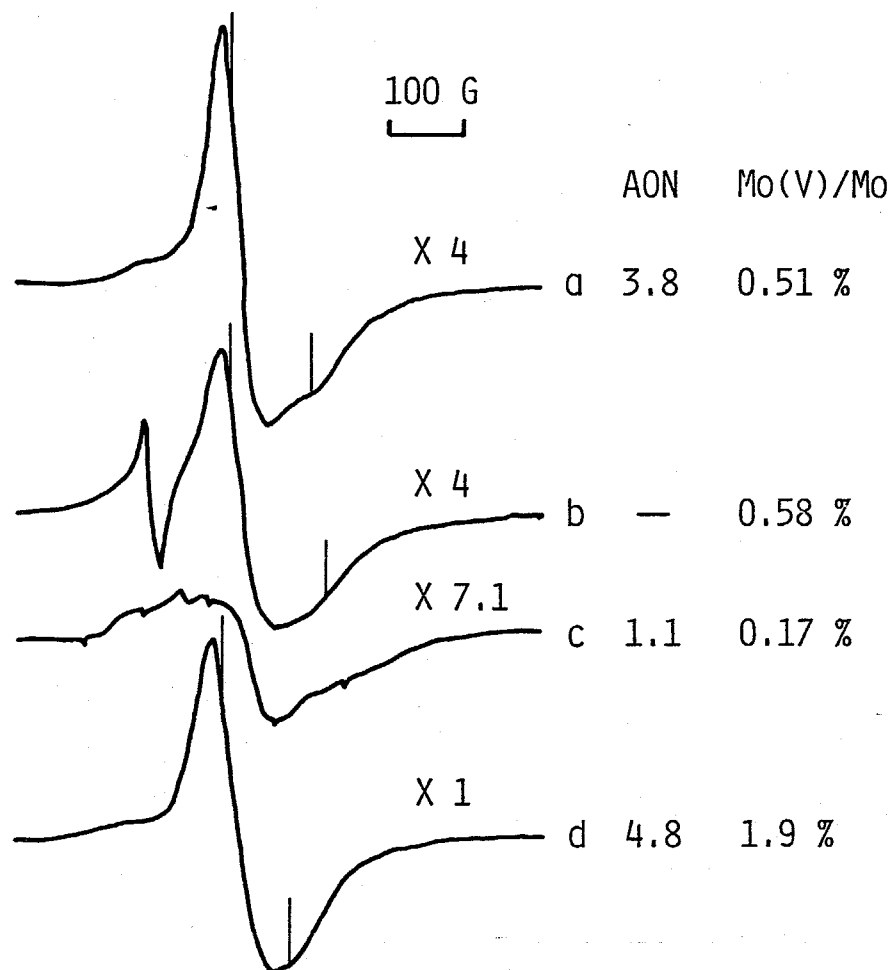


Fig. 16 ESR spectra of Mo/H(82)Na-Y

- a: Dehydration, 200°C; decomposition, 300°C
- b: Sample a exposed to air at 25°C
- c: Dehydration, 400°C; decomposition, 300°C
- d: Sample c reduced at 500°C after oxidation at 500°C

Table 7
ESR data of Mo(V) species in Mo supported catalysts

| Catalyst | g _I | g _{II} | Reference |
|--|------------------|------------------|-----------|
| Mo(CO) ₆ /H(82)Na-Y decomposed at 300°C | 1.948 - 1.949 | 1.882 - 1.883 | This work |
| Mo(CO) ₆ /H(80)Na-Y decomposed at 400°C | 1.96 | 1.88 | [21] |
| Mo(CO) ₆ /Al ₂ O ₃ decomposed at 400°C | 1.954 | 1.897 | [22] |
| MoO ₃ /Al ₂ O ₃ reduced at 500°C | 1.943 | 1.900 | [23] |
| MoCl ₅ /HNa-Y decomposed at 400°C | 1.956 | 1.884 | [24] |

ca. 1.95) was detected. After the oxidation of this Mo/H(82)Na-Y (spectrum c) at 500°C and the subsequent reduction at 500°C, spectrum (d) was obtained ($g_{\perp} = 1.946$, $g_{\parallel} = 1.902$). This signal is also attributed to Mo(V) species, but the g-values were slightly different from the spectrum (a). This may be due to the different environment of the Mo(V) species due to the treatment at the high temperature. The fraction of Mo(V) in the reduced sample (spectrum d) corresponded to 1.9 % of the total Mo, while the AON of Mo was +4.8. The fraction of Mo(V) calculated from the ESR spectrum seems low compared with the AON. Such a difference in the Mo(V) concentration has been reported to result from the formation of ESR inactive Mo(V) pairs for MoO₃/Al₂O₃ catalysts [26,27]. In the case of Mo/HNa-Y, two Mo(CO)₆ molecules are adsorbed per supercage of HNa-Y, so that such a Mo(V) pair seems possible to be formed. Thus only a small amount of Mo(V) species which are detected by ESR are found to consist in Mo/HNa-Y.

3-4 Conclusion

During the thermal decomposition of Mo(CO)₆ adsorbed on HNa-Y zeolites, molybdenum is oxidized by the hydroxyl groups of zeolites. By controlling this oxidation, the oxidation state of the supported molybdenum can be widely altered. The higher oxidation states are obtained under the following conditions;

- (a) Low dehydration temperature of HNa-Y zeolites
- (b) High degree of proton exchange in Y zeolites

(c) High decomposition temperature of $\text{Mo}(\text{CO})_6/\text{HNa-Y}$

The average oxidation number of molybdenum is adjusted in the range from +0.3 to +3.8 by changing above conditions. Thus the Mo species with the low oxidation states (AON < 4) which can hardly be prepared by the reduction of $\text{MoO}_3/\text{Al}_2\text{O}_3$ under mild conditions can be prepared. The Mo species in $\text{Mo}/\text{HNa-Y}$ can be oxidized easily up to Mo(VI) by O_2 treatments. Therefore, it may be possible to clarify the catalytic properties of molybdenum in the low oxidation states by using $\text{Mo}/\text{HNa-Y}$ as a catalyst and by comparing with the catalytic properties of Mo(IV) - Mo(VI).

From the in situ XPS spectra, it is found that Mo(0) is mainly formed on the Na-Y support and that $\text{Mo}/\text{H}(65)\text{Na-Y}$ contains Mo(0) and Mo(II). The presence of Mo(0) species is also indicated by the IR spectra of adsorbed CO. However, the results of the IR study suggest that $\text{Mo}/\text{H}(65)\text{Na-Y}$ contains Mo(I) species as well as Mo(0) and Mo^{n+} ($n \geq 2$). In addition, these characterizations imply the heterogeneity in the oxidation state of molybdenum. This heterogeneity is also suggested by the fact that most of $\text{Mo}/\text{HNa-Y}$ does not exhibit an integral AON. However, ESR study reveals that little Mo(V) is formed during the decomposition of $\text{Mo}(\text{CO})_6/\text{HNa-Y}$.

References

- 1 R. Nakamura, R. G. Bowman and R. L. Burwell, Jr., *J. Am. Chem. Soc.*, 103, 673 (1981); R. Nakamura, D. Pioch, R. G. Bowman and R. L. Burwell, Jr., *J. Catal.*, 93, 388 (1985)
- 2 J. B. Perl, *J. Phys. Chem.*, 86, 1615 (1982)
- 3 R. G. Bowman and R. L. Burwell, Jr., *J. Catal.*, 63, 463 (1980)
- 4 P. A. Jacobs, "Carboniogenic Activity of Zeolite", Elsevier Sci. Pub. Co., Amsterdam, 1977, p. 59
- 5 Y. I. Yermakov and B. N. Kuznetsov, Prepr. 2nd Japan-Soviet Catalysis Seminar, (Tokyo, 1973), p. 65
- 6 G. Leclercq, T. Romero, S. Pietrzyk, J. Grimblot and L. Leclercq, *J. Mol. Catal.*, 25, 67 (1984)
- 7 S. O. Grim and L. J. Matienzo, *Inorg. Chem.*, 14, 1014 (1975)
- 8 A. D. Hammer and R. A. Walton, *Inorg. Chem.*, 13, 1446 (1974)
- 9 T. A. Patterson, J. C. Carver, D. E. Leyden and D. M. Hercules, *J. Phys. Chem.*, 80, 1700 (1976)
- 10 W. E. Swartz, Jr. and D. M. Hercules, *Anal. Chem.*, 43, 1774 (1971)
- 11 J. C. Vedrine, M. Dufaux, C. Naccacha and B. Imelik, *J. Chem. Soc., Faraday Trans. I*, 74, 440 (1978)
- 12 L. A. Pedersen and J. H. Lunsford, *J. Catal.*, 61, 39 (1980)
- 13 J. Strutz, H. Diegruber, N. I. Jaeger and R. Moseler, *Zeolites*, 3, 102 (1983)
- 14 S. Badrinarayanan, R. I. Hegde, I. Balakrishnan, S. B. Kulkarni and P. Ratnasamy, *J. Catal.*, 71, 439 (1981)
- 15 T. M. Tri, J. -P. Candy, F. Gallezot, J. Massardier, M. Primet, J. C. Vedrine and B. Imelik, *J. Catal.*, 79, 396 (1983)

- 16 M. C. Kung and H. H. Kung, *Catal. Rev. Sci. Eng.*, 27, 425 (1985)
- 17 Y. A. Lakhov and A. A. Davydov, *Kinet. Catal.*, 21, 1093 (1980)
- 18 N. Giordano, M. Padovan, A. Vaghi, J. C. J. Bart and A. Castellan, *J. Catal.*, 38, 1 (1975)
- 19 R. V. Morris, D. R. Waywell and J. W. Shepard, *J. Less-Common Metals*, 36, 395 (1974)
- 20 K. Hashimoto, S. Watanabe and K. Tarama, *Bull. Chem. Soc. Japan*, 49, 12 (1976)
- 21 S. Abdo and R. F. Howe, *J. Phys. Chem.*, 87, 1722 (1983)
- 22 R. F. Howe and I. R. Leith, *J. Chem. Soc., Faraday Trans. I*, 69, 1967 (1973)
- 23 K. S. Seshadri and L. Petrakis, *J. Catal.*, 30, 195 (1973)
- 24 P. -S. E. Dai and J. H. Lunsford, *J. Catal.*, 64, 173 (1980)
- 25 O. V. Krylov, G. B. Pariiskii and K. N. Spiridonov, *J. Catal.*, 23, 301 (1971)
- 26 S. Abdo, R. B. Clarkson and W. K. Hall, *J. Phys. Chem.*, 80, 2431 (1976); S. Abdo, A. Kazusaka and R. F. Howe, *ibid.*, 85, 1380 (1981)
- 27 H. Weigold, *J. Catal.*, 83, 85 (1983)

Chapter 4 Dispersion of molybdenum

4-1 Introduction

In the case of MoO_3 supported catalysts, the dispersion of molybdenum has been one of the main subjects to be studied. It has been generally reported that the dispersion of molybdenum becomes lower with increasing the content of molybdenum. If large particles of MoO_3 are present, the dispersion can be estimated by transmission electron microscopy or X-ray diffraction. However, when the content of Mo corresponds to monolayer coverage or less, the dispersion of Mo is often too high to be determined by these techniques.

The chemisorption of oxygen has been reported to provide certain informations about the dispersion of Mo for the MoO_3 supported catalysts. Reduction or sulfidation of the supported MoO_3 leads to the formation of O_2 chemisorption sites. These chemisorption sites are thought to be the coordinatively unsaturated sites (CUS) on Mo(IV) [1,2] or parts of the CUS [3]. Parekh and Weller [4] have determined the surface area of Mo species supported on alumina from the amount of chemisorbed oxygen regarding the Mo species after reduction as the crystalline MoO_2 . About a quarter of the alumina surface was covered with the Mo species even if the content of MoO_3 corresponded to above monolayer coverage. They have suggested that the dispersion of Mo is low.

In the first step of the preparation of Mo/HNa-Y, $\text{Mo}(\text{CO})_6$ molecules are dispersed within the zeolite crystallites in the ratio of two molecules per supercage of HNa-Y, so that the dis-

persion of Mo is 100 %. When the CO ligands are removed through the thermal decomposition, the migration of molybdenum may occur if the interaction between molybdenum and the support is weak. Consequently, the dispersion may become less than 100 % during the decomposition.

In this chapter, I discuss the dispersion of the supported molybdenum from the results of the chemisorption of oxygen on Mo/HNa-Y and the ultraviolet spectra of the oxidized Mo/HNa-Y.

4-2 Experimental

4-2-1 Chemisorption of oxygen

The amount of chemisorbed oxygen was measured with a static system. A specific amount of HNa-Y (0.4 g) was placed in a quartz tube, and Mo/HNa-Y was prepared in the same manner described previously (see 2-2-2). At a certain temperature, a known amount of oxygen was introduced onto the Mo/HNa-Y and the first adsorption isotherm was obtained. The Mo/HNa-Y was evacuated for 30 min at this temperature except that the evacuation temperature was -78°C when the adsorption was carried out at -190°C . The second isotherm was then obtained at the same adsorption temperature. The amount of the chemisorbed oxygen was calculated from the difference between the two isotherms and was expressed in terms of the number of the adsorbed oxygen atoms per Mo atom (O/Mo).

4-2-2 Ultraviolet spectroscopy

The diffuse reflectance technique was used on a Shimadzu

UV-240 spectrometer to obtain the ultraviolet (UV) spectra.

HNa-Y (28 - 60 mesh) was put into a Pyrex tube having a branch of quartz UV cell. After Mo/HNa-Y was prepared in the tube, molybdenum was oxidized by O_2 at $400^\circ C$. Then Mo(VI)/HNa-Y sample was transferred into the quartz cell in vacuo. The UV-diffuse reflectance spectra were recorded at room temperature in the range of 190 - 700 nm using the parent HNa-Y as a reference.

4-3 Results and discussion

4-3-1 Chemisorption of oxygen

The chemisorption of oxygen has been applied to some MoO_3 supported catalysts in order to get the information about the dispersion of molybdenum. In the case of MoO_3/Al_2O_3 catalysts, it has been reported that the adsorption manner of oxygen differs significantly depending on the adsorption temperature [4]. I measured the amount of chemisorbed oxygen on Mo/HNa-Y at various temperatures to determine the effect of the adsorption temperature. The results are shown in Fig. 17. Irrespective of the temperature, the amount of chemisorbed oxygen on Mo/H(74)Na-Y was nearly constant ($O/Mo \approx 1.2$). Assuming that one oxygen atom is chemisorbed on one Mo atom, the dispersion of Mo corresponds to about 100 %, though parts of the oxygen seem to be chemisorbed in the ratio of $O/Mo > 1$. It has been reported for the MoO_3/Al_2O_3 catalysts that one oxygen atom is chemisorbed on one CUS [1], that is, the stoichiometry of the chemisorption is $O/Mo = 1$. In these catalysts, the oxidation numbers of Mo are mainly +4 and +5, so that this stoichiometry of chemisorption cannot be applied

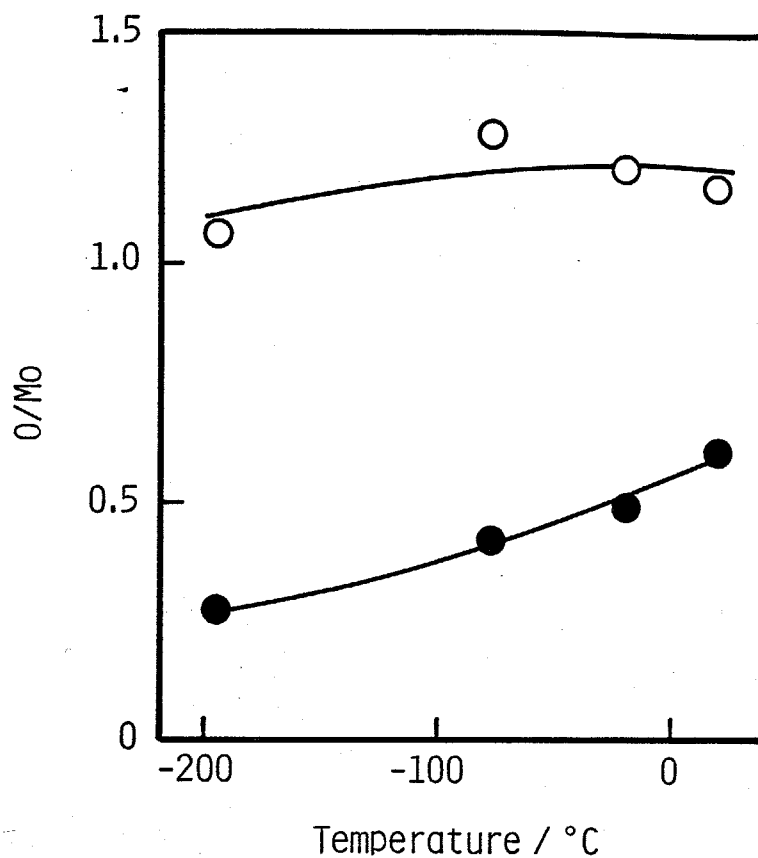


Fig. 17 Effect of adsorption temperature on the amount of chemisorbed oxygen

● : Mo/Na-Y ○ : Mo/H(74)Na-Y
 Dehydration temperature of Y zeolite: 300°C
 Decomposition temperature of Mo(CO)₆: 300°C
 Mo content: 2 Mo-atoms/supercage

directly to the Mo/HNa-Y which contains the Mo species of lower oxidation numbers than +4. Yermakov et.al. [5] and Iwasawa et. al. [6] have reported that on the catalysts prepared from π -allyl complexes, oxygen is consumed on Mo(II) species in the ratio of O/Mo = 1 at room temperature. In the case of the Mo metal, however, oxygen was adsorbed on the Mo (100) face in the ratio of O/Mo = 1.5 at room temperature [7]. I discuss this stoichiometry taking into account the results from UV-spectra in the next section.

In the case of Mo/Na-Y, Fig. 17 clearly shows that the less amount of oxygen was chemisorbed compared with Mo/H(74)Na-Y. This indicates the lower dispersion of Mo in the Mo/Na-Y. The O/Mo ratio increased with increasing the adsorption temperature. When a certain amount of O₂ was introduced onto the Mo/Na-Y at 25°C, the O₂ uptake increased gradually for more than 40 hours and the O/Mo ratio became more than twice as much as that measured at -196°C. These results indicate that the oxidation of molybdenum in bulk phase occurs at higher temperatures. Consequently, in order to determine the amount of the surface Mo, it is better to adsorb oxygen at -196°C.

The low O/Mo ratios for Mo/Na-Y imply the correlation between the dispersion of Mo and the proton concentration of HNa-Y. Figure 18 shows the amount of oxygen chemisorbed on Mo/HNa-Y with various degrees of proton exchange in Y zeolites. The oxygen chemisorption was carried out at -196°C. When the degree of proton exchange was 65 or 74 %, the O/Mo ratio was about 1, which indicates the high dispersion of Mo. However, the O/Mo

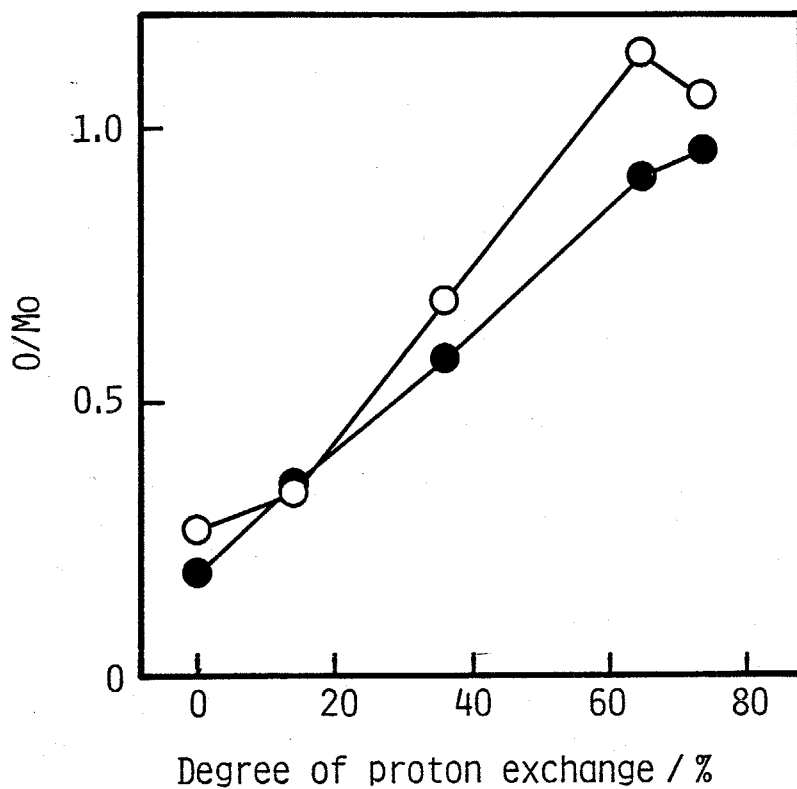


Fig. 18 Effect of the degree of proton exchange in Y zeolites on the amount of chemisorbed oxygen

Dehydration temperature of Y zeolite:

○ : 300°C ● : 500°C

Decomposition temperature of $\text{Mo}(\text{CO})_6$: 300°C

Mo content: 2 Mo-atoms/supercage

Adsorption temperature of oxygen: -196°C

ratio decreased with decreasing the degree of proton exchange below 65 %. This is attributed to the aggregation of Mo. In addition, the dehydration temperature of HNa-Y had an effect on the amount of chemisorbed oxygen, that is, the O/Mo ratio was low when the dehydration temperature was high. The dehydration at 500°C should cause the decrease in the concentration of the OH groups, so that it corresponds to lowering the degree of proton exchange. Thus the lower proton concentration in Y zeolites leads to the decrease in the amount of chemisorbed oxygen, probably because free Mo(0) atoms which are formed by the decomposition of Mo(CO)₆ and are not oxidized by the OH groups can migrate to form aggregates.

Table 8 shows the amount of chemisorbed oxygen (O/Mo) measured with two Mo/HNa-Y samples in which Mo species with higher oxidation states are contained. The O/Mo ratios measured with MoO₃ supported catalysts [1,4,8,9,] are also shown in Table 8. In the case of Mo/H(74)Na-Y oxidized to Mo(VI) and subsequently reduced with H₂ at 500°C, the O/Mo ratio was rather low compared with the Mo/H(82)Na-Y, though two samples had nearly the same AON of Mo. Therefore, the aggregation might occur during the oxidation and/or the reduction at the high temperatures. The MoO₃ supported catalysts exhibit lower O/Mo ratios than the reduced Mo(VI)/H(74)Na-Y, which indicates the more extensive aggregation of Mo species in the former catalysts. It is found that the Mo/HNa-Y system has an advantage to obtaining the high dispersion of Mo compared with the MoO₃ supported catalysts.

Table 8
Amounts of oxygen chemisorbed on various molybdenum supported catalysts

| Catalyst | Amount of chemisorbed oxygen: O/Mo | Reference |
|---|------------------------------------|-----------|
| Mo/H(82)Na-Y (AON = 2.3) | 0.78 | This work |
| Reduced Mo ⁶⁺ /H(74)Na-Y (AON = 2.6) ^a | 0.38 | This work |
| Reduced MoO ₃ /Al ₂ O ₃ | 0.21 - 0.34 | [1,4,8] |
| Reduced MoO ₃ /SiO ₂ | 0.26 | [9] |
| Reduced MoO ₃ /CeO ₂ | 0.29 | [9] |

^a Mo/H(74)Na-Y was oxidized at 400°C followed by reduction at 500°C

4-3-2 Ultraviolet spectra

I studied the dispersion of molybdenum also by ultraviolet diffuse reflectance spectroscopy. It has been reported [10,11] that Mo(VI) with tetrahedrally and octahedrally coordinated O^{2-} exhibits UV absorption bands at 260 - 280 nm and 300 - 320 nm, respectively. An additional band at 220 - 240 nm is common to the tetrahedral and octahedral configurations. These bands are attributed to the charge transfer from O^{2-} to Mo(VI). The Mo(VI) species in the tetrahedral configuration are thought to be monomeric or dimeric species, while those in the octahedral configuration are attributed to polymeric species with bridging O^{2-} [12].

Figure 19 shows the UV diffuse reflectance spectra of two different Mo/HNa-Y measured after the oxidation of all the Mo species to Mo(VI). The spectra of sodium molybdate (a) and ammonium paramolybdate (c) are also shown. The spectrum of Mo(VI)/H(65)Na-Y (b) had a peak at about 255 nm and a shoulder at about 220 nm similarly to the spectrum of sodium molybdate (a) which consists of the tetrahedrally coordinated molybdenum. The spectrum of Mo(VI)/Na-Y (d) had a peak at about 295 nm and three shoulders at about 230, 270 and 320 nm. Ammonium paramolybdate which consists of the octahedrally coordinated molybdenum exhibited two absorption peaks at about 260 and 295 nm and two shoulders at about 220 and 320 nm.

It is clear that the Mo species in Mo(VI)/H(65)Na-Y consist almost exclusively of the tetrahedrally coordinated molybdenum. Therefore, the Mo species in this sample should be dispersed on the zeolite corresponding to the monolayer coverage

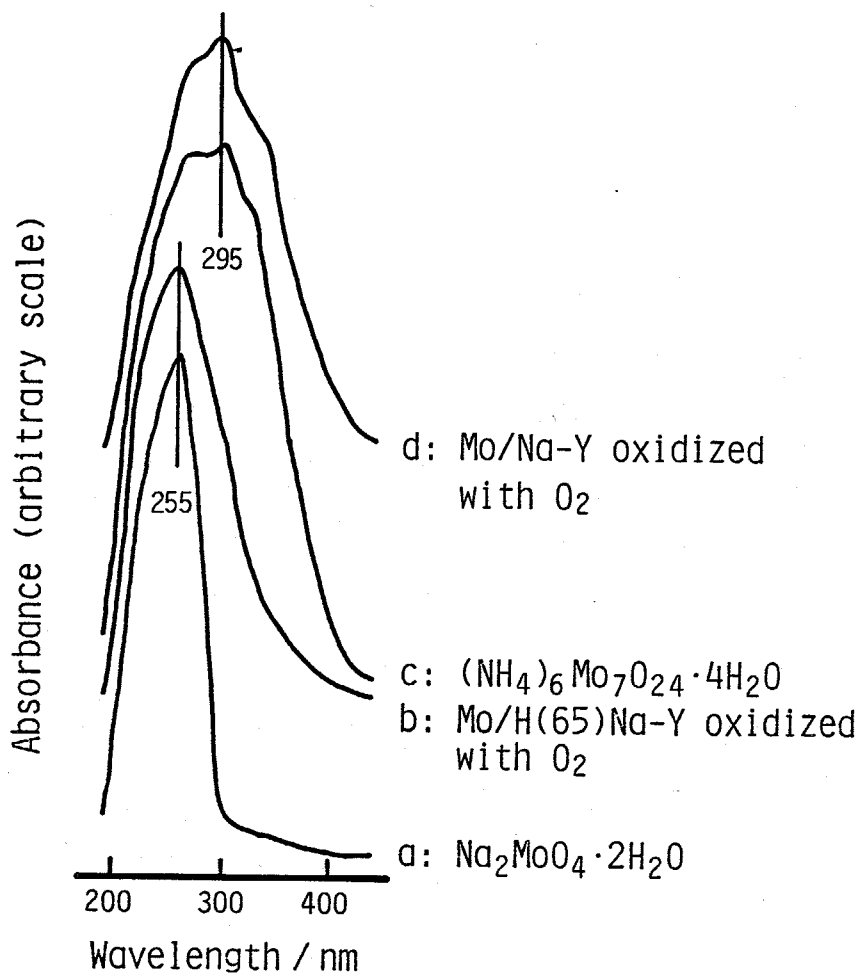


Fig. 19 UV diffuse reflectance spectra

or less. It seems impossible that the redispersion of Mo atoms in aggregates occurs during the oxidation of Mo/H(65)Na-Y, so that the dispersion of molybdenum in the Mo/H(65)Na-Y before oxidation is nearly 100 %. As mentioned in the previous section (4-3-1), the amount of chemisorbed oxygen on the Mo/H(65)Na-Y at -196°C corresponded to $\text{O}/\text{Mo} = \text{ca. } 1$. Therefore, the previous assumption that the O/Mo stoichiometry is 1 for the chemisorption of oxygen at -196°C (see 4-3-1) is found to be reasonable.

It seems that most of the Mo species in Mo(VI)/Na-Y have the octahedral coordination, that is, the Mo species are probably aggregated to form bulk oxide. The bulk MoO_3 phase in $\text{MoO}_3/\text{Al}_2\text{O}_3$ catalysts can be detected by Raman spectroscopy. It has been reported that the Raman peaks at about 820 and 1000 cm^{-1} are attributed to the bulk MoO_3 on alumina [11,13] or titania [14]. However, I could not obtain significant Raman spectra of Mo(VI)/HNa-Y because of the intense background.

When the Mo(0) cluster with a considerable size is oxidized at a high temperature, the framework of the zeolite may hinder the formation of bulk MoO_3 , because the formation of MoO_3 is accompanied with the increase in the particle size. This consideration was confirmed by two findings. First, the oxidation of molybdenum on Na-Y proceeded slowly compared with Mo/H(65)Na-Y or Mo/H(74)Na-Y. Second, after the oxidation of Mo/Na-Y, its surface area decreased by about $200 \text{ m}^2/\text{g}$, while that of Mo/H(74)Na-Y did not change during the oxidation. These findings imply that the partial destruction of the framework of Y zeolite results from the formation of the bulk MoO_3 .

4-4 Conclusion

The dispersion of the supported molybdenum is estimated from the results of the oxygen chemisorption and the ultraviolet diffuse reflectance spectra. The amount of chemisorbed oxygen at -196°C corresponds to the number of Mo atoms exposed on the surface. When HNa-Y with the higher proton concentration is used as a support, the dispersion of Mo is about 100 %. This is confirmed by the UV spectra, that is, the Mo species in Mo(VI)/H(65)Na-Y consist almost exclusively of the tetrahedrally coordinated molybdenum. It is concluded that Mo/HNa-Y system is advantageous for the preparation of the highly dispersed Mo species (about 100 % dispersion) compared with MoO_3 supported catalysts.

The aggregation of molybdenum occurs when H(36)Na-Y, H(14)Na-Y and Na-Y are used as supports, which leads to the formation of Mo(0) cluster. After the oxidation of molybdenum to Mo(VI), UV spectra of these samples demonstrate the presence of the octahedrally coordinated molybdenum. This is explained by the formation of bulk MoO_3 .

References

- 1 W. S. Millman and W. K. Hall, *J. Catal.*, 59, 311 (1979); J. Valyon and W. K. Hall, *J. Catal.*, 84, 216 (1983)
- 2 W. Zmierczak, G. Muralidhar and F. E. Massoth, *J. Catal.*, 77, 432 (1982)
- 3 N. K. Nag, *J. Catal.*, 92, 432 (1985)
- 4 B. S. Parekh and S. W. Weller, *J. Catal.*, 47, 100 (1977)
- 5 Y. I. Yermakov and B. N. Kuznetsov, *Prepr. 2nd Japan-Soviet Catalysis Seminar, (Tokyo, 1973), P.65*
- 6 Y. Iwasawa and S. Ogasawara, *J. Chem. Soc., Faraday Trans. I*, 75, 1465 (1979)
- 7 R. Riwan, C. Guillot and J. Paigne, *Surf. Sci.*, 47, 183 (1975)
- 8 H. -c. Liu and S. W. Weller, *J. Catal.*, 66, 65 (1980)
- 9 G. Muralidhar, B. E. Concha, G. L. Bartholomew and C. H. Bartholomew, *J. Catal.*, 89, 274 (1984)
- 10 M. Che, F. Figueras, M. Forissier, J. McAteer, M. Perrin, J. L. Portefaix and H. Praliaud, *Proc. 6th Intern. Congr. Catal.*, (London, 1976), P. 261
- 11 N. Giordano, J. C. J. Bart, A. Vaghi, A. Castellan and G. Martinotti, *J. Catal.*, 36, 81 (1975)
- 12 L. Wang and W. K. Hall, *J. Catal.*, 77, 232 (1982)
- 13 H. Jeziorowski and H. Knozinger, *J. Phys. Chem.*, 83, 1166 (1979)
- 14 K. Y. S. Ng and E. Gulari, *J. Catal.*, 92, 340 (1985)

5-1 Introduction

Molybdenum supported catalysts, especially MoO₃ supported catalysts have been used for a variety of reactions. It is known that the catalytic activity of the MoO₃ supported catalysts for various reactions such as hydrogenation of olefins, hydrogenolysis of parafins, etc. increases by the reduction of Mo species. The reduction is usually carried out with hydrogen at about 500 °C. Most of the Mo(VI) species are reduced to Mo(V) and Mo(IV) during this reduction. Therefore, in the case of the MoO₃/Al₂O₃ catalysts, the studies on the catalytic properties of Mo(IV), Mo(V) and Mo(VI) are usually performed. In many cases, the activity increases with increasing the extent of the reduction. If a significant amount of the Mo species whose oxidation numbers are less than +4 is formed during this reduction, it may be probable that these Mo species are active for the specific reactions.

Recently, new type catalysts have been prepared from some molybdenum complexes, and the catalytic activity of the Mo species in low oxidation states has been studied with these new catalysts. For example, Mo(II) species derived from Mo(π -C₃H₅)₄/Al₂O₃ or SiO₂ have exhibited the high activity for ethylene hydrogenation [1]. In the case of Mo(CO)₆/Al₂O₃ or SiO₂, it has been reported that Mo(III) is active for propylene metathesis [2] and Mo(0) is active for propane hydrogenolysis [3].

As mentioned in chapter 3, the Mo species whose average oxidation numbers are between +0.3 and +3.8 as well as +6 can be

prepared by changing the preparation conditions of Mo/HNa-Y. This wide range of the oxidation state obtained with the Mo/HNa-Y is advantageous for the study on the catalytic properties of the Mo species in the low oxidation states. In this chapter, I refer to the catalytic activity of the Mo species in the low oxidation states using Mo/HNa-Y with various oxidation states. The polymerization of ethylene, the hydrogenation of ethylene and the metathesis of propylene are selected as test reactions because it has been reported that the reduction of Mo(VI) in MoO₃/Al₂O₃ catalysts generates higher activity for these three reactions compared with the activity observed with the catalysts without reduction.

5-2 Experimental

5-2-1 Polymerization of ethylene

The polymerization of ethylene on Mo/HNa-Y was carried out at 60°C with a static system of 110 ml dead volume. The Mo/HNa-Y catalyst was prepared in situ from 0.70 g of HNa-Y and a certain amount of Mo(CO)₆ (typically, 0.68 Mo atoms per supercage of HNa-Y). Ethylene was purified by a freeze-pump-thaw technique. The initial pressure of ethylene was 290 torr.

The reaction products in gas phase were analyzed by gas chromatography using a 4 m column of VZ-7 and a FID detector. The extent of the reaction was monitored by measuring the pressure in the system.

5-2-2 Hydrogenation of ethylene

The hydrogenation of ethylene on Mo/HNa-Y was carried out at 1°C with a closed circulation system of 230 ml dead volume. The Mo/HNa-Y catalyst was prepared in situ from 0.040 g of HNa-Y and a certain amount of Mo(CO)₆ which corresponds to the molybdenum content of 2.0 Mo atoms per supercage. Traces of oxygen was removed from hydrogen by passage through a trap of Mn/SiO₂. Both of the initial pressures of ethylene and hydrogen were 135 torr.

The reaction products were analyzed by gas chromatography using a 2 m column of Porapak Q and the FID detector. The extent of the reaction was monitored by measuring the pressure in the system.

5-2-3 Metathesis of propylene

The metathesis of propylene on Mo/HNa-Y was carried out at 1°C with the closed circulation system of 230 ml dead volume. The Mo/HNa-Y catalyst was prepared in situ from 0.20 g of HNa-Y in the same manner as described above (5-2-2). Propylene was purified using a freeze-pump-thaw technique. The initial pressure of propylene was 190 torr.

The reaction products were analyzed by gas chromatography using a 4 m column of propylene carbonate and the FID detector.

5-3 Results and discussion

5-3-1 Polymerization of ethylene

When a certain amount of ethylene was introduced onto Mo/HNa-Y at 60°C, the immediate decrease in pressure was observed. After 1 hour of the reaction, trace amounts of propylene and butenes were detected in the gas phase in addition to the

remaining ethylene, which implies that the side reactions such as dimerization and metathesis occurred. However, the total amount of these by-products was less than 5 mol% of the amount of the consumed ethylene. Therefore, the rate of the pressure decrease corresponds to the reaction rate of the ethylene polymerization. Figure 20 is an example of first-order plot for the ethylene polymerization on Mo/HNa-Y. The linear relationship was observed for 10 minutes of the reaction, which indicates the first-order reaction with respect to the pressure of ethylene. I describe the activity of Mo/HNa-Y for the ethylene polymerization in terms of the first-order rate constant obtained at the initial stage of the reaction.

The gradual deactivation took place with the reaction time. The polyethylene formed by the polymerization probably hinders the diffusion of ethylene molecules within the zeolite crystallites. In order to confirm the formation of the polyethylene, IR spectra was measured with Mo/HNa-Y after the exposure to ethylene. The result is shown in Fig. 21. The exposure to 300 torr of ethylene at 60°C caused four IR bands as shown in spectrum (b). These bands result from methylene groups and are attributed as follows [4];

| | |
|-----------------------|----------------------------------|
| 2925 cm^{-1} | : Asymmetrical stretching |
| 2850 cm^{-1} | : Symmetrical stretching |
| 1470 cm^{-1} | : In-plane bending (scissoring) |
| 1370 cm^{-1} | : Out-of-plane bending (wagging) |

Therefore, the formation of the chain structure consisted of the methylene groups occurred on the Mo/HNa-Y sample. The intensity

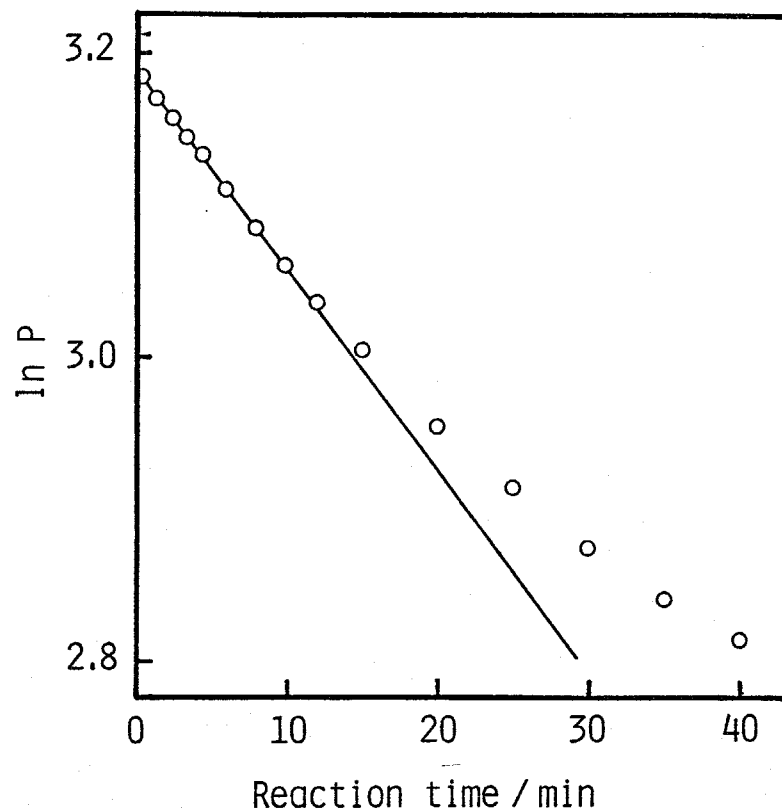


Fig. 20 First-order plot for ethylene polymerization on Mo/H(82)Na-Y

Dehydration temperature of H(82)Na-Y: 300°C

Decomposition temperature of Mo(CO)₆: 400°C

Reaction temperature: 60°C

Initial pressure of ethylene: 290 torr

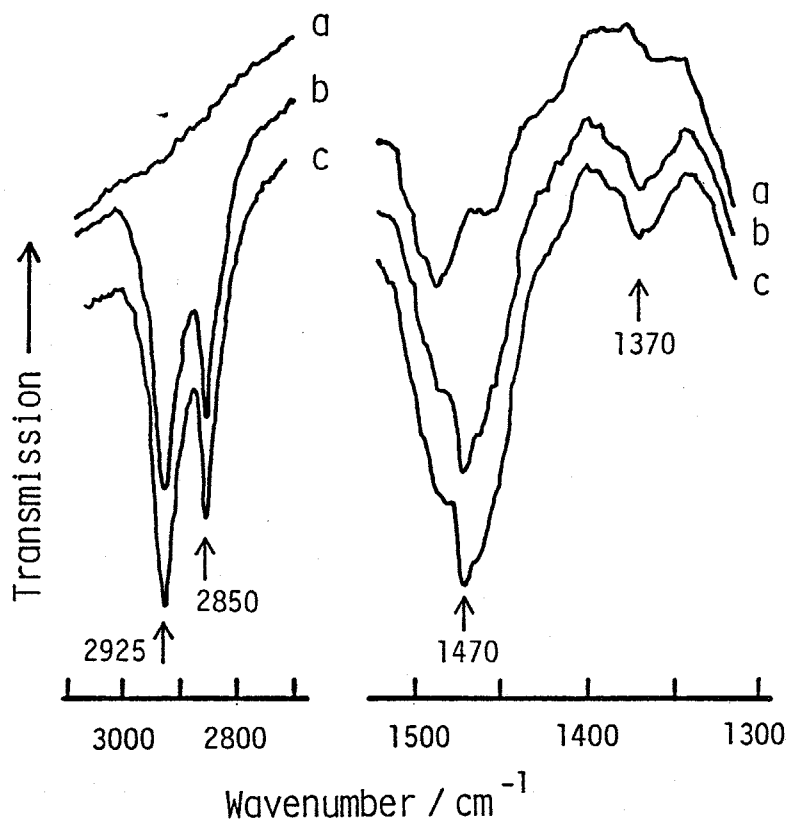


Fig. 21 IR spectra of polyethylene on Mo/H(82)Na-Y

a: Mo/H(82)Na-Y; dehydration temperature was 400°C, decomposition temperature was 300°C.

b: Sample a exposed to ethylene (300 torr) at 60°C.

c: Sample b evacuated at 100°C for 1 h.

of these bands were almost constant after the evacuation of the sample at 100°C for 1 hour (c), and no obvious band due to methyl groups was observed. Consequently, it is concluded that long and less branched chains of polyethylene are produced on the Mo/HNa-Y.

In order to clarify the effect of the oxidation state of molybdenum on the activity for the ethylene polymerization, various kinds of Mo/HNa-Y having different AON of Mo were used as catalysts. The relation between the activity and the AON of Mo are shown in Fig. 22. The catalysts were prepared at various dehydration and decomposition temperatures as shown in Fig. 9 (see 3-3-1). Two curves correspond to two series of Mo/HNa-Y which differ in the decomposition temperature of the adsorbed Mo(CO)_6 . At the decomposition temperature of 300°C, the activity reached the maximum at the AON of about +1.1. This maximum activity was about 25 fold as higher as the activity reported with reduced $\text{MoO}_3/\text{Al}_2\text{O}_3$ [5]. At the AON of +3.8, the activity was very low, and the activity became nearly zero after the oxidation of Mo to form Mo(VI)/HNa-Y. The fraction of Mo(V) determined from the ESR spectra had the inverse correlation with the activity, that is, the Mo/HNa-Y exhibiting the maximum activity gave the Mo(V)/Mo ratio of 0.17 % and the Mo/HNa-Y of lower activity (AON = +3.8) gave the ratio of 0.51 % as described in Fig. 16. Therefore, the Mo(V) which is detected by ESR is not the active site for the ethylene polymerization.

In the case of the decomposition temperature of 400°C, the activity reached the maximum at the AON of about +1. The two series of Mo/HNa-Y which differ in the decomposition temperature

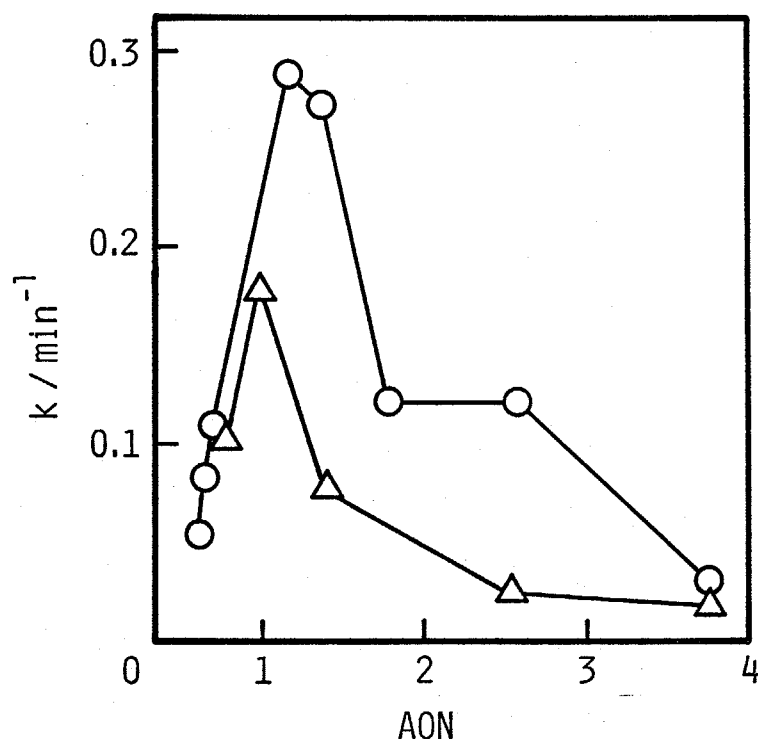


Fig. 22 Effect of average oxidation number on activity for ethylene polymerization

Catalyst: Mo/H(82)Na-Y (0.76 g)

Mo content: 0.68 Mo-atoms/supercage

Reaction temperature: 60°C

Initial pressure of ethylene: 290 torr

Decomposition temperature of Mo(CO)₆:

○ - 300°C; △ - 400°C

show the similar curves with the maximum activity at the nearly equal AON. These curves imply that the Mo species in the low oxidation state around +1 is the active site. However, the higher decomposition temperature led to the lower activity. This decrease in activity at the decomposition temperature of 400°C may result from the decrease in the dispersion of Mo. The amount of chemisorbed oxygen was measured with the Mo/HNa-Y which exhibited the maximum activity with the decomposition temperature of 400°C (AON = +0.98). The amount of oxygen corresponded to the O/Mo ratio of 0.85, which implies that the certain aggregation of Mo occurs in this catalyst.

Olsthoorn and Moulijn [6] have reported that the $\text{Mo}(\text{CO})_6/\text{Al}_2\text{O}_3$ heated at 100°C shows the catalytic activity for the ethylene polymerization. They have suggested that the adsorbed subcarbonyl species, $\text{Mo}(\text{CO})_3$ (ads), is the active species and that the oxidation number of Mo in this species is low. In the case of the $\text{Mo}(\text{CO})_6/\text{HNa-Y}$, the activity decreased with decreasing the decomposition temperature of $\text{Mo}(\text{CO})_6$ from 300°C to 100°C. This indicates that the remaining CO ligands on Mo lower the polymerization activity, that is, subcarbonyl species are not the most active species. From the above discussion, I conclude that the most active species for the ethylene polymerization is the molybdenum in low oxidation state, probably Mo(I) or Mo(II).

5-3-2 Hydrogenation of ethylene

When the 1:1 mixture of ethylene and hydrogen was intro-

duced onto Mo/HNa-Y at 1°C, the pressure decreased immediately to approach the half of the initial value. After the decrease in the pressure became negligible, trace amounts of propane and methane were detected in the gas phase in addition to ethane. However, the total amount of these by-products corresponded to 0.4 mol% of the amount of produced ethane, so that the side reactions can be ignored. Therefore, the rate of the pressure decrease represents the reaction rate of the ethylene hydrogenation. The reaction rates were measured with various values of the initial pressure of one reactant keeping that of the other reactant constant. The results indicate that the hydrogenation of ethylene on Mo/HNa-Y was the first order reaction with respect to the pressure of hydrogen and that it was about zero order to that of ethylene. Figure 23 shows an example of the first-order plot with respect to the pressure of hydrogen for the ethylene hydrogenation on Mo/H(14)Na-Y. The pressure decrease differed gradually from the linear relationship with the reaction time. Side reactions such as oligomerization of ethylene may occur. Therefore, the activity of Mo/HNa-Y is described in terms of the first-order rate constant determined in the initial stage of the reaction (1.5 minutes of the reaction).

Figure 24 shows the relation between the activity and the AON of Mo. Various Mo/HNa-Y (AON = +0.4 - +2.8) were prepared by changing both the degree of proton exchange in Y zeolites and their dehydration temperatures as shown in Fig. 11 (see 3-3-1). The activity increased with decreasing the AON of Mo when H(36)Na-Y, H(65)Na-Y or H(74)Na-Y was used as a support. After the oxygen treatment at -196°C which increased the AON to +3.6,

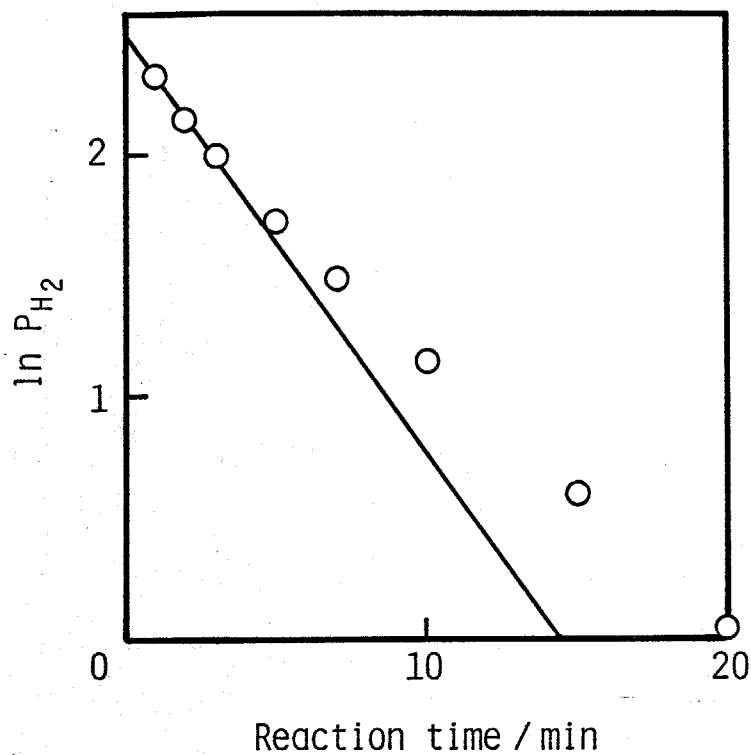


Fig. 23 First-order plot for ethylene hydrogenation on Mo/H(14)Na-Y

Dehydration temperature of H(14)Na-Y: 500°C

Decomposition temperature of Mo(CO)₆: 300°C

Mo content: 2 Mo-atoms/supercage

Reaction temperature: 1°C

Initial pressure of ethylene and H₂: 135 torr

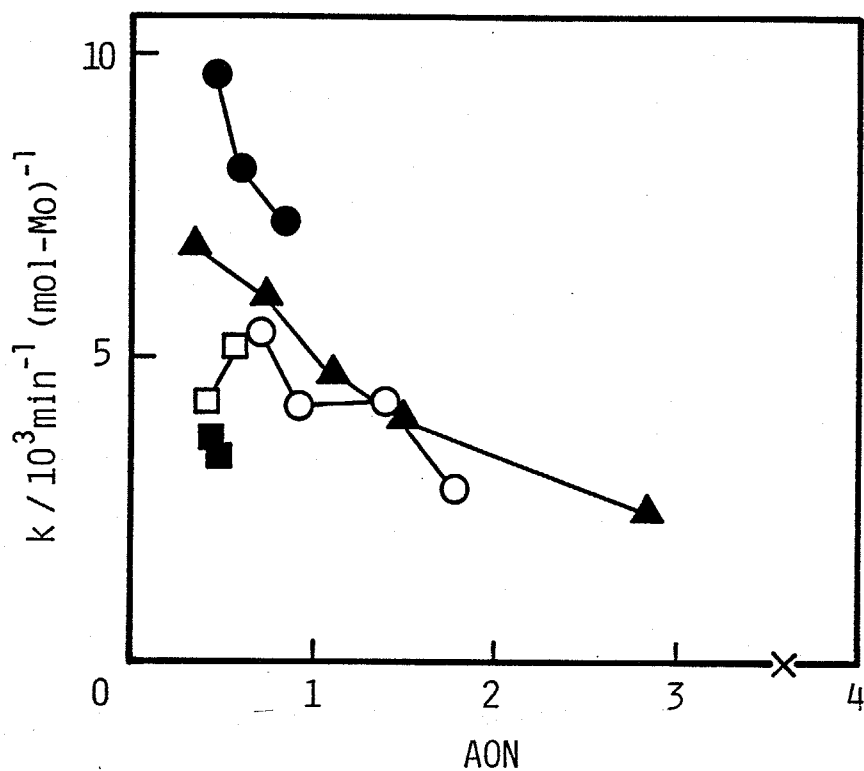


Fig. 24 Change in activity for ethylene hydrogenation with average oxidation number of Mo

Mo content: 2 Mo-atoms/supercage

Decomposition temperature of $\text{Mo}(\text{CO})_6$: 300°C

Reaction temperature: 1°C

Initial pressure of ethylene and H_2 : 135 torr

Degree of proton exchange (%):

■ - 0; □ - 14; ● - 36; ○ - 65; ▲ - 74

X : Oxidized with O_2 at 25°C

the activity of Mo/H(74)Na-Y decreased nearly to zero. These results implies that the Mo species in low oxidation state are the active sites for the ethylene hydrogenation.

Several studies have been carried out in relation to the active site for the ethylene hydrogenation with molybdenum supported catalysts. In the case of MoO₃/Al₂O₃, Lombardo et al. [7] have found that the reduction of Mo causes the higher activity. They considered the coordinatively unsaturated sites (CUS) on Mo(IV) to be the active site. However, the reduction of Mo(VI) in MoO₃/β-TiO₂ to the oxidation number below +4 has made the activity several fold as higher as that of Mo(IV) species [8]. In the case of the catalysts prepared from the π-allyl complex of Mo, Mo(II) has been the most active among the Mo species with the oxidation states of +2 - +6 [2]. Brenner [9] has reported for the catalysts derived from Mo(CO)₆ and alumina that the Mo(0) subcarbonyl species is active but that the further decomposition accompanied with the oxidation of Mo lowers the activity. In the above studies, the activity for the ethylene hydrogenation always increases with decreasing the oxidation state of Mo. This tendency is consistent with my results with the Mo/HNa-Y catalysts.

When Na-Y or H(14)Na-Y was used as a support, the activity was lower than that of Mo/H(36)Na-Y and Mo/H(74)Na-Y which had the AON of Mo in the similar range (+0.3 - +0.6). The Mo species in Mo/Na-Y and Mo/H(14)Na-Y exhibited the low dispersion of Mo as shown in Fig. 18 (see 4-3-1). To clarify the effect of the dispersion of Mo, the activity per surface Mo atom was calculated from the amount of chemisorbed oxygen (O/Mo) at -196°C. The

results are shown in Fig. 25. The plots for the activity were obviously divided into two groups. The lower activity group contained Mo/H(65)Na-Y and Mo/H(74)Na-Y where the dispersion of Mo was about 100 %. The higher activity group contained Mo/Na-Y, Mo/H(14)Na-Y and Mo/H(36)Na-Y. In these catalysts, the dispersion of Mo was low and the formation of Mo(0) cluster was suggested as described in chapter 4. Thus it is considered that the activity per Mo atom increases when the metallic cluster of Mo is formed. Mo metal has been reported to be active for the ethylene hydrogenation, though the activity is 1/18 as active as that of Pt metal [10]. It is concluded that the active site for the ethylene hydrogenation is the Mo(0) species and that when the Mo(0) species are aggregated to form metallic clusters, the activity of the surface Mo(0) atoms becomes higher.

5-3-3 Metathesis of propylene

The metathesis of propylene was carried out at 1°C on various Mo/HNa-Y catalysts. Immediately after propylene was introduced on Mo/HNa-Y, propylene was converted into ethylene and butenes. After 1 hour of the reaction, ethylene, trans- and cis-2-butenes and a trace amount of 1-butene were detected as reaction products. The amount of ethylene formed was larger than the total amount of butenes in every case. I expressed the catalytic activity of Mo/HNa-Y for the propylene metathesis in terms of the apparent turnover frequency calculated from the amount of ethylene formed in 1 hour of the reaction and the total amount of

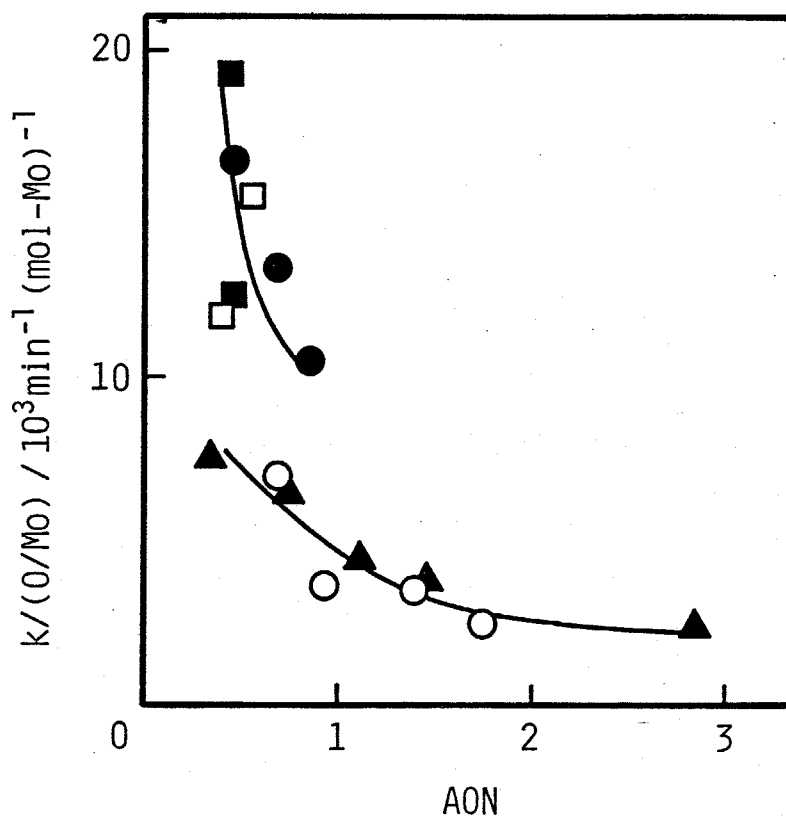


Fig. 25 Activity per surface Mo atom for ethylene hydrogenation

Mo content: 2 Mo-atoms/supercage

Decomposition temperature of $\text{Mo}(\text{CO})_6$: 300°C

Reaction temperature: 1°C

Initial pressure of ethylene and H_2 : 135 torr

Degree of proton exchange (%):

■ - 0; □ - 14; ● - 36; ○ - 65; ▲ - 74

O/Mo was measured at -196°C

molybdenum in the catalyst.

Figure 26 shows the relation between the catalytic activity of Mo/HNa-Y and the AON of Mo. The Mo/HNa-Y catalysts with various oxidation states (AON = +0.3 - +6) were prepared by changing the proton concentration of the HNa-Y supports as shown in Fig. 11 (see 3-3-1). In addition, Mo/H(82)Na-Y (Mo content = 0.68 Mo-atoms/supercage; AON = +3.75) and several Mo/HNa-Y catalysts oxidized with oxygen at room temperature or 300°C were used as catalysts.

In the cases of Mo/H(74)Na-Y, Mo/H(65)Na-Y and Mo/H(36)Na-Y, the catalytic activity increased with decreasing the AON of molybdenum. After the oxidation of three Mo/HNa-Y catalysts with oxygen at room temperature, the AON became +2.23, +2.99 and +4.94, while Mo/HNa-Y oxidized at 300°C had the AON of +6. These oxidized catalysts exhibited very low activities compared with the parent Mo/HNa-Y.

The Mo species whose oxidation numbers are +2 - +5 have been reported to be the active sites for the propylene metathesis. In the case of $\text{MoO}_3/\text{Al}_2\text{O}_3$ catalysts, from the relation between the ESR signal intensity of Mo(V) and the catalytic activity, Giordano et al. [11] have suggested that Mo(V) pair is the active site. Nakamura et al. [12] have reported that the Mo species whose oxidation number is less than +5, probably +4, is the active site from their ESR studies. In the case of the catalysts prepared from $\text{Mo}(\pi\text{-C}_3\text{H}_5)_4$, the most active species among Mo(II) - Mo(VI) was Mo(IV) formed from Mo(II) by oxidation at 0°C [13,14]. From the studies with $\text{Mo}(\text{CO})_6/\text{SiO}_2$ catalyst systems, Brenner et al. [15] have suggested that Mo(II) species

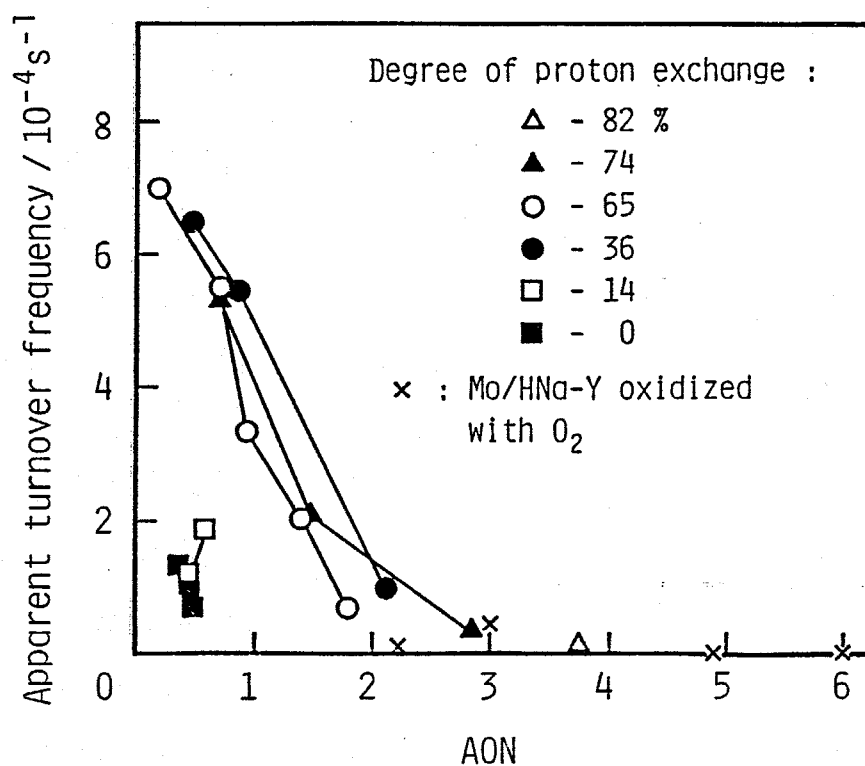


Fig. 26 Change in activity for propylene metathesis with average oxidation number of Mo

Mo content: 2 Mo-atoms/supercage

Decomposition temperature of Mo(CO)₆: 300°C

Reaction temperature: 1°C

Initial pressure of propylene: 190 torr

or Mo(IV) species formed from the Mo(II) by oxidation at room temperature are active for the propylene metathesis. Howe and Kemball [2] have also studied on the active site present in the catalysts prepared from Mo(CO)_6 and silica by infrared spectroscopy with NO as probe molecules. They have concluded that the Mo(III) species which can adsorb the NO molecule is the active site.

My results with the Mo/HNa-Y catalysts indicate that the activity of the Mo species whose AONs are +2 - +6 are much lower than that of Mo species in the lower oxidation state. The initial activity of the most active Mo/HNa-Y with Mo species in the low oxidation state is nearly comparable to that of the oxomolybdenum species with an oxidation number of +4 in $\text{Mo}(\pi\text{-C}_3\text{H}_5)_4/\text{Al}_2\text{O}_3$ catalyst system [14], which is the most active Mo catalyst for the propylene metathesis. The former activity corresponds to about 60 % of the latter. When the activity per surface Mo is compared, the former activity corresponds to about 110 % of the latter. These facts mean that such a high activity of the Mo/HNa-Y catalyst cannot result from a small amount of Mo(IV) species probably contained in the Mo/HNa-Y. Besides, the oxygen treatment on the Mo species in the low oxidation states caused the decrease in activity to a considerable extent. Therefore, it is concluded that the oxidation number of the most active Mo species for the propylene metathesis is not +4 but less than +2, probably 0.

When H(14)Na-Y and Na-Y were used as supports, however, the catalytic activities were relatively low, though the AONs of

Mo in these catalysts were as low as those in more active catalysts with H(36)Na-Y or H(65)Na-Y support. On the H(14)Na-Y or Na-Y support, the aggregation of Mo species occurs to lower the dispersion of Mo (see Fig. 18, in section 4-3-1). Therefore, it seems that the low dispersion of Mo species results in the low activity. However, the aggregation also occurs in the case of Mo/H(36)Na-Y whose activity was as high as that of Mo/H(65)Na-Y or Mo/H(74)Na-Y with the higher dispersion of Mo.

Figure 27 shows the relation between the metathesis activity per surface Mo atom and the AON of Mo. The number of the surface Mo atoms was determined by the oxygen chemisorption at -196°C as described previously (4-3-1). In the region of low AON, Mo/H(36)Na-Y exhibited the highest activity. The Mo species in Mo/H(36)Na-Y have medium dispersion ($\text{O}/\text{Mo} = 0.6 - 0.7$) compared with those in Mo/H(74)Na-Y ($\text{O}/\text{Mo} \approx 1$) and Mo/Na-Y ($\text{O}/\text{Mo} = 0.2 - 0.3$).

Consequently, I suggest that the activity for the propylene metathesis increases with the formation of small Mo(0) clusters but that the activity decreases with the formation of large Mo(0) clusters by the further aggregation of Mo(0). The propylene metathesis is believed to proceed through a metallocyclobutane intermediate. Therefore, the effect of the dispersion on the metathesis activity probably results from the steric hindrance caused by the large Mo(0) cluster located in the supercage of zeolites. However, the effect of the dispersion may result also from the structure sensitivity sometimes reported in supported metal particles or slight differences in the oxidation state of Mo caused by the metal-support interaction.

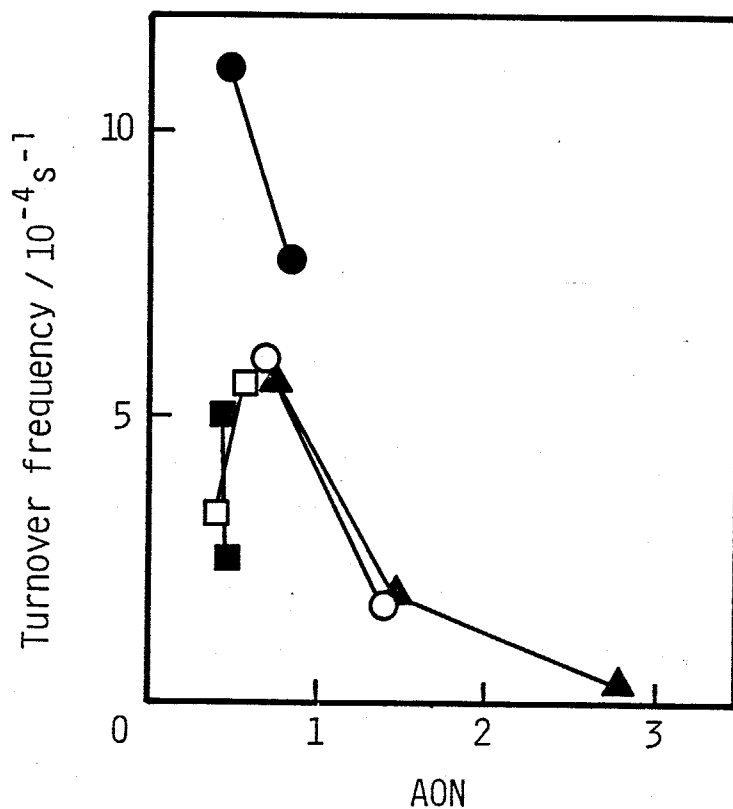


Fig. 27 Activity per surface Mo atom for propylene metathesis

Mo content: 2 Mo-atoms/supercage

Decomposition temperature of $\text{Mo}(\text{CO})_6$: 300°C

Reaction temperature: 1°C

Initial pressure of propylene: 190 torr

Degree of proton exchange (%):

■ - 0; □ - 14; ● - 36; ○ - 65; ▲ - 74

O/Mo was measured at -196°C

$$\text{Turnover frequency} = \frac{\text{Apparent turnover frequency}}{\text{O/Mo}}$$

5-4 Conclusion

The catalytic activity of molybdenum was studied by using the Mo/HNa-Y catalysts with various oxidation states of molybdenum. For the polymerization of ethylene, the slightly oxidized Mo species, probably Mo(I) or Mo(II), is suggested to be the active site. For the hydrogenation of ethylene and the metathesis of propylene, Mo(0) species is the most active species compared with that with the higher oxidation states. The aggregation of Mo(0) to form a small metallic cluster results in the higher activity per surface Mo atom for these two reactions. In the case of the propylene metathesis, excess aggregation lowers the activity.

For any reaction studied, the Mo species in extremely low oxidation states which can hardly be prepared in MoO₃ supported catalysts exhibit the high activities. These activities are much higher than those reported for the MoO₃ supported catalysts. It seems that the extent of coordinative unsaturation as well as the electronic effect affects the activities. This is obvious because the subcarbonyl species which consist of Mo(0) are less active than the Mo(0) clusters without any CO ligand formed after the complete decomposition of the subcarbonyls.

References

- 1 Y. Iwasawa, M. Yamagishi and S. Ogasawara, *J. Chem. Soc., Chem. Comm.*, 871 (1980)
- 2 R. F. Howe and C. Kemball, *J. Chem. Soc., Faraday Trans. I*, 70, 1153 (1974)
- 3 R. Nakamura, R. G. Bowman and R. L. Burwell, Jr., *J. Am. Chem. Soc.*, 103, 673 (1981); R. Nakamura, D. Pioch, R. G. Bowman and R. L. Burwell, Jr., *J. Catal.*, 93, 388 (1985)
- 4 R. M. Silverstein, G. C. Bassler and T. C. Morrill, "Spectrometric Identification of Organic Compounds", 4th Ed., p. 106, John Willey & Sons, 1981
- 5 R. V. Morris, D. R. Waywell and J. W. Shepard, *J. Less-Common Metals*, 36, 395 (1974)
- 6 A. A. Olsthoorn and J. A. Moulijin, *J. Mol. Catal.*, 8, 147 (1980)
- 7 E. A. Lombardo, M. Houalla and W. K. Hall, *J. Catal.*, 51, 256 (1978)
- 8 K. Tanaka, K. Miyahara and K. Tanaka, *J. Mol. Catal.*, 15, 133 (1982); K. Tanaka, K. Miyahara and K. Tanaka, *Proc. 7th Intern. Congr. Catal.*, (Tokyo, 1980), p. 1318
- 9 A. Brenner, *J. Mol. Catal.*, 5, 157 (1979)
- 10 A. Kouskova, J. Adamek and V. Ponec, *Collect. Czech. Chem. Comm.*, 35, 2538 (1970)
- 11 N. Giordano, M. Padovan, A. Vaghi, J. C. J. Bart and A. Castellan, *J. Catal.*, 38, 1 (1975)
- 12 R. Nakamura, Y. Morita and E. Echigoya, *Nippon Kagaku Kaishi*, 244 (1973)

- 13 Y. I. Yermakov, B. N. Kuznetzov, Y. P. Grabovski, A. N. Startzev, A. M. Lazutkin, V. A. Zakharov and A. I. Lazutkina, *J. Mol. Catal.*, 1, 93 (1975/76); B. N. Kuznetsov, A. N. Statsev and Y. I. Yermakov, *ibid.*, 8, 135 (1980)
- 14 Y. Iwasawa, H. Ichinose, S. Ogasawara and M. Soma, *J. Chem. Soc., Faraday Trans. I*, 77, 1763 (1981); Y. Iwasawa, H. Kubo and H. Hamamura, *J. Mol. Catal.*, 28, 191 (1985)
- 15 A. Brenner, D. A. Hucul and S. J. Hardwick, *Inorg. Chem.*, 18, 1478 (1979); A. Brenner and R. L. Burwell, Jr., *J. Catal.*, 52, 364 (1978)

In order to clarify the catalytic properties of molybdenum, I prepared Mo/HNa-Y catalysts with various oxidation states of molybdenum and carried out the characterization of the supported molybdenum species. Three kinds of reactions were performed with the various Mo/HNa-Y catalysts and the active sites for these reactions were discussed based on the results of the characterization.

In the first stage of the preparation of Mo/HNa-Y, $\text{Mo}(\text{CO})_6$ is adsorbed in the supercage of the dehydrated HNa-Y zeolite. The adsorption is saturated when every supercage adsorbs two $\text{Mo}(\text{CO})_6$ molecules irrespective of the proton concentration of HNa-Y. The second stage involves the heating of the adsorbed $\text{Mo}(\text{CO})_6$ in vacuo to decompose the $\text{Mo}(\text{CO})_6$. Above 300°C , the $\text{Mo}(\text{CO})_6$ is completely decomposed to form Mo/HNa-Y. When the amount of added $\text{Mo}(\text{CO})_6$ does not exceed the amount of its saturated adsorption, all of the added molybdenum is supported on the HNa-Y zeolite through the thermal decomposition. From the Mo/Si ratio estimated from XPS spectra, it is found that the molybdenum species in Mo/HNa-Y are distributed within the zeolite crystallites.

Molybdenum is oxidized by the surface hydroxyl groups of HNa-Y during the thermal decomposition of the adsorbed $\text{Mo}(\text{CO})_6$. This oxidation causes the formation of certain amounts of hydrogen and methane. The average oxidation number (AON) of the supported molybdenum is determined by an O_2 titration method and by measuring the amount of H_2 and CH_4 evolved during the decomposition

of $\text{Mo}(\text{CO})_6/\text{HNa-Y}$. The $\text{Mo}/\text{HNa-Y}$ catalysts with various AON of molybdenum are prepared by changing the preparation conditions. The lower AON of molybdenum is obtained by using the HNa-Y supports with the lower concentrations of the surface hydroxyl groups and by decomposing the $\text{Mo}(\text{CO})_6$ at the lower temperatures. Thus I can prepare the $\text{Mo}/\text{HNa-Y}$ in which the AONs of molybdenum are in the range from +0.3 to +3.8.

The existence of $\text{Mo}(0)$ species is confirmed from in situ XPS spectra of the supported molybdenum and from IR spectra of CO adsorbed on the $\text{Mo}/\text{HNa-Y}$. The XPS spectra also indicate the existence of $\text{Mo}(\text{II})$ species when HNa-Y with the high proton concentration is used as a support. In the similar $\text{Mo}/\text{HNa-Y}$, the existence of $\text{Mo}(\text{I})$ and Mo^{n+} ($n \geq 2$) is indicated from the IR spectra of the adsorbed CO . In the case of the impregnation $\text{MoO}_3/\text{Al}_2\text{O}_3$ catalyst, the Mo species with the low oxidation states as $\text{Mo}(0)$, $\text{Mo}(\text{I})$ and $\text{Mo}(\text{II})$ have only be prepared by the reduction with H_2 at high temperatures above 800°C . Treatments at such high temperatures may cause the aggregation of Mo species. It is concluded that the $\text{Mo}/\text{HNa-Y}$ prepared from $\text{Mo}(\text{CO})_6$ is the useful system to obtain the molybdenum with the low oxidation states.

The dispersion of the supported Mo species is estimated by the amount of chemisorbed oxygen (O/Mo) at -196°C . When HNa-Y with a high degree of proton exchange is used as a support, about one oxygen atom is chemisorbed on one Mo atom ($\text{O}/\text{Mo} \approx 1$). After oxidation of this sample to $\text{Mo}(\text{VI})$, its UV spectrum shows that most of the Mo species have the tetrahedral coordination with the oxygens, which indicates that few Mo atoms form the bulk MoO_3 .

Therefore, the dispersion of molybdenum in this Mo/HNa-Y is about 100 %. On the other hand, when HNa-Y with the lower degree of proton exchange is used as a support, the O/Mo ratio becomes lower than 1. The UV spectrum after the oxidation shows that the Mo species with the octahedral coordination are contained in the sample. Therefore, the bulk MoO₃ is formed and lowers the dispersion of molybdenum.

The Mo/HNa-Y catalysts with various oxidation states of molybdenum are used as catalysts to clarify the catalytic properties of molybdenum in the low oxidation states. Three reactions are performed, that is, the polymerization of ethylene, the hydrogenation of ethylene and the metathesis of propylene. In the case of the polymerization of ethylene, slightly oxidized species, probably Mo(I) or Mo(II), are considered to be the active site. On the other hand, Mo(0) species is found to be the active site for the ethylene hydrogenation and the propylene metathesis. The formation of Mo(0) clusters leads to the increase in the activity per surface molybdenum for these two reactions. However, the extensive aggregation (O/Mo < 0.4) lowers the activity for the propylene metathesis. The activities of the Mo/HNa-Y catalysts observed in this study are higher than those reported with MoO₃ supported catalysts which consist mainly of Mo(IV), Mo(V) and Mo(VI) species.

It is concluded that I can prepare the various molybdenum species by using Mo(CO)₆ and HNa-Y zeolites. The oxidation state and the dispersion of the molybdenum species can be altered over the wide range by changing the preparation conditions. The Mo species with the low oxidation states such as Mo(0), Mo(I) and

Mo(II) are found to be very active species for certain reactions. The Mo/HNa-Y catalyst system is advantageous for clarifying the catalytic properties of molybdenum especially in the low oxidation states.

ACKNOWLEDGMENT

I would like to give my hearty gratitude to Associate Professor Tatsuaki Yashima and Dr. Seitaro Namba for their continuing advice, helpful discussion and encouragement.

I also wish to thank Professor Takaharu Onish and Dr. Kazunari Domen for their assistance and valuable discussion in XPS study. I am grateful to Lecturer Koichi Segawa and Mr. Yoshihiro Tomatsu (Sophia University) for their valuable suggestion and assistance in UV spectroscopic study. I am also grateful to Professor Yoshio Ono and Dr. Nobumasa Kitajima for their assistance and useful advice in ESR study, and also grateful to Associate Professor Ichiro Okura for his assistance and encouragement during this study.

I would like to express my gratitude to Professor Mitsuo Abe for his advice and encouragement during this study. My special thanks are given to Professor Eizo Miyazaki and Dr. Isao Kojima for their support and suggestion in XPS study. I would like to thank Professor Hiroshi Kobayashi and Associate Professor Yoko Kaizu for their support and suggestion in Raman spectroscopic study. I also wish to thank Professor Ikuzo Tanaka, Associate Professor Kinichi Obi and Dr. Takashi Imamura for their assistance and suggestion in ESR study.

It is with great pleasure that I thank all the members who have belonged to Yashima laboratory from 1980 to 1986 and assisted my work for this study by drawing figures, typing manuscripts, giving valuable suggestions, etc.. My special gratitude is given to Mr. Tokuzo Komatsu, my father, and his family, Mr.

Goro Okuni, my father-in-law, and his family and my wife for their precious assistance and continuing encouragement.